

**GSFC JPSS CMO  
November 9, 2012  
Released**

**Joint Polar Satellite System (JPSS) Ground Project  
Code 474  
474-00090**

**Joint Polar Satellite System (JPSS)  
Operational Algorithm Description (OAD)  
Document for VIIRS Geolocation (GEO)  
Sensor Data Record (SDR) and Calibration  
(CAL) SDR Software**

**For Public Release**

The information provided herein does not contain technical data as defined in the International Traffic in Arms Regulations (ITAR) 22 CFC 120.10. This document has been approved For Public Release to the NOAA Comprehensive Large Array-data Stewardship System (CLASS).



---

**Goddard Space Flight Center  
Greenbelt, Maryland**

---

National Aeronautics and  
Space Administration

# **Joint Polar Satellite System (JPSS) Operational Algorithm Description (OAD) Document for VIIRS Geolocation (GEO) Sensor Data Record (SDR) and Calibration (CAL) SDR Software**

## **JPSS Electronic Signature Page**

Prepared by (Book Boss), Reviewed by (if reviewer approved in MIS), Approved by (CCB Chair).

### **Prepared By:**

Neal Baker  
JPSS Data Products and Algorithms, Senior Engineering Advisor  
(Electronic Approvals available online at ([https://jpssmis.gsfc.nasa.gov/mainmenu\\_dsp.cfm](https://jpssmis.gsfc.nasa.gov/mainmenu_dsp.cfm)))

### **Approved By:**

Heather Kilcoyne  
DPA Manager  
(Electronic Approvals available online at ([https://jpssmis.gsfc.nasa.gov/mainmenu\\_dsp.cfm](https://jpssmis.gsfc.nasa.gov/mainmenu_dsp.cfm)))

**Goddard Space Flight Center  
Greenbelt, Maryland**

## Preface

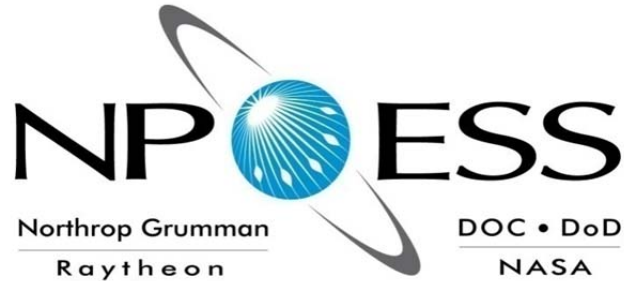
This document is under JPSS Ground Algorithm ERB configuration control. Once this document is approved, JPSS approved changes are handled in accordance with Class I and Class II change control requirements as described in the JPSS Configuration Management Procedures, and changes to this document shall be made by complete revision.

Any questions should be addressed to:

JPSS Configuration Management Office  
NASA/GSFC  
Code 474  
Greenbelt, MD 20771

## Change History Log

| Revision   | Effective Date | Description of Changes<br>(Reference the CCR & CCB/ERB Approve Date)  |
|------------|----------------|---|
| Original   | 08/24/2011     | This version incorporates <b>474-CCR-11-0105</b> : (This version baselines D41868, Rev A dated 09/22/2010. This is the version that was approved for NPP launch. Per NPOESS CDFCB - External, Volume V – Metadata, doc number D34862-05, this has been approved for Public Release into CLASS.) to create JPSS version, Rev-. This was approved by the JPSS Ground Algorithm ERB on August 24, 2011.  |
| Revision A | 01/18/2012     | <b>474-CCR-11-0250</b> : This version baselines 474-00090, Joint Polar Satellite System (JPSS) Operational Algorithm Description (OAD) Document for VIIRS Geolocation (GEO) Sensor Data Record (SDR) and Calibration (CAL) SDR Software, for the Mx 6 IDPS release. This CCR was approved by the JPSS Algorithm ERB on January 18, 2012.  |
| Revision B | 10/09/2012     | <b>474-CCR-12-0627</b> : This version authorizes 474-00090, Joint Polar Satellite System (JPSS) Operational Algorithm Description (OAD) Document for VIIRS Geolocation (GEO) Sensor Data Record (SDR) and Calibration (CAL) SDR Software, for the Mx 6.1 – 6.3 IDPS releases. Includes: <b>ECR-ALG-0035</b> which contains Raytheon PCR030210; OAD: Implement 474-CCR-12-362 (VIIRS SDR Code and LUT Mods for scan-by-scan RSB Calibration) (ADR 4586) updated Table 19. Raytheon PCR030559, OAD: Implement 474-CCR-12-0402 (Add Mirror Side Information to VIIRS SDR Geolocation Files) (ADR 4703), updated Table 13 and section 2.2.2.28. Raytheon PCR030617; OAD: Implement 474-CCR-12-0406 (VIIRS-SDR Reflective Band Limits SZA Modified to 89 Degrees from 85 Degrees) (ADR 4277), updated Section 2.3.2.3. Raytheon PCR031579; OAD: Implement 474-CCR-12-0490 (Modify Cal Sector Data in VIIRS OBC-IP) (ADR 4743, 4744, 4745, 4820) updated Tables 3, 18 & 31. Raytheon PCR031615, OAD: Implement 474-CCR-12-0489 (Add VIIRS Scan Encoder Electronics Side Indicator to VIIRS SDR GEO QF's) (ADR 4759), updated Tables 9-13. |
|            |                |   |
|            |                |   |
|            |                |   |
|            |                |   |
|            |                |   |



# **NATIONAL POLAR-ORBITING OPERATIONAL ENVIRONMENTAL SATELLITE SYSTEM (NPOESS)**

## **OPERATIONAL ALGORITHM DESCRIPTION DOCUMENT FOR VIIRS GEOLOCATION (GEO) SENSOR DATA RECORD (SDR) and CALIBRATION (CAL) SDR**

**SDRL No. S141  
SYSTEM SPECIFICATION SS22-0096**

**RAYTHEON COMPANY  
INTELLIGENCE AND INFORMATION SYSTEMS (IIS)  
NPOESS PROGRAM  
OMAHA, NEBRASKA**

**Copyright © 2004-2012  
Raytheon Company  
Unpublished Work  
ALL RIGHTS RESERVED**

Portions of this work are the copyrighted work of Raytheon. However, other entities may own copyrights in this work. Therefore, the recipient should not imply that Raytheon is the only copyright owner in this work.

This data was developed pursuant to Contract Number F04701-02-C-0502 with the US Government under subcontract number 7600002744. The US Government's right in and to this copyrighted data are as specified in DFAR 252.227-7013, which was made part of the above contract.



Northrop Grumman Space & Mission Systems Corp.  
**Space Technology**  
One Space Park  
Redondo Beach, CA 90278

**NORTHROP GRUMMAN**

**Raytheon**



Engineering & Manufacturing Development (EMD) Phase  
Acquisition & Operations Contract

CAGE NO. 11982

**Operational Algorithm Description  
VIIRS SDR**

**Document Date: Nov 04, 2011**

**Document Number: D41868  
Revision: B7**

**PREPARED BY:**

\_\_\_\_\_  
Ronson Chu *Date*  
*AM&S VIIRS SDR Lead*

\_\_\_\_\_  
Paul D. Siebels *Date*  
*IDPS PRO SW Manager*

**ELECTRONIC APPROVAL SIGNATURES:**

\_\_\_\_\_  
Roy Tsugawa *Date*  
*SEIT Lead & ACCB Chair*

\_\_\_\_\_  
Bob Hughes *Date*  
*Algorithm Implementation Thread Lead*

\_\_\_\_\_  
Bob Hughes *Date*  
*Data Product System Engineering Lead*

\_\_\_\_\_  
Stephen E. Ellefson *Date*  
*IDPS Processing SI Lead*

Prepared by  
**Northrop Grumman Space Technology**  
One Space Park  
Redondo Beach, CA 90278

Prepared for  
**Department of the Air Force**  
NPOESS Integrated Program Office  
C/O SMC/CIK  
2420 Vela Way, Suite 1467-A8  
Los Angeles AFB, CA 90245-4659

Under  
**Contract No. F04701-02-C-0502**

This document has been identified per the NPOESS Common Data Format Control Book – External Volume 5 Metadata, D34862-05, Appendix B as a document to be provided to the NOAA Comprehensive Large Array-data Stewardship System (CLASS) via the delivery of NPOESS Document Release Packages to CLASS.

Northrop Grumman Space & Mission Systems Corp.  
**Space Technology**  
 One Space Park  
 Redondo Beach, CA 90278

**NORTHROP GRUMMAN**

**Raytheon**

**Revision/Change Record**

**Document Number D41868**

| <b>Revision</b> | <b>Date</b> | <b>Revision/Change Description</b>   | <b>Pages Affected</b> |
|-----------------|-------------|--|-----------------------|
| ---             | 8-31-04     | Initial Release VIIRS Geolocation (GEO) SDR Software.  | All                   |
| ---             | 9-30-04     | Initial Release VIIRS SDR Calibration Software.  | All                   |
| A1              | 6-8-06      | <p>06Oct05 - Reflects continued Science To Operational Code Conversion combining VIIRS GEO SDR OAD and VIIRS Calibration SDR OAD since official delivery of separate documents to NGST on 15Sep05.</p> <p>14Mar06 – Updated copyright on coversheet; inserted latest Unit Test dated 9Mar06 (31 pages); updated Table of Content page numbers and List of Table page numbers; addressed Omaha QA comments from Code Completion Peer Review (CCPR) on 14Mar06.</p> <p>15Mar06 – Continued to edit based on Omaha QA comments, individually listing all 60 TBDs versus lumping them together per the Table they reside in; fixing Table references in the text, etc.</p> <p>20Mar06 – Updated Section 1.3.3 Source Code and Test Data References.</p> <p>28Mar06 – Minor edits to fix Doug Rishel CCPR comments.</p> <p>29Mar06 – Changed upper right header document number to only use the originally dropped VIIRS Geolocation SDR OAD (D39300) number although this document incorporates a lot of information from the originally dropped VIIRS SDR Calibration OAD (D39553).</p> <p>21Apr06 – Added viirs_decmp function information and updated TOC</p> <p>11May06 – Updated for SDR Optimization modifications</p> <p>08 Jun06 – Updated Document Numbers. Original VIIRS Geolocation OAD D39300. Original VIIRS Calibration OAD D39553. These 2 OADs combined into this single OAD.</p> | All                   |
| A2              | 12-11-06    | Add Section 2.3.1.4 for new “createRadianProducts()” method.   | All                   |
| A3              | 2-16-07     | Updated for DDPR AIs.  | All                   |
| A4              | 5-3-07      | Rename and modify Section 2.3.1.4.   | All                   |
| A5              | 6-18-07     | Updated for CCPR AIs.  | All                   |

Northrop Grumman Space & Mission Systems Corp.  
**Space Technology**  
 One Space Park  
 Redondo Beach, CA 90278



## Revision/Change Record

Document Number **D41868**

| Revision | Document Date | Revision/Change Description  | Pages Affected |
|----------|---------------|--|----------------|
| A6       | 7-3-07        | Updated for the implementation of<br>NP-EMD.2005.510.0122_VIIRS_CAL_SD_Detailed_Code_Changes_Oct_2005<br>NP-EMD-2007.510.0014_VIIRS_SDR_Cal_Modif_Implement_OAD<br>NP-EMD-2007.510.0009_VIIRS_SDR_Even_odd_subframe_design<br>NP-EMD-2007.510.0010_VIIRS_SDR_Robust_Alg_design<br>NP-EMD-2007.510.0012_NPP_VIIRS_CAL_EV_Detailed_Code_Changes_Feb_2007   | All            |
| A7       | 8-2-07        | Delivered to NGST.   | All            |
| A8       | 9-27-07       | Implemented NP-EMD-2007.510.0029_NPP_VIIRS_SDR_DNB_FirstFrameAnomaly.  | All            |
| A9       | 11-9-07       | Added S/C Attitude to non-gridded geolocation outputs. Responded to PR comments – ECR A-122.   | All            |
| A10      | 12-17-07      | ECR A-103, EDR-PR 1.8 CP 3, and CDFCB-X compliance updates: updated non-gridded geolocation output structures and quality flags and the SDR scan-level quality flags.  | All            |
| A11      | 2-22-08       | Reformatted in accordance to new template. Implementation of NP-EMD.2005.510.0134, NP-EMD.2005.510.0119, NP-EMD.2005.510.0065, NP-EMD.2005.510.0067, NP-EMD.2005.510.0069, NP-EMD.2005.510.0071, NP-EMD.2005.510.0074, NP-EMD.2005.510.0081, MP-EMD.2005.510.0064, NP-EMD.2005.510.0075, NP-EMD.2005.510.0004, NP-EMD.2005.510.0012, NP-EMD.2005.510.0068, NP-EMD.2005.510.0125, NP-EMD.2006.510.0098, NP-EMD-2007.510.0011, NP-EMD-2007.510.0013.<br>Added Bright Pixel sections.<br>Incorporated updates from NGST comments pertaining to previous delivery.<br>Delivered to NGST. | All            |
| A12      | 2-25-08       | Accept all track changes for re-baselined version.   | All            |
| A13      | 8-18-08       | Updated in accordance with NP-EMD.2008.510.0027.   | All            |
| A14      | 10-17-08      | Updated in accordance with NP-EMD-2008.510.0019. Remove moon_vector field from VIIRS-OBC-IP. Incorporated comments from previous delivery. Updated cover sheet and Acronym list. Delivered to NGST.  | All            |
| A15      | 11-12-08      | Minor changes for PCR 18378, VIIRS SDR Refactor, to remove specific references to ProSdrViirs.   | 5, 7           |

Northrop Grumman Space & Mission Systems Corp.  
**Space Technology**  
 One Space Park  
 Redondo Beach, CA 90278



| <b>Revision/Change Record</b> |             |   | <b>Document Number</b>                        |
|-------------------------------|-------------|---|---|
|                               |             |   | <b>D41868</b>                                 |
| <b>Revision</b>               | <b>Date</b> | <b>Revision/Change Description</b>  | <b>Pages Affected</b>                         |
| A16                           | 3-18-09     | Incorporated comments from SDRL Delivery. Fixed definition of Moon Phase, typo in definition of SolarAzimuth, bit numbering in Scan Level Geolocation Quality Byte, and updated OBC structure definition. Updated Table 9 for IPO Issue. Prepared OAD for TIM – (All pages).  | 20-25, 45-47                                  |
| A17                           | 6-15-09     | Incorporated TIM comments and prepared for ARB/ACCB. Updated the obc-ip output structure – PCR19290/PCR 20614. ARB actions delayed until after Sep 09, revision increment returned to header(s).  | All Table 31                                  |
| A18                           | 7-06-09     | PCR 15261 Removed Sensor Dependent column since all AUX items are sensor dependent. Updated the obc-ip output structure ECR 878 changes.  | Table 19, Table 31                            |
| A19                           | 7-07-09     | NP-EMD.2008.510.0050 VIIRS GEO EVtimes Updates  | Tables 9, 10, 11, 12, and 31, Section 2.1.2.5 |
| A20                           | 11-04-09    | Updated for ECR-878 Changes which fixed packet info.  | All   |
| A21                           | 01-13-10    | Implemented:<br><br>NP-EMD.2009.510.0047_VIIRS_GEO_DNB_AggZoneFix,<br>NP-EMD.2009.510.0048 Rev A VIIRS Geo Quality Flags Logic Updates,<br>NP-EMD-2009.510.0033 Rev A VIIRS SDR OAD Updates to the Geolocation Parameters Table,<br>NP-EMD-2009.510.0031 Rev A Solar Diffuser LUT Read Update,<br>NP-EMD-2009.510.0042 Solar Diffuser Cal SDSM Angle Fix. k<br>Updated for 878 Changes which fixed packet info.<br>NP-EMD-2009.510.0041 SDR Calibration Imagery Even Odd Parity Fix Code Update | All   |
| A22                           | 02-25-10    | Implemented: NP-EMD-2009.510.0052 VIIRS Bright Pixel ID Algorithm Update  | Tables 1, 2                                   |

Northrop Grumman Space & Mission Systems Corp.  
**Space Technology**  
 One Space Park  
 Redondo Beach, CA 90278



**Revision/Change Record**

**Document Number D41868**

| <b>Revision</b> | <b>Document Date</b> | <b>Revision/Change Description</b>   | <b>Pages Affected</b> |
|-----------------|----------------------|--|-----------------------|
| A23             | 06-17-10             | Implemented ECR-A280:<br>NP-EMD.2010.510.0003_SDR_and_SDCal_RVS_LUT_Update<br>NP-EMD.2010.510.0007-Rev-A_SDR_Calibration_Thermistor_LUT_Update<br>NP-EMD.2010.510.0008_VIIRS_SDR_Calibration_OBC_Blackbody_Calibration_Update<br>NP-EMD.2010.510.0011_SDR_Calibration_RSR_LUT_Update<br>NP-EMD.2010.510.0012_VIIRS_SDR_Cal_DNB_Stray_Light_Quality_Flag<br>NP-EMD.2010.510.0013_VIIRS_SDR_Cal_DG_Anomaly_Quality_Flag<br>NP-EMD.2010.510.0021_VIIRS_SDR_Calibration_EMI_Spike_Filter<br>NP-EMD.2010.510.0016_Solar_Diffuser_LUT_Update | All                   |
| A24             | 6-22-10              | Updated Tables 1 & 2, coversheets, font, and format throughout document.   | All                   |
| A25             | 7-08-10              | Updated for SDRL   | All                   |
| A26             | 8-17-10              | Incorporated TM 2010.510.0004  | All                   |
| A27             | 8-23-10              | Incorporated VIIRS SDR fixes for ADCM-010  | Tables 1 & 2          |
| A28             | 9-16-10              | Updated for TIM/ARB  | All                   |
| A               | 9-22-10              | Incorporated TIM and ARB comments in preparation for ACCB (ECR-A325)   | All                   |
| B1              | 9-29-10              | Updated for Algorithm Development Library  | Section 2.0           |
| B2              | 10-12-10             | Updated due to document convergence, to include tech memos 2010.510.0011, 2010.510.0012, 2010.510.0013, 2010.510.0014, & 2010.510.0016,  | All                   |
| B3              | 11-29-10             | Updates for PCR025126 – Revert OBC-IP to UInt16s (Rev B3 undone in Rev B7)   | All                   |
| B4              | 02-10-11             | Updates for ISTN_VIIRS_NGST_4.19.2 & ISTN_VIIRS_NGST_4.23.1 (NP-EMD.2010.510.0094)   | All                   |
| B5              | 06-29-11             | Implemented TM NP-EMD.2011.510.0003_VIIRS_inst2sc.pdf  | All                   |
| B6              | 09-28-11             | Updated for PCR026634.   | All                   |
| B7              | 11-04-11             | Updated for PCR027965 Solar diffuser dim fixes. Undo of PCR025126. And updated for PCR027896.  | All                   |

**Table of Contents**

|           |   |    |
|-----------|---|----|
| 1.0       | INTRODUCTION.....                                       | 1  |
| 1.1       | Objective.....  | 1  |
| 1.2       | Scope .....   | 1  |
| 1.3       | References .....  | 1  |
| 1.3.3     | Document References .....                               | 1  |
| 1.3.3     | Source Code References .....                            | 4  |
| 2.0       | ALGORITHM OVERVIEW .....                                | 8  |
| 2.1       | VIIRS SDR Verified RDR Description.....                 | 11 |
| 2.1.1     | Interfaces .....  | 13 |
| 2.1.1.1   | Inputs .....  | 13 |
| 2.1.1.2   | Outputs .....   | 18 |
| 2.1.2     | Algorithm Processing.....                               | 18 |
| 2.1.2.1   | createVerifiedRDR().....                                | 19 |
| 2.1.2.2   | ProViirsVerifiedRDRConverter() .....                    | 19 |
| 2.1.2.3   | ViirsCalAppPacket().....                                | 20 |
| 2.1.2.4   | ViirsEngAppPacket().....                                | 20 |
| 2.1.2.5   | ViirsHrdAppPacket() .....                               | 20 |
| 2.1.3     | Graceful Degradation.....                               | 20 |
| 2.1.3.1   | Graceful Degradation Inputs .....                       | 20 |
| 2.1.3.2   | Graceful Degradation Processing .....                   | 20 |
| 2.1.3.3   | Graceful Degradation Outputs .....                      | 20 |
| 2.1.4     | Exception Handling .....                                | 20 |
| 2.1.5     | Data Quality Monitoring .....                           | 20 |
| 2.1.6     | Computational Precision Requirements .....              | 21 |
| 2.1.7     | Algorithm Support Considerations .....                  | 21 |
| 2.1.8     | Assumptions and Limitations .....                       | 21 |
| 2.2       | VIIRS SDR Geolocation Description .....                 | 21 |
| 2.2.1     | Interfaces .....  | 22 |
| 2.2.1.1   | Inputs .....  | 22 |
| 2.2.1.2   | Outputs .....   | 28 |
| 2.2.1.2.1 | Geolocation Gridded Outputs.....                        | 36 |
| 2.2.2     | Algorithm Processing.....                               | 38 |
| 2.2.2.1   | Main driver for Geolocation ( geolocateGranule() )..... | 39 |
| 2.2.2.2   | GEO_absolute_limit_check() .....                        | 40 |

|          |   |    |
|----------|---|----|
| 2.2.2.3  | GEO_determine_DNB_sample_time_offsets() ..... | 41 |
| 2.2.2.4  | GEO_determine_sample_time_offsets().....      | 41 |
| 2.2.2.5  | GEO_determine_thermal_corrections() .....     | 41 |
| 2.2.2.6  | GEO_determine_view_vectors().....             | 41 |
| 2.2.2.7  | GEO_evaluate_polynomial().....                | 42 |
| 2.2.2.8  | GEO_find_next_flag() .....                    | 42 |
| 2.2.2.9  | GEO_get_grid().....                           | 42 |
| 2.2.2.10 | GEO_interp_mod_unagg().....                   | 43 |
| 2.2.2.11 | GEO_interpolate_mirror_encoder() .....        | 43 |
| 2.2.2.12 | GEO_interpolate_telescope_encoder().....      | 43 |
| 2.2.2.13 | GEO_process_parameters().....                 | 43 |
| 2.2.2.14 | GEO_relative_limit_check() .....              | 43 |
| 2.2.2.15 | GEO_validate_scan_encoder_data().....         | 43 |
| 2.2.2.16 | geolocatePixel() .....                        | 43 |
| 2.2.2.17 | geolocateDecim().....                         | 44 |
| 2.2.2.18 | geolocateFullFromDecim().....                 | 44 |
| 2.2.2.19 | calcModFromImg().....                         | 44 |
| 2.2.2.20 | createInterpRctngls() .....                   | 44 |
| 2.2.2.21 | initGeoDataStructs() .....                    | 44 |
| 2.2.2.22 | storeGranule().....                           | 44 |
| 2.2.2.23 | fixSatAngles().....                           | 44 |
| 2.2.2.24 | quadInterp() .....                            | 44 |
| 2.2.2.25 | geolocateAllRecPix().....                     | 45 |
| 2.2.2.26 | interpLocations() .....                       | 45 |
| 2.2.2.27 | interpAngles().....                           | 45 |
| 2.2.2.28 | Geolocation Quality Flag Logic .....          | 45 |
| 2.2.2.29 | Create Degree GEO Products .....              | 45 |
| 2.2.3    | Graceful Degradation.....                     | 45 |
| 2.2.3.1  | Graceful Degradation Inputs .....             | 46 |
| 2.2.3.2  | Graceful Degradation Processing .....         | 46 |
| 2.2.3.3  | Graceful Degradation Outputs .....            | 46 |
| 2.2.4    | Exception Handling .....                      | 46 |
| 2.2.5    | Data Quality Monitoring .....                 | 46 |
| 2.2.6    | Computational Precision Requirements .....    | 46 |
| 2.2.7    | Algorithm Support Considerations .....        | 47 |

|           |   |    |
|-----------|---|----|
| 2.2.8     | Assumptions and Limitations .....                       | 47 |
| 2.2.8.1   | Sci2Ops Issues .....                                    | 47 |
| 2.2.8.2   | Numerical Computation Considerations.....               | 47 |
| 2.2.8.3   | Additional Assumptions.....                             | 47 |
| 2.2.8.4   | Additional Limitations .....                            | 48 |
| 2.3       | VIIRS SDR Calibration Description .....                 | 48 |
| 2.3.1     | Interfaces .....  | 50 |
| 2.3.1.1   | Inputs .....  | 50 |
| 2.3.1.2   | Outputs .....   | 51 |
| 2.3.1.2.1 | Definitions of the Calibration VIIRS SDR Outputs.....   | 52 |
| 2.3.1.2.2 | VIIRS On-Board Calibrator Intermediate Product .....    | 56 |
| 2.3.2     | Algorithm Processing.....                               | 62 |
| 2.3.2.1   | Sub-frame Offset Compensation .....                     | 64 |
| 2.3.2.2   | Robust Algorithm Design .....                           | 64 |
| 2.3.2.3   | Earth View Radiometric Calibration Error Handling ..... | 64 |
| 2.3.2.4   | calibrateSDR() .....                                    | 64 |
| 2.3.2.5   | PreprocessRDR() and PreprocessDNB().....                | 64 |
| 2.3.2.6   | SDRSetup().....   | 65 |
| 2.3.2.7   | Combine_Reduced_Quality_Flags().....                    | 65 |
| 2.3.2.8   | Calibrate_Emissive_Bands().....                         | 65 |
| 2.3.2.9   | Find_SV_Scan_Index().....                               | 65 |
| 2.3.2.10  | Calibrate_Reflective_Bands() .....                      | 65 |
| 2.3.2.11  | Calibrate_DayNight_Bands() .....                        | 65 |
| 2.3.2.12  | Aggregate_750M_DG().....                                | 65 |
| 2.3.2.13  | viirs_decmp() .....                                     | 66 |
| 2.3.3     | Graceful Degradation.....                               | 66 |
| 2.3.3.1   | Graceful Degradation Inputs .....                       | 66 |
| 2.3.3.2   | Graceful Degradation Processing .....                   | 66 |
| 2.3.3.3   | Graceful Degradation Outputs .....                      | 66 |
| 2.3.4     | Exception Handling .....                                | 66 |
| 2.3.5     | Data Quality Monitoring .....                           | 66 |
| 2.3.6     | Computational Precision Requirements .....              | 67 |
| 2.3.7     | Algorithm Support Considerations .....                  | 67 |
| 2.3.8     | Assumptions and Limitations .....                       | 67 |
| 2.3.8.1   | I/O Timeliness .....                                    | 67 |

|           |   |    |
|-----------|---|----|
| 2.3.8.2   | Sci2Ops Issues .....                                      | 67 |
| 2.3.8.3   | Numerical Computation Considerations.....                 | 67 |
| 2.3.8.4   | Additional Assumptions.....                               | 67 |
| 2.3.8.5   | Additional Limitations .....                              | 68 |
| 2.4       | VIIRS SDR Solar Diffuser Description.....                 | 68 |
| 2.4.1     | Interfaces .....  | 68 |
| 2.4.1.1   | Inputs .....  | 68 |
| 2.4.1.2   | Outputs for Solar Diffuser View Data Processing Unit..... | 70 |
| 2.4.2     | Algorithm Processing.....                                 | 72 |
| 2.4.2.1   | Solar Diffuser View Data Processing Logic .....           | 72 |
| 2.4.2.2   | Calibration Symbols and Units .....                       | 73 |
| 2.4.2.3   | Reflective Calibration Core Equations .....               | 76 |
| 2.4.2.4   | Emissive Calibration Core Equations.....                  | 76 |
| 2.4.2.5   | Day Night Band Calibration Core Equations.....            | 77 |
| 2.4.2.6   | Solar Diffuser View Data Processing Core Equations .....  | 77 |
| 2.4.2.7   | Solar Diffuser SDSM.....                                  | 78 |
| 2.4.2.7.1 | SDSM Processing Logic.....                                | 78 |
| 2.4.3     | Graceful Degradation.....                                 | 80 |
| 2.4.3.1   | Graceful Degradation Inputs .....                         | 80 |
| 2.4.3.2   | Graceful Degradation Processing .....                     | 81 |
| 2.4.3.3   | Graceful Degradation Outputs .....                        | 81 |
| 2.4.4     | Exception Handling .....                                  | 81 |
| 2.4.5     | Data Quality Monitoring .....                             | 81 |
| 2.4.6     | Computational Precision Requirements .....                | 81 |
| 2.4.7     | Algorithm Support Considerations .....                    | 81 |
| 2.4.8     | Assumptions and Limitations .....                         | 81 |
| 2.5       | Viirs SDR Bright Pixel Description.....                   | 81 |
| 2.5.1     | Interfaces .....  | 81 |
| 2.5.1.1   | Inputs .....  | 81 |
| 2.5.1.2   | Outputs .....   | 82 |
| 2.5.2     | Algorithm Processing.....                                 | 83 |
| 2.5.2.1   | Estimating % Scattered Light.....                         | 83 |
| 2.5.2.2   | “Calculation Unreliable” Flag.....                        | 85 |
| 2.5.2.3   | Creation of Non-Saturated Scene.....                      | 85 |
| 2.5.2.4   | Common Adjacency Use In Bright Pixel .....                | 86 |

|         |  |    |
|---------|--|----|
| 2.5.2.5 | Data Convolution .....                     | 87 |
| 2.5.3   | Graceful Degradation.....                  | 87 |
| 2.5.3.1 | Graceful Degradation Inputs .....          | 87 |
| 2.5.3.2 | Graceful Degradation Processing .....      | 87 |
| 2.5.3.3 | Graceful Degradation Outputs .....         | 87 |
| 2.5.4   | Exception Handling .....                   | 88 |
| 2.5.5   | Data Quality Monitoring .....              | 88 |
| 2.5.6   | Computational Precision Requirements ..... | 88 |
| 2.5.7   | Algorithm Support Considerations .....     | 88 |
| 2.5.8   | Assumptions and Limitations .....          | 88 |
| 3.0     | GLOSSARY/ACRONYM LIST .....                | 89 |
| 3.1     | Glossary .....                             | 89 |
| 3.2     | Acronyms.....                              | 92 |
| 4.0     | OPEN ISSUES .....                          | 93 |

### List of Figures

|  |    |
|--|----|
| Figure 1 IPO Model Interface to INF and DMS (Calibration) .....                    | 8  |
| Figure 2 VIIRS Verified RDR Flow Diagram .....                                     | 9  |
| Figure 3 VIIRS Geolocation Flow Diagram .....                                      | 10 |
| Figure 4 VIIRS Calibration Flow Diagram .....                                      | 10 |
| Figure 5 Instrument Engineering Order and Product Order Illustration.....          | 12 |
| Figure 6 Create Verified VIIRS RDR Flow Diagram .....                              | 19 |
| Figure 7 Geolocation Processing Chain .....  | 22 |
| Figure 8 geolocateGranule() Flow Diagram.....                                      | 40 |
| Figure 9 GEO_determine_view_vectors() Block Diagram (Geolocation).....             | 42 |
| Figure 10 Calibration Processing Chain .....                                       | 49 |
| Figure 11 Radiometric Calibration Main Program Flow .....                          | 63 |
| Figure 12 Solar Diffuser View Data Processing Main Program Flow.....               | 73 |
| Figure 13 SDSM Processing Block Diagram .....                                      | 78 |
| Figure 14 Interpolation of Solar Position From Scan Fraction of Sample Times ..... | 80 |

**List of Tables**

|   |    |
|---|----|
| Table 1 Document References .....   | 1  |
| Table 2 Source Code References.....   | 4  |
| Table 3 Verified VIIRS RDR Engineering Packet Data Inputs .....                       | 13 |
| Table 4 Verified VIIRS RDR Science Packet Data Inputs .....                           | 16 |
| Table 5 Verified VIIRS RDR Calibration Packet Data Inputs .....                       | 17 |
| Table 6 VIIRS Geolocation Inputs.....   | 22 |
| Table 7 S/C Ephemeris and Attitude Data .....   | 23 |
| Table 8 Geolocation Parameter Inputs .....  | 23 |
| Table 9 DNB Geolocation Output Structure.....   | 29 |
| Table 10 MOD Geolocation Output Structure .....                                       | 31 |
| Table 11 Unaggregated MOD Geolocation Output Structure .....                          | 32 |
| Table 12 IMG Geolocation Output Structure.....  | 33 |
| Table 13 Scan Level Geolocation Quality Bytes.....                                    | 35 |
| Table 14 Pixel Level Geolocation Quality Byte .....                                   | 35 |
| Table 15 Map Data Set (mds_type) (Geolocation) .....                                  | 36 |
| Table 16 Gridded Geolocation Moderate Output (Geolocation) .....                      | 37 |
| Table 17 Gridded Geolocation Imagery Output (Geolocation).....                        | 38 |
| Table 18 Earth View Radiometric Calibration Unit Inputs .....                         | 50 |
| Table 19 Earth View Radiometric Calibration Parameter & LUT Inputs .....              | 50 |
| Table 20 Outputs from the Earth View Radiometric Calibration Unit (Calibration) ..... | 51 |
| Table 21 Imagery Resolution SDR .....   | 53 |
| Table 22 Moderate Resolution SDR .....  | 53 |
| Table 23 Day/Night Band SDR .....   | 54 |
| Table 24 Imagery Resolution Scaled SDR .....  | 54 |
| Table 25 Moderate Resolution Scaled SDR .....   | 55 |
| Table 26 Scan Quality Byte .....  | 55 |
| Table 27 Pixel Quality Byte.....  | 56 |
| Table 28 RDR Scan Quality Int.....  | 56 |
| Table 29 Reduced Quality Flag Byte .....  | 56 |
| Table 30 VIIRS SDR Header .....   | 56 |
| Table 31 OBC IP Output.....   | 57 |
| Table 32 VIIRS SDR Calibration Data Quality Monitoring .....                          | 66 |
| Table 33 Solar Diffuser View Data Processing Unit Inputs (Calibration) .....          | 69 |

|  |    |
|--|----|
| Table 34 SD View Data Processing Unit Calibration Parameter Input Files .....  | 69 |
| Table 35 Solar Diffuser: Table Output .....                                    | 71 |
| Table 36 Calibration Symbols and Units .....                                   | 73 |
| Table 37 Reflective Calibration Core Equations (Calibration).....              | 76 |
| Table 38 Emissive Calibration Core Equations (Calibration) .....               | 76 |
| Table 39 Day Night Band Calibration Core Equations (Calibration) .....         | 77 |
| Table 40 Solar Diffuser View Data Processing Core Equations (Calibration)..... | 77 |
| Table 41 Determining Good Data Set.....  | 79 |
| Table 42 VIIRS Bright Pixel Algorithm Inputs .....                             | 82 |
| Table 43 VIIRS Bright Pixel Output Files .....                                 | 82 |
| Table 44 Glossary .....  | 89 |
| Table 45 Acronyms .....  | 92 |
| Table 46 List of TBD/TBR .....   | 93 |

## 1.0 INTRODUCTION

### 1.1 Objective

The purpose of the Operational Algorithm Description (OAD) document is to express, in computer-science terms, the remote sensing algorithms that produce the National Polar-Orbiting Operational Environmental Satellite System (NPOESS) end-user data products. These products are individually known as Raw Data Records (RDRs), Temperature Data Records (TDRs), Sensor Data Records (SDRs) and Environmental Data Records (EDRs). In addition, any Intermediate Products (IPs) produced in the process are also described in the OAD.

The science basis of an algorithm is described in a corresponding Algorithm Theoretical Basis Document (ATBD). The OAD provides a software description of that science as implemented in the operational ground system -- the Data Processing Element (DPE).

The purpose of an OAD is two-fold:

1. Provide initial implementation design guidance to the operational software developer.
2. Capture the "as-built" operational implementation of the algorithm reflecting any changes needed to meet operational performance/design requirements.

An individual OAD document describes one or more algorithms used in the production of one or more data products. There is a general, but not strict, one-to-one correspondence between OAD and ATBD documents.

### 1.2 Scope

The scope of this document is limited to the description of the core operational algorithm(s) required to create the GEO, CAL, Solar Diffuser, and Bright Pixel products for the VIIRS SDR. It provides a general overview and is intended to supplement in-line software documentation and interface control documentation for maintenance of the operational software. The theoretical basis for these algorithms is described Section 3.3 of the ATBD documents, VIIRS Geolocation Algorithm Theoretical Basis Document (ATBD), 474-00053 and VIIRS Radiometric Calibration Algorithm Theoretical Basis Document ATBD, 474-00027.

### 1.3 References

#### 1.3.3 Document References

The science and system engineering documents relevant to the algorithms described in this OAD are listed in Table 1.

**Table 1 Document References**

| Document Title  | Document Number/Revision | Revision Date |
|---|--------------------------|---------------|
| VIIRS Geolocation Unit Software Architecture                  | Y2479a Ver. 5 Rev. 5     | 31 Aug 2004   |
| VIIRS Geolocation Unit Detailed Interface Control Document    | Y3243 Ver. 5 Rev. 3      | 31 Aug 2004   |
| VIIRS Geolocation Unit Detailed Data Dictionary               | Y3248 Ver. 5 Rev. 3      | 31 Aug 2004   |
| VIIRS Geolocation Unit Detailed Design                        | Y3245 Ver. 5 Rev. 4      | 31 Aug 2004   |
| VIIRS Geolocation Algorithm Theoretical Basis Document (ATBD) | 474-00053                | 22 Apr 2011   |

| Document Title  | Document Number/Revision | Revision Date |
|---|--------------------------|---------------|
| JPSS Environmental Data Record (EDR) Production Report for NPP  | 474-00012 Rev. A         | 09 Feb 2011   |
| JPSS Environmental Data Record (EDR) Interdependency Report (IR) for NPP                                      | 474-0007 Rev. A          | 09 Feb 2011   |
| JPSS Internal Data Format Control Book<br>Volume III – Retained Intermediate Product Formats (IDFCB)          | 474-00020-03, Rev -      | 18 Feb 2011   |
| NPP Mission Data Format Control Book and App A (MDFCB)  | 472-REF-00057, Rev B     | 06 Jan 2011   |
| JPSS Common Data Format Control Book - External - Volume I - Overview   | 474-00001-01, Rev-       | 10-Dec-10     |
| JPSS Common Data Format Control Book - External - Volume II - RDR Formats                                     | 474-00001-02, Rev-       | 10-Dec-10     |
| JPSS Common Data Format Control Book - External - Volume III - SDR/TDR Formats                                | 474-00001-03, Rev-       | 16-Feb-11     |
| JPSS Common Data Format Control Book - External - Volume IV - Part I - IPs, ARPs, and Geolocation Data        | 474-00001-04-01, Rev-    | 10-Dec-10     |
| JPSS CDFCB - External - Volume IV - Part II - Imagery, Atmospheric, and Cloud EDRs                            | 474-00001-04-02, Rev-    | 10-Dec-10     |
| JPSS Common Data Format Control Book - External - Volume IV - Part III - Land and Ocean/Water EDRs            | 474-00001-04-03, Rev-    | 10-Dec-10     |
| JPSS Common Data Format Control Book - External - Volume IV - Part IV - Earth Radiation Budget and Space EDRs | 474-00001-04-04, Rev-    | 18-Feb-11     |
| JPSS Common Data Format Control Book - External - Volume V - Metadata   | 474-00001-05, Rev-       | 16-Feb-11     |
| JPSS CDFCB - External - Volume VI - Ancillary Data, Auxiliary Data, Messages, and Reports                     | 474-00001-06, Rev-       | 10-Dec-10     |
| JPSS Common Data Format Control Book - External - Volume VII - Part I - JPSS Downlink Data Formats            | 474-00001-07-01, Rev-    | 16-Feb-11     |
| JPSS CDFCB - External - Volume VII - Part 2 - JPSS Downlink Data Formats - CrIS                               | 474-00001-07-02, Rev-    | 16-Feb-11     |
| JPSS CDFCB - External - Volume VII - Part 3 - JPSS Downlink Data Formats - OMPS                               | 474-00001-07-03, Rev-    | 16-Feb-11     |
| JPSS CDFCB - External - Volume VII - Part 4 - JPSS Downlink Data Formats - ATMS                               | 474-00001-07-04, Rev-    | 16-Feb-11     |
| JPSS CDFCB - External - Volume VII - Part 5 - JPSS Downlink Data Formats - VIIRS                              | 474-00001-07-05, Rev-    | 16-Feb-11     |
| JPSS Common Data Format Control Book - External - Volume VIII - Look Up Table Formats                         | 474-00001-08, Rev-       | 10-Dec-10     |
| NPP Command and Telemetry (C&T) Handbook  | D568423 Rev. C           | 30 Sep 2008   |
| JPSS CGS Data Processor Inter-subsystem Interface Control Document (DPIS ICD) Vol I – IV                      | IC60917-IDP-002, Rev C   | 29-Sep-11     |
| Operational Algorithm Description Document for Common Geolocation   | 474-00091, Rev A         | 27 Jan 2012   |
| VIIRS Radiometric Calibration Component Software Architecture   | Y2479b Ver. 5 Rev. 5     | 30 Sep 2004   |
| VIIRS Radiometric Calibration Component Interface Control Document  | Y3242 Ver. 5 Rev. 2      | 11 Aug 2004   |
| VIIRS Radiometric Calibration Component Data Dictionary   | Y3273 Ver. 5 Rev. 3      | 11 Aug 2004   |
| VIIRS Radiometric Calibration Unit Level Detailed Design  | Y2490 Ver. 5 Rev. 4      | 30 Sep 2004   |
| VIIRS Radiometric Calibration Algorithm Theoretical Basis Document ATBD                                       | 474-00027                | 22 Apr 2011   |
| VIIRS Radiometric Calibration Equations   | D36966 Rev. 1            | 2 Aug 2004    |
| JPSS CGS Acronyms and Glossary  | LI60917-GND-005, Rev -   | 17-Oct-11     |

| Document Title  | Document Number/Revision      | Revision Date |
|---|-------------------------------|---------------|
| NGST/SE technical memo –<br>VIIRS_CAL_SD_Detailed_Code_Changes_Oct_2005   | NP-EMD.2005.510.0122 Rev. --- | 12 Oct 2005   |
| NGST/SE technical memo –<br>VIIRS_SDR_Cal_Modif_Implement_OAD   | NP-EMD-2007.510.0014 Rev. --- | 14 Feb 2007   |
| NGST/SE technical memo –<br>VIIRS_SDR_Even_odd_subframe_design  | NP-EMD-2007.510.0009 Rev. --- | 14 Feb 2007   |
| NGST/SE technical memo – VIIRS_SDR_Robust_Alg_design  | NP-EMD-2007.510.0010 Rev. --- | 14 Feb 2007   |
| NGST/SE technical memo –<br>NPP_VIIRS_CAL_EV_Detailed_Code_Changes_Feb_2007   | NP-EMD-2007.510.0012 Rev. --- | 14 Feb 2007   |
| NGST/SE technical memo –<br>NPP_VIIRS_SDR_DNB_FirstFrameAnomaly   | NP-EMD-2007.510.0029 Rev. --- | 23 Apr 2007   |
| NGST/SE technical memo – viirsLUTconfigMethod   | NP-EMD.2005.510.0134 Rev. --- | 12 Oct 2005   |
| NGST/SE technical memo – RevA_viirsCAL_sdIO_description   | NP-EMD.2005.510.0119 Rev. A   | 11 June 2007  |
| NGST/SE technical memo – EM061405_viirsCAL_moon_in_SV   | NP-EMD.2005.510.0065 Rev. --- | 14 Dec 2005   |
| NGST/SE technical memo –<br>EM052405_viirsRDR_HDF_description   | NP-EMD.2005.510.0067 Rev. --- | 24 May 2005   |
| NGST/SE technical memo –<br>EM061005_viirsCAL_evIO_description  | NP-EMD.2005.510.0069 Rev. --- | 6 Oct 2005    |
| NGST/SE technical memo –<br>EM061005_viirsCAL_sdIO_description  | NP-EMD.2005.510.0071 Rev. --- | 6 Oct 2005    |
| NGST/SE technical memo –<br>EM060305VIIRS_CAL_EV_Detailed_Code_Changes  | NP-EMD.2005.510.0074 Rev. --- | 2 June 2005   |
| NGST/SE technical memo – VIIRS_CAL_testProc   | NP-EMD.2005.510.0081 Rev. --- | 25 July 2005  |
| NGST/SE technical memo – cal_Sdcode_change_Description  | NP-EMD.2005.510.0064 Rev. --- | 3 June 2005   |
| NGST/SE technical memo –<br>EM060305VIIRS_CAL_SD_Detailed_Code_Changes  | NP-EMD.2005.510.0075 Rev. --- | 3 June 2005   |
| NGST/SE technical memo – EM050106Parameters-M   | NP-EMD.2005.510.0004 Rev. --- | 6 Jan 2005    |
| NGST/SE technical memo – VIIRS_GEO_OADtables_memo   | NP-EMD.2005.510.0012 Rev. --- | 17 Jan 2005   |
| NGST/SE technical memo –<br>VIIRS_CAL_Sdcode_changes_011905   | NA                            | 19 Jan 2005   |
| NGST/SE technical memo –<br>EM060605_viirsGEO_IP_description  | NP-EMD.2005.510.0068 Rev. --- | 6 June 2005   |
| NGST/SE technical memo –<br>EM101005_geo_OADupdates_Rev_A   | NP-EMD.2005.510.0125 Rev. A   | 30 Nov 2005   |
| NGST/SE technical memo –<br>NPP_Geo_AtmosphericCorrectionSZAcac   | NP-EMD.2006.510.0098 Rev. --- | 15 Dec 2006   |
| NGST/SE technical memo –<br>Rev.A_VIIRS_SDR_BrightPixel_ID_design_Rev_A   | NP-EMD-2007.510.0011 Rev. A   | 11 May 2007   |
| NGST/SE technical memo –<br>VIIRS_SDR_BrightPixel_ID_Implement_OAD  | NP-EMD-2007.510.0013 Rev. --- | 14 Feb 2007   |
| NGST/SE technical memo – VIIRS_GEO_BugFixes   | NP-EMD.2008.510.0044 Rev. --- | 3 July 2008   |
| NGST/SE technical memo – VIIRS_GEO_OAD_Updates  | NP-EMD.2008.510.0027 Rev. A   | 19 Aug 2008   |
| NGST/SE technical memo – SDSM_OAD_Update  | NP-EMD-2008.510.0019 Rev. --- | 20 Mar 2008   |
| NGAS/A&DP technical memo – SDSM_OAD_Update  | NP-EMD-2009.510.0006          | 21 Jan 2009   |
| NGST/SE technical memo –VIIRS GEO EvtimesUpdates  | NP-EMD-2008.510.0050          | 29 Oct 2008   |
| NGAS/SE technical memo –<br>Direction for Setting the VIIRS Pixel Level SDR Quality flag for<br>VIIRS SDR Calibration | NP-EMD.2009.510.0038          | 24 Jun 2009   |
| NGAS/SE technical memo –<br>VIIRS Geo Quality Flags Logic Updates   | NP-EMD.2009.510.0048 Rev A    | 12 Oct 2009   |

| Document Title   | Document Number/Revision   | Revision Date   |
|--|--|---|
| NGAS/SE technical memo –<br>VIIRS SDR OAD Updates to the Geolocation Parameters Table  | NP-EMD.2009.510.0033 Rev A   | 12 Oct 2009   |
| NGAS/SE technical memo –<br>Solar Diffuser LUT Read Update   | NP-EMD.2009.510.0031 Rev A   | 03 Dec 2009   |
| NGAS/SE technical memo –<br>Solar Diffuser Cal SDSM Angle Fix  | NP-EMD.2009.510.0042   | 23 Jul 2009   |
| NGAS/SE technical memo –<br>Solar Diffuser Cal SDSM Angle Fix  | NP-EMD.2009.510.0047   | 15 Sep 2009   |
| VIIRS Bright Pixel ID Algorithm Update   | NP-EMD-2009.510.0052   | 09 Oct 2009   |
| NGAS/SE technical memo –<br>SDR/SDCal RVS Update   | NP-EMD-2010.510.0003   | 10 Feb 2010   |
| NGAS/SE technical memo –<br>VIIRS SDR Cal Thermistor Update  | NP-EMD-2010.510.0007 revA  | 22 Mar 2010   |
| NGAS/SE technical memo –<br>VIIRS SDR OBC Cal Update   | NP-EMD-2010.510.0008   | 24 Feb 2010   |
| NGAS/SE technical memo –<br>VIIRS SDR Cal RSR Update   | NP-EMD-2010.510.0011   | 26 Feb 2010   |
| NGAS/SE technical memo –<br>VIIRS SDR Cal DNB Stray Light QF   | NP-EMD-2010.510.0012   | 05 Mar 2010   |
| NGAS/SE technical memo –<br>VIIRS SDR Cal DG Anomaly QF  | NP-EMD-2010.510.0013   | 12 Mar 2010   |
| NGAS/SE technical memo –<br>VIIRS Solar Diffuser LUT Update  | NP-EMD-2010.510.0016   | 05 Mar 2010   |
| NGAS/SE technical memo –<br>VIIRS SDR Cal EMI Spike Filter   | NP-EMD-2010.510.0021   | 16 Mar 2010   |
| NGAS/SE technical memo –<br>VIIRS_SDR_SD_Calibration_Off_During_Manuever   | NP-EMD-2010.510.0004   | 11 Feb 2010   |
| NGST/SE technical memos:<br>LUT_OAD_Drop_History_Corrections<br>LUT_Format_Corrections<br>PC_OAD_Last_Drop_Corrections<br>PC_Format_Corrections<br>SAD_Formatand Usage_Corrections | NPOESS GJM-2010.510.0011<br>NPOESS GJM-2010.510.0012<br>NPOESS GJM-2010.510.0013<br>NPOESS GJM-2010.510.0014<br>NPOESS GJM-2010.510.0016 | 21 Sep 2010<br>21 Sep 2010<br>22 Sep 2010<br>22 Sep 2010<br>22 Sep 2010 |
| NGST/SE technical memo –<br>VIIRS_SDR-GEO_CODE_LUT_Update_Dec_2010   | NP-EMD.2010.510.0094   | 1 Dec 2010  |
| NGST/SE technical memo –<br>VIIRS_inst2sc.pdf  | NP-EMD.2011.510.0003   | 21 Feb 2011   |
| Joint Polar Satellite System (JPSS) Common Ground System<br>(CGS) IDPS PRO Software User's Manual Part 2   | UG60917-IDP-026 Rev -  | 18 Jul 2011   |

### 1.3.3 Source Code References

The science and operational code and associated documentation relevant to the algorithms described in this OAD are listed in Table 2.

**Table 2 Source Code References**

| Reference Title   | Reference Tag/Revision         | Revision Date |
|---|--------------------------------|---------------|
| VIIRS SDR --- Science-grade Software                        | ISTN_VIIRS_NGST_2.9            | 30 Sep 2004   |
| NGST/SE technical memo – EM050106Parameters-M               | NP-EMD.2005.510.0004 Rev. ---  | 6 Jan 2005    |
| VIIRS SDR --- Operational-grade Software                    | Build 1.3 (OAD D39553 Rev ---) | 30 Sep 2004   |
| NGST/SE technical memo –<br>VIIRS_CAL_Sdcode_changes_011905 | NA [Build 1.3]                 | 19 Jan 2005   |

| Reference Title  | Reference Tag/Revision                    | Revision Date |
|--|---|---------------|
| VIIRS SDR --- Science-grade Software                                     | ISTN_VIIRS_NGST_2.9.1                     | 27 Jul 2005   |
| NGST/SE technical memo – EM052405_viirsRDR_HDF_description               | NP-EMD.2005.510.0067 Rev. --- [Build 1.3] | 24 May 2005   |
| NGST/SE technical memo – EM061405_viirsCAL_moon_in_SV                    | NP-EMD.2005.510.0065 Rev. --- [Build 1.3] | 14 Dec 2005   |
| NGST/SE technical memo – EM061005_viirsCAL_evIO_description              | NP-EMD.2005.510.0069 Rev. --- [Build 1.3] | 6 Oct 2005    |
| NGST/SE technical memo – EM061005_viirsCAL_sdIO_description              | NP-EMD.2005.510.0071 Rev. --- [Build 1.3] | 6 Oct 2005    |
| NGST/SE technical memo – cal_Sdcode_change_Description                   | NP-EMD.2005.510.0064 Rev. --- [Build 1.3] | 3 June 2005   |
| NGST/SE technical memo – EM060305VIIRS_CAL_SD_Detailed_Code_Changes      | NP-EMD.2005.510.0075 Rev. --- [Build 1.3] | 3 June 2005   |
| NGST/SE technical memo – EM060605_viirsGEO_IP_description                | NP-EMD.2005.510.0068 Rev. --- [Build 1.3] | 6 June 2005   |
| NGST/SE technical memo – VIIRS_CAL_testProc                              | NP-EMD.2005.510.0081 Rev. --- [Build 1.3] | 25 July 2005  |
| NGST/SE technical memo – VIIRS_CAL_SD_Detailed_Code_Changes_Oct_2005     | NP-EMD.2005.510.0122 Rev. --- [Build 1.3] | 12 Oct 2005   |
| NGST/SE technical memo – EM060305VIIRS_CAL_EV_Detailed_Code_Changes      | NP-EMD.2005.510.0074 Rev. --- [Build 1.3] | 2 June 2005   |
| VIIRS SDR --- Operational-grade Software                                 | Build 1.4 (follow-on)                     | 27 Jul 2005   |
| VIIRS SDR --- Science-grade Software (GEO)                               | ISTN_VIIRS_NGST_2.7.2 (ECR-A080C)         | 01 Dec 2005   |
| VIIRS SDR --- Science-grade Software                                     | ISTN_VIIRS_NGST_2.9.2                     | 06 Dec 2005   |
| NGST/SE technical memo – viirsLUTconfigMethod                            | NP-EMD.2005.510.0134 Rev. --- [Build 1.4] | 12 Oct 2005   |
| NGST/SE technical memo –viirsCAL_sdIO_description                        | NP-EMD.2005.510.0119 [Build 1.4]          | 12 Oct 2005   |
| VIIRS SDR --- Science-grade Software                                     | ISTN_VIIRS_NGST_2.9.3                     | 06 Apr 2006   |
| VIIRS SDR --- Operational-grade Software                                 | Build 1.4 (follow-on)                     | 06 Apr 2006   |
| Combined CAL and GEO OADs (D39300) into D41868                           | Build 1.4 (D41868 Rev A1)                 | 08 Jun 2006   |
| NGST/SE technical memo – NPP_Geo_AtmosphericCorrectionSZacalc            | NP-EMD.2006.510.0098 Rev. --- [Build 1.4] | 15 Dec 2006   |
| VIIRS SDR --- Operational-grade Software                                 | Build 1.5 (OAD Revs A3-A8)                | 1 Jan 2007    |
| NGST/SE technical memo – VIIRS_SDR_Even_odd_subframe_design              | NP-EMD.2007.510.0009 Rev. --- [Build 1.5] | 14 Feb 2007   |
| NGST/SE technical memo – VIIRS_SDR_Robust_Alg_design                     | NP-EMD.2007.510.0010 Rev. --- [Build 1.5] | 14 Feb 2007   |
| NGST/SE technical memo – Rev.A_VIIRS_SDR_BrightPixel_ID_design_Rev_A     | NP-EMD.2007.510.0011 Rev. A [Build 1.5]   | 11 May 2007   |
| NGST/SE technical memo – NPP_VIIRS_CAL_EV_Detailed_Code_Changes_Feb_2007 | NP-EMD.2007.510.0012 Rev. --- [Build 1.5] | 14 Feb 2007   |
| NGST/SE technical memo – VIIRS_SDR_BrightPixel_ID_Implement_OAD          | NP-EMD.2007.510.0013 Rev. --- [Build 1.5] | 14 Feb 2007   |
| NGST/SE technical memo – VIIRS_SDR_Cal_Modif_Implement_OAD               | NP-EMD.2007.510.0014 Rev. --- [Build 1.5] | 14 Feb 2007   |
| NGST/SE technical memo – NPP_VIIRS_SDR_DNB_FirstFrameAnomaly             | NP-EMD.2007.510.0029 Rev. --- [Build 1.5] | 23 Apr 2007   |

| Reference Title   | Reference Tag/Revision  | Revision Date |
|---|---|---------------|
| NGST/SE technical memo –<br>RevA_viirsCAL_sdIO_description  | NP-EMD.2005.510.0119 Rev. A<br>[Build 1.5]  | 11 June 2007  |
| VIIRS SDR --- Science-grade Software  | ISTN_VIIRS_NGST_2.9.4   | 13 Aug 2007   |
| VIIRS SDR operational software  | B1.5.x.1 (OAD Revs A9-A16)  | 1 Oct 2007    |
| NGST/SE technical memo – SDSM_OAD_Update  | NP-EMD-2008.510.0019 Rev. ---<br>[Build 1.5.x.1]  | 20 Mar 2008   |
| VIIRS SDR --- Science-grade Software  | ISTN_VIIRS_NGST_2.9.5   | 14 May 2008   |
| VIIRS Geolocation – Science-grade Software  | ISTN_VIIRS_NGST_4.10 (ECR-<br>A157)   | 18 Jun 2008   |
| NGST/SE technical memo – VIIRS_GEO_BugFixes   | NP-EMD.2008.510.0044 Rev. ---<br>[Build 1.5.x.1]  | 3 Jul 2008    |
| VIIRS SDR --- Science-grade Software (Model 'E' LUT<br>update)  | ISTN_VIIRS_NGST_2.9.7   | 08 Aug 2008   |
| VIIRS_SDR_DNB_Calibration_Saturation_Value_Bug_Fix<br>(PCR019689)   | NP-EMD.2009.510.0006- [Build Post-<br>X-C] (No update to OAD required)                    | 31 Mar 2009   |
| PCR019290   | Build Post-X-E (OAD Rev-A17)  | 23 Apr 2009   |
| VIIRS SDR --- Science-grade Software  | ISTN_VIIRS_NGST_2.9.8   | 25 Jul 2009   |
| NGAS/SE technical memo –<br>Direction for Setting the VIIRS Pixel Level SDR Quality flag<br>for VIIRS SDR Calibration (PCR20858)  | NP-EMD.2009.510.0038--Build 1.5<br>Sensor Characterization Build SC 3<br>(No OAD updates) | 01 Sep 2009   |
| VIIRS SDR --- Science-grade Software (Calibration)  | ISTN_VIIRS_NGST_4.18  | 11 Nov 2009   |
| VIIRS SDR --- Science-grade Software (Geo)  | ISTN_VIIRS_NGST_4.19  | 11 Nov 2009   |
| VIIRS SDR operational software<br>Includes Tech Memos (not listed in Table 1):<br>NP-EMD.2009.510.0071_VIIRS_SDR_Cal_14bit_<br>Conversion (PCR22051)<br>NP-EMD-2009.510.0041_SDR_Cal_Imagery_Even_<br>Odd_Parity_Fix (PCR21468)<br>NP-EMD-2009.510.0044_VIIRS_Calibration_3rd_Order_<br>Coefficient_Fix (PCR21467)<br>NP-EMD.2009.510.0028_RevB_VIIRS_GEO_<br>MissingEncoderRobustness (PCR20616)       | Build 1.5 Sensor Characterization<br>Build SC 6 (OAD Rev A21)                             | 20 Jan 2010   |
| VIIRS SDR Bright Pixel<br>Identification science algorithm drop 4.21  | ISTN_VIIRS_NGST_4.21 (ECR A-<br>259B)   | 14 Dec 2009   |
| NP-EMD-2009.510.0052 VIIRS Bright Pixel ID Algorithm<br>Update (PCR021472)  | Build 1.5 Sensor Characterization<br>Build SC 8 (OAD Rev A22)                             | 25 Feb 2010   |
| VIIRS SDR --- Science-grade Software (Geo)  | ISTN_VIIRS_NGST_4.19.1 (ECR-<br>A280A)  | 07 Apr 2010   |
| VIIRS SDR --- Science-grade Software (Calibration)<br>includes:<br>NP-EMD-2010.510.0003 – SDR/SDCal RVS Update<br>NP-EMD-2010.510.0007 revA – VIIRS SDR Cal<br>Thermistor Update<br>NP-EMD-2010.510.0008 – VIIRS SDR OBC Cal Update<br>NP-EMD-2010.510.0011 – VIIRS SDR Cal RSR Update<br>NP-EMD-2010.510.0012 – VIIRS SDR Cal DNB Stray<br>Light QF<br>NP-EMD-2010.510.0013 – VIIRS SDR Cal DG Anomaly | ISTN_VIIRS_NGST_4.23  | 09 Apr 2010   |

| Reference Title   | Reference Tag/Revision  | Revision Date                            |
|---|---|--|
| QF<br>NP-EMD-2010.510.0016 – VIIRS Solar Diffuser LUT Update<br>NP-EMD-2010.510.0021 – VIIRS SDR Cal EMI Spike Filter             |   |  |
| VIIRS SDR operational software  | Build 1.5 Sensor Characterization<br>Build SC 11 (OAD Rev A23)              | 16 Jun 2010                              |
| SDRL  | (OAD Rev A25)   | 08 Jul 2010                              |
| PCRs 19655, 22912, 22913 (TM 2010.510.0004)   | Build 1.5 Sensor Characterization<br>Build SC 13 (OAD Rev A26)              | 17 Aug 2010                              |
| ACCB  | OAD Rev A   | 22 Sep 2010                              |
| VIIRS SDR Algorithm Development Library   | Mx1.5.4.00 (OAD Rev B1)   | 29 Sep 2010                              |
| Convergence Update (No code updates)  | Mx1.5.4.00 (OAD Rev B2)   | 12 Oct 2010                              |
| PCR025126 Revert OBCIP to UIIn16s   | Mx1.5.5_A (OAD Rev B3)  | 29 Oct 2010                              |
| VIIRS SDR --- Science-grade Software (Calibration)<br>includes:<br>VIIRS_SDR-GEO_CODE_LUT_Update_Dec_2010 (PCRs 025836 & 026160)  | ISTN_VIIRS_NGST_4.19.2,<br>ISTN_VIIRS_NGST_4.23.1<br>Mx1.5.5_A (OAD Rev B4) | 1 Dec 2010<br>& 29 Jun 2011<br>(OAD)     |
| VIIRS SDR --- Science-grade Software (Calibration)<br>includes:<br>NP-EMD.2011.510.0003_VIIRS_inst2sc.pdf4<br>PCRs026129 & 026130 | ISTN_VIIRS_NGST_4.19.3,<br>Mx1.5.5_E (OAD Rev B5)                           | 08 Mar 2011<br>&<br>29 Jun 2011<br>(OAD) |
| PCR026634 (OAD update for ADL)  | (OAD Rev B6)  | 28 Sep 2011                              |
| PCR027965 (& undo of PCR025126) and PCR027896   | (OAD Rev B7)  | 04 Nov 2011                              |

## 2.0 ALGORITHM OVERVIEW

To begin data processing, the VIIRS SDR algorithms (Verified RDR, Geolocation and Calibration) are initiated or retasked by the Infrastructure (INF) Subsystem Software Item (SI). The INF SI provides tasking information to the VIIRS SDR algorithms indicating which granule number and version to process. The Data Management Subsystem (DMS) SI provides data storage and retrieval capability. A library of C++ classes is used to implement the SI interfaces (for more information refer to document UG60917-IDP-026 particularly sections regarding PRO Common processing and the IPO Model). The VIIRS SDR algorithms are identified as a persistent retaskable process. When it completes processing for a specified granule, instead of shutting down, the algorithm requests new tasking data in order to process another granule. Figure 1 shows the IPO (Input, Processing, Output) model interface to INF and DMS for calibration only but the Verified RDR and Geolocation algorithms follow the same IPO model.

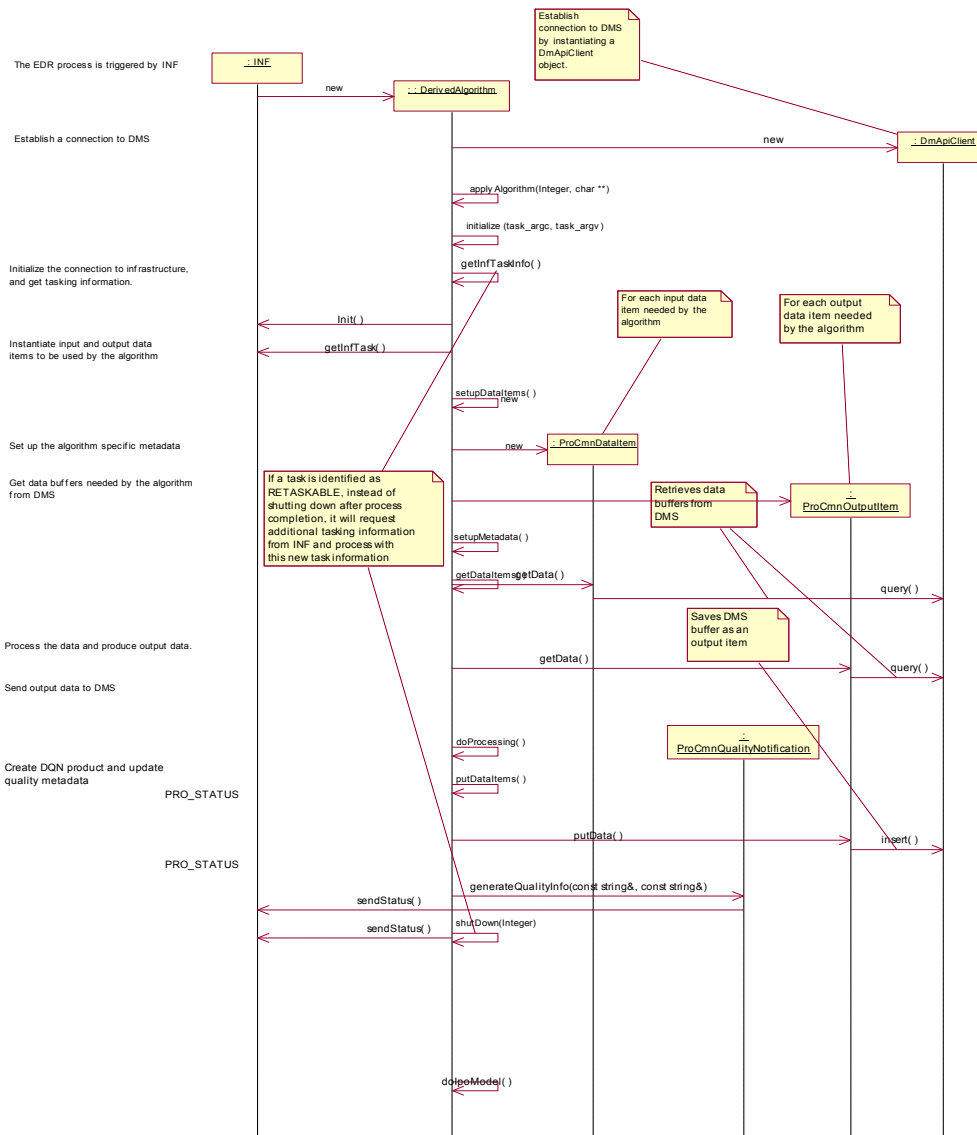


Figure 1 IPO Model Interface to INF and DMS (Calibration)

When the VIIRS SDR algorithms are called, they first initialize values such as routine name and software version number, then call `setupDataItems()` to create data items handlers for retrieving input data from, and storing output data to, DMS. Next, `doPtrAssignmentToInputAndOutput()` assigns pointers to input and output data items. The Verified RDR algorithm, `ProSdrViirsVerifiedRDR`, produces the Verified RDR. The geolocation algorithm, `ProSdrViirsGeo` controls the execution and processing of the geolocation outputs.

In the `ProSdrViirsGeo` algorithm, consecutive calls are made to the GEO method, `geolocateGranule`, with appropriate resolution parameter structures to produce GEO products in the following order (first to last): imagery (non-terrain corrected and terrain corrected items); moderate (non-terrain corrected and terrain corrected items); moderate unaggregated; DNB.

The `ProSdrViirsCal` algorithm calls the Radiometric Calibration routine to produce TOA radiances, reflectances (reflective bands only), and brightness temperatures (emissive bands only) for each pixel in the imagery bands, moderate bands, and day/night band .

Finally, outputs are checked for data quality, and select outputs are scaled before all output data items are written to DMS. A flow diagram of the VIIRS SDR algorithms is provided in Figure 2, Figure 3 and Figure 4 for clarification.

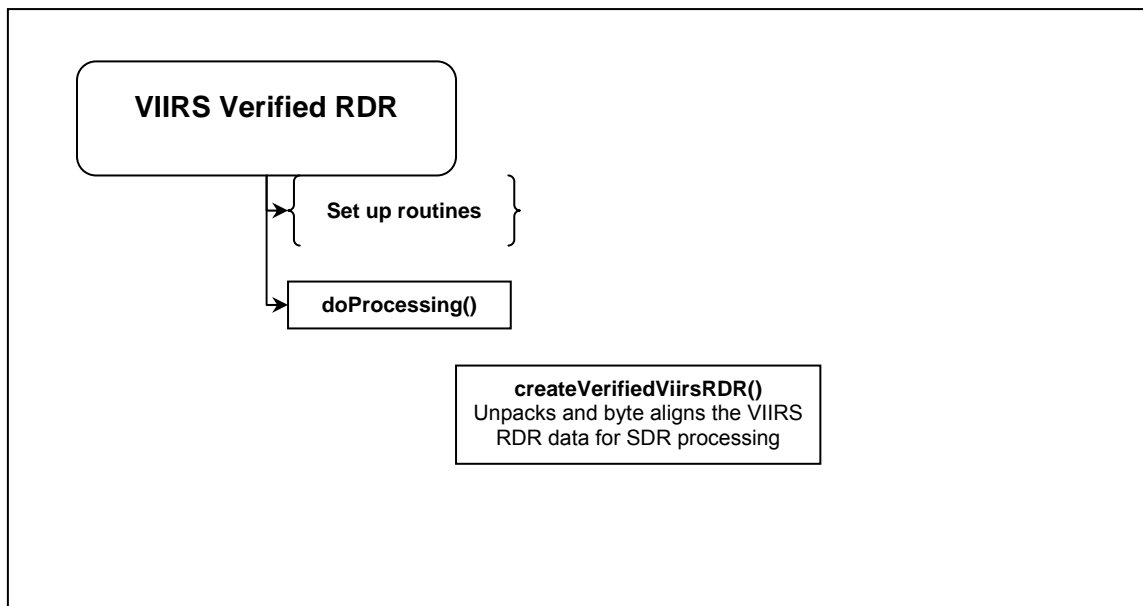


**Figure 2 VIIRS Verified RDR Flow Diagram**

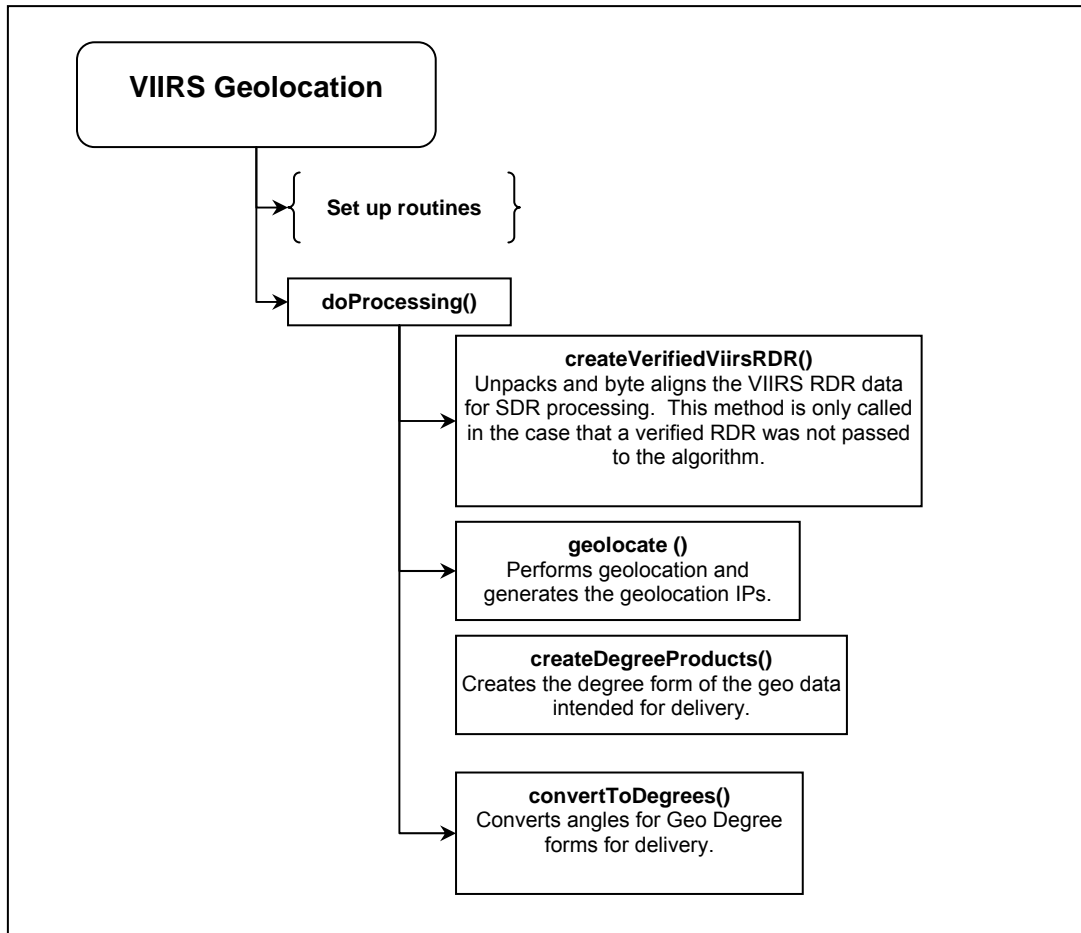


Figure 3 VIIRS Geolocation Flow Diagram

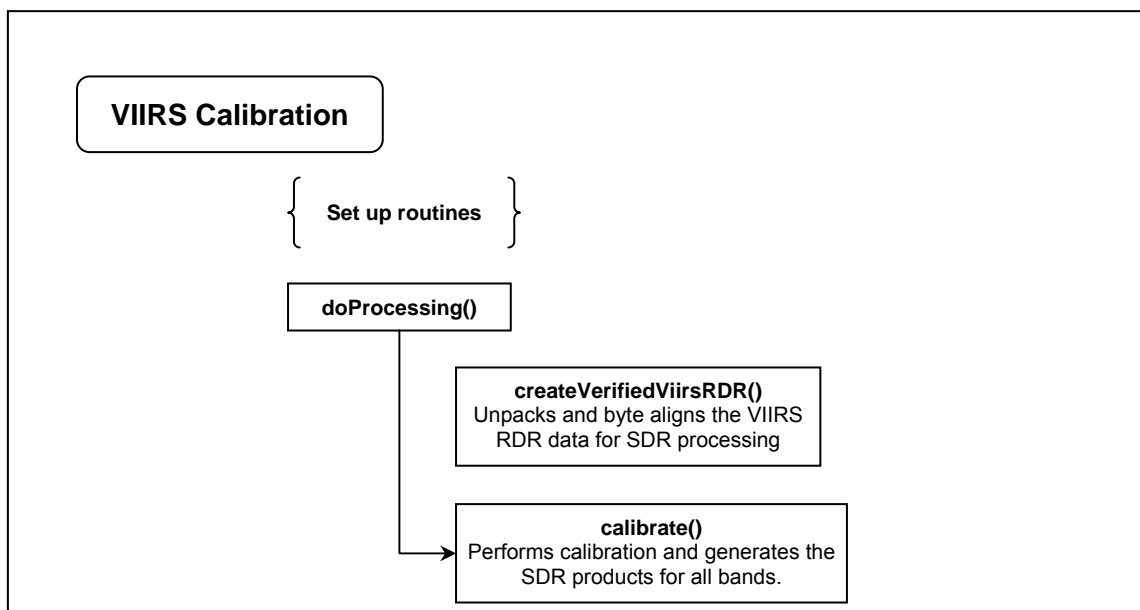


Figure 4 VIIRS Calibration Flow Diagram

## 2.1 VIIRS SDR Verified RDR Description

Before the geolocation or calibration components can be run the RDR packets must be assembled into what is called the Verified RDR. The RDR packets must first be decompressed. There are four stages of decompression. All stages are lossless. The stages in order of application on the compression side for the earth-view (EV) data are:

- Removal of unused bits
- Piecewise linear offset for dual-gain bands only
- Differential Encoding using a predictor band
- Universal Source Encoder for Space (USES), an industry standard for lossless encoding.

The decompression reverses the compression steps and is therefore applied in the reverse of the order listed above. The decompressed EV packets are then assembled into matrices in the order needed by the calibration algorithm. The calibration views must also be assembled into matrices called granules. The granules have  $n$  full scans (either  $n_{scan}=47$  or  $48$  in the current configuration). The scans are assembled from first to last in time, with increasing scan line indices corresponding to later times. This is referred to as the in-track index. The detector focal plane arrays (FPA) are positioned so that detector 1 is at the leading edge of the FPA in the track direction. Unfortunately, this is the opposite of what is needed to produce the verified RDR with the scan lines increasing in the in-track direction. Therefore, the order of the detectors must be reversed in creating granules from packets. The numbering of the detectors on the FPA is referred to as Instrument Engineering Order (IEO). The reversed ordering that is used in the verified RDR (as well as the SDR and EDR) is referred to as Product Order (PO). All look-up tables that have per detector values should be in Product Order. Figure 5 provides an illustration of the different detector ordering.

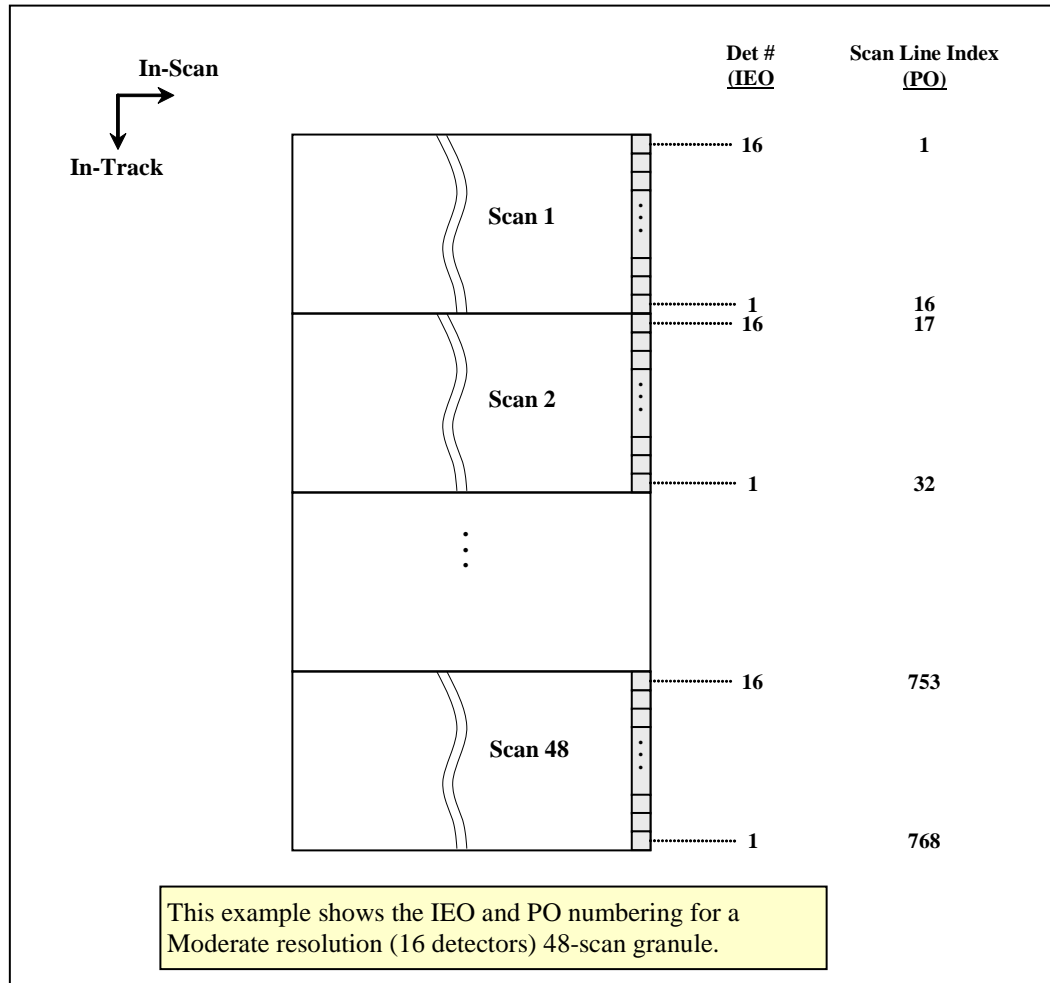


**Figure 5 Instrument Engineering Order and Product Order Illustration**

The other dimension is in the scan direction, referred to as the scan index, and has increasing indices from start of scan to end of scan. The imagery bands (I1 to I5) have 6400 samples in the scan index for the EV verified RDR. The dual gain moderate resolution bands (M1 to M5, M7 and M13) have 6304 samples and the other moderate resolution bands have 3200. The DNB has 4064 EV samples in-scan.

The Cal views have 96 samples in scan for imagery bands I1 to I5, and 48 samples in-scan for the moderate resolution bands. The number of samples per view for the DNB band is 64 except for Aggregation Modes 34 and 35 when it is 16. The DNB aggregation mode in the Cal view changes every two scans, cycling over aggregation Modes 1 to 36 in 72 scans. The DNB Cal data is split between the four FPAs used by the DNB: HGA, HGB, MGS, and LGS. Because the M16 detectors use TDI, it contains calibration data for both M16A and M16B detectors. The EV data, however, is aggregated before transmission for M16, so there is no separate A and B data in the verified RDR. When the Verified RDR granule arrays are created, fill values must be put in pixels where there is missing data.

Verified engineering application packet data is also produced and byte aligned as part of this process.

For the geolocation algorithm the Verified Spacecraft E&A RDR is generated from the RDR packets. This is S/C Ephemeris and Attitude RDR data that has been byte aligned. This process is done as part of the geolocation algorithm. The onboard S/C ephemeris and attitude data (in APID 11) includes: spacecraft ECR (GPS ECEF) position vectors (X, Y, Z components in meters), ECR velocity vectors (X, Y, Z components in meters per second) and attitude quaternion data (4 dimensionless numbers). The attitude quaternion data are used to create a quaternion matrix providing unambiguous rotation from J2000 ECI coordinates to spacecraft coordinates.

## 2.1.1 Interfaces

### 2.1.1.1 Inputs

The VIIRS Verified RDR process takes as input the VIIRS RDR data as shown in Table 3, Table 4, and Table 5.

**Table 3 Verified VIIRS RDR Engineering Packet Data Inputs**

| Input                | Type/<br>Dimensions  | Description  | Units/<br>Valid Range                    | Fill<br>Value    |
|----------------------|----------------------|--|--|------------------|
| startIETusec         | Int64/<br>(nscans)   | IET time at the start of the scan which is the number of microseconds since 1/1/1958 | IET<br>microseconds                      | MISS_IN<br>T64   |
| startTAIsec          | Float64/ (nscans)    | TAI time at the start of the scan which is the number of seconds since 1/1/1958      | TAI seconds                              | MISS_FL<br>OAT64 |
| mirror_side          | uint8/ (nscans)      | mirror side in optical path – “0” for side 1 and “1” for side 2                      | Unitless/<br>[0 1]                       | MISS_UI<br>NT8   |
| dpp_config           | uint8/ (nscans)(128) | digital PreProcessor Configuration   | Unitless/<br>Count                       | MISS_UI<br>NT8   |
| mf_ao_blkhd_px_nz    | int16/<br>(nscans)   | MF_AO_BLKHD_PX_NZ Therm 44   | Unitless/<br>Count                       | MISS_IN<br>T16   |
| mf_ao_blkhd_nx_pz    | int16/<br>(nscans)   | MF_AO_BLKHD_NX_PZ Therm 45   | Unitless/<br>Count                       | MISS_IN<br>T16   |
| mf_stopassy_baff_nz  | int16/<br>(nscans)   | On Baffle NZ of Apert Stop Assy between HAM and FM2 Therm 14                         | Unitless/<br>Count                       | MISS_IN<br>T16   |
| mf_fold_mir_bkhd_ct  | int16/<br>(nscans)   | MF_FOLD MIRROR BLKHD Center Therm 6  | Unitless/<br>Count                       | MISS_IN<br>T16   |
| mf_tel_blkhd_py      | int16/<br>(nscans)   | Mainframe Telescope Bulkhead Therm 33, RT16 (Node 1022 in Radiometry Model)          | Unitless/<br>Count                       | MISS_IN<br>T16   |
| ap_lw_cca            | int16/<br>(nscans)   | Long wave IR CCA Information stored in the Engineering packet.                       | Unitless/<br>Count                       | MISS_IN<br>T16   |
| ap_sm_cca            | int16/<br>(nscans)   | Short/Med wave IR CCA information stored in the Engineering packet.                  | Unitless/<br>Count                       | MISS_IN<br>T16   |
| ap_vn_cca            | int16/<br>(nscans)   | Visible/Near IR CCA information stored in the Engineering packet                     | Unitless/<br>Count                       | MISS_IN<br>T16   |
| ct_prec_tref_mux1ca1 | int16/<br>(nscans)   | Precision Thermistor Cal Ref Resistor 1  | Unitless/<br>Count                       | MISS_IN<br>T16   |
| ct_prec_tref_mux1ca2 | int16/<br>(nscans)   | Precision Thermistor Cal Ref Resistor 2  | Unitless/<br>Count                       | MISS_IN<br>T16   |
| ct_prec_tref_mux1ca3 | int16/<br>(nscans)   | Precision Thermistor Cal Ref Resistor 3  | Unitless/<br>Count                       | MISS_IN<br>T16   |
| ft_lw_cfpa_hi_rsl    | int16/ (nscans)      | focal plane Temperature Controller Long Wave IR CFPA high resolution temperature     | degrees<br>Kelvin/ 70 –<br>89K<br>Note 1 | MISS_IN<br>T16   |

| Input             | Type/<br>Dimensions     | Description  | Units/<br>Valid Range               | Fill<br>Value  |
|-------------------|-------------------------|--|-------------------------------------|----------------|
| ft_lw_cfpa_lo_rsl | int16/ (nscans)         | focal plane Temperature Controller Long Wave IR CFPA wide range temperature          | degrees Kelvin/ 52 – 330K<br>Note 1 | MISS_IN<br>T16 |
| ft_sm_cfpa_hi_rsl | int16/ (nscans)         | focal plane Temperature Controller Short Midwave IR CFPA high resolution temperature | degrees Kelvin/ 70 – 89K<br>Note 1  | MISS_IN<br>T16 |
| ft_sm_cfpa_lo_rsl | int16/ (nscans)         | focal plane Temperature Controller Short Midwave IR CFPA wide range temperature      | degrees Kelvin/ 51-330K<br>Note 1   | MISS_IN<br>T16 |
| ft_vis_nir_fpa    | int16/ (nscans)         | focal plane Temperature Controller Visual/Near IR fpa                                | degrees Kelvin/ 245-319K<br>Note 1  | MISS_IN<br>T16 |
| m1_asp_offset     | int16/ (nscans)(2)( 16) | moderate band 1 Analog Signal Processor offset                                       | Unitless                            | MISS_IN<br>T16 |
| m2_asp_offset     | int16/ (nscans)(2)( 16) | moderate band 2 Analog Signal Processor offset                                       | Unitless                            | MISS_IN<br>T16 |
| m3_asp_offset     | int16/ (nscans)(2)( 16) | moderate band 3 Analog Signal Processor offset                                       | Unitless                            | MISS_IN<br>T16 |
| m4_asp_offset     | int16/ (nscans)(2)( 16) | moderate band 4 Analog Signal Processor offset                                       | Unitless                            | MISS_IN<br>T16 |
| m5_asp_offset     | int16/ (nscans)(2)( 16) | moderate band 5 Analog Signal Processor offset                                       | Unitless                            | MISS_IN<br>T16 |
| m6_asp_offset     | int16/ (nscans)(2)( 16) | moderate band 6 Analog Signal Processor offset                                       | Unitless                            | MISS_IN<br>T16 |
| m7_asp_offset     | int16/ (nscans)(2)( 16) | moderate band 7 Analog Signal Processor offset                                       | Unitless                            | MISS_IN<br>T16 |
| m8_asp_offset     | int16/ (nscans)(2)( 16) | moderate band 8 Analog Signal Processor offset                                       | Unitless                            | MISS_IN<br>T16 |
| m9_asp_offset     | int16/ (nscans)(2)( 16) | moderate band 9 Analog Signal Processor offset                                       | Unitless                            | MISS_IN<br>T16 |
| m10_asp_offset    | int16/ (nscans)(2)( 16) | moderate band 10 Analog Signal Processor offset                                      | Unitless                            | MISS_IN<br>T16 |
| m11_asp_offset    | int16/ (nscans)(2)( 16) | moderate band 11 Analog Signal Processor offset                                      | Unitless                            | MISS_IN<br>T16 |
| m12_asp_offset    | int16/ (nscans)(2)( 16) | moderate band 12 Analog Signal Processor offset                                      | Unitless                            | MISS_IN<br>T16 |
| m13_asp_offset    | int16/ (nscans)(2)( 16) | moderate band 13 Analog Signal Processor offset                                      | Unitless                            | MISS_IN<br>T16 |
| m14_asp_offset    | int16/ (nscans)(2)( 16) | moderate band 14 Analog Signal Processor offset                                      | Unitless                            | MISS_IN<br>T16 |
| m15_asp_offset    | int16/ (nscans)(2)( 16) | moderate band 15 Analog Signal Processor offset                                      | Unitless                            | MISS_IN<br>T16 |
| m16a_asp_offset   | int16/ (nscans)(2)( 16) | moderate band 16 Analog Signal Processor offset                                      | Unitless                            | MISS_IN<br>T16 |
| m16b_asp_offset   | int16/ (nscans)(2)( 16) | day/night band Analog Signal Processor offset  | Unitless                            | MISS_IN<br>T16 |
| i1_asp_offset     | int16/ (nscans)(2)( 32) | imagery band 1 Analog Signal Processor offset  | Unitless                            | MISS_IN<br>T16 |
| i2_asp_offset     | int16/ (nscans)(2)( 32) | imagery band 2 Analog Signal Processor offset  | Unitless                            | MISS_IN<br>T16 |
| i3_asp_offset     | int16/ (nscans)(2)( 32) | imagery band 3 Analog Signal Processor offset  | Unitless                            | MISS_IN<br>T16 |
| i4_asp_offset     | int16/ (nscans)(2)( 32) | imagery band 4 Analog Signal Processor offset  | Unitless                            | MISS_IN<br>T16 |
| i5_asp_offset     | int16/ (nscans)(2)( 32) | imagery band 5 Analog Signal Processor offset  | Unitless                            | MISS_IN<br>T16 |

| Input                 | Type/<br>Dimensions | Description  | Units/<br>Valid Range                   | Fill<br>Value  |
|-----------------------|---------------------|--|---|----------------|
| bb_tmps               | int16/ (nscans)(6)  | black body temperatures, OT shutdown=315K                                    | degrees Kelvin/ 243 to 336 K<br>Note 1  | MISS_IN<br>T16 |
| ham_tmp1              | int16/ (nscans)     | half angle mirror T1 prec therm 07, radiatively coupled                      | degrees Celsius/ -30 to 65 °C<br>Note 1 | MISS_IN<br>T16 |
| ham_tmp2              | int16/ (nscans)     | half angle mirror T2 prec therm 08, radiatively coupled                      | degrees Celsius/ -30 to 65 °C<br>Note 1 | MISS_IN<br>T16 |
| mf_nadir_rad_nxp      | int16/ (nscans)     | mainframe Nadir radiator nxpy  | degrees Celsius/ -25 to 65 °C<br>Note 1 | MISS_IN<br>T16 |
| mf_scan_cavity_nxp    | int16/ (nscans)     | mainframe scan cavity nx pz therm 46   | degrees Celsius/ -25 to 60°C<br>Note 1  | MISS_IN<br>T16 |
| mf_scan_cavity_baf_nz | int16/ (nscans)     | mainframe scan cavity baffle NZ prec therm 10                                | degrees Celsius/ -25 to 60°C<br>Note 1  | MISS_IN<br>T16 |
| mf_scan_cavity_baf_pz | int16/ (nscans)     | mainframe scan cavity baffle PZ prec therm 9 temperature                     | degrees Celsius/ -25 to 60°C<br>Note 1  | MISS_IN<br>T16 |
| mf_scan_cavity_bknd_n | int16/ (nscans)     | mainframe scan cavity bulkhead ny therm 8                                    | degrees Celsius/ -25 to 60°C<br>Note 1  | MISS_IN<br>T16 |
| dp_dnb_cca            | int16/ (nscans)     | digital preprocessor DNB cca thermistor 60                                   | degrees Celsius/ -25 to 60°C<br>Note 1  | MISS_IN<br>T16 |
| dp_dpp_cca            | int16/ (nscans)     | digital preprocessor DPP cca thermistor 61                                   | degrees Celsius/ -25 to 60°C<br>Note 1  | MISS_IN<br>T16 |
| dp_fpie_clk_cca       | int16/ (nscans)     | digital preprocessor focal plane interface electronics clk cca thermistor 51 | degrees Celsius/ -25 to 60°C<br>Note 1  | MISS_IN<br>T16 |
| power_supply1         | int16/ (nscans)     | power supply 1 thermistor 52   | degrees Celsius/ -25 to 60°C<br>Note 1  | MISS_IN<br>T16 |
| power_supply2         | int16/ (nscans)     | power supply 2 thermistor 53   | degrees Celsius/ -25 to 60°C<br>Note 1  | MISS_IN<br>T16 |
| se_a_cca              | int16/ (nscans)     | scan control electronics A cca thermistor 31                                 | degrees Celsius/ -25 to 60°C<br>Note 1  | MISS_IN<br>T16 |
| se_b_cca              | int16/ (nscans)     | scan control electronics B cca thermistor 12                                 | degrees Celsius/ -25 to 60°C<br>Note 1  | MISS_IN<br>T16 |

| Input          | Type/<br>Dimensions  | Description   | Units/<br>Valid Range                         | Fill<br>Value  |
|----------------|--|---|---|----------------|
| sdsd_position  | Uint8/<br>(nscans)   | SDSM position<br>0=home, 1=SD view and 2=sun<br>view              | Unitless/<br>0- 2                             | MISS_UI<br>NT8 |
| sdsd_samples   | int16/<br>[nscans]<br>[n_sdsd_samples(5)]<br>[n_sdsd_detectors(8)] | SDSM Samples  | Volts/<br>-2.5 to 2.5 V<br>Note 1             | MISS_IN<br>T16 |
| sdsd_preamp    | int16/<br>[nscans]   | SDSM Preamp Thermistor 57   | degrees<br>Celsius/ -70<br>to 120°C<br>Note 1 | MISS_IN<br>T16 |
| tel_enc        | uint16/<br>[nscans x (num. of TEL<br>enc. Pulses)]                 | contains the raw encoder values<br>for each scan in the granule   | Scan time<br>counter<br>ticks/[0 –<br>65535]  | MISS_IN<br>T16 |
| ham_enc        | uint16/<br>[nscans x (num. Of<br>HAM enc. Pulses)]                 | contains the raw encoder values<br>for each scan in the granule   | Scan time<br>counter<br>ticks/[0 –<br>65535]  | MISS_IN<br>T16 |
| tel_start_enc  | uint16 /<br>[nscans]   | Telescope start of scan encoder<br>value (15-bit encoder)         | 15-bit<br>encoder ticks/<br>[0 – 32768]       | MISS_IN<br>T16 |
| ham_start_enc  | uint16 /<br>[nscans]   | Half angle mirror start of scan<br>encoder value (15-bit encoder) | 15-bit<br>encoder ticks/<br>[0 – 32768]       | MISS_IN<br>T16 |
| act_scans      | int32/ 1   | number of actual scans  | N/A/ 0 – 16                                   | MISS_IN<br>T32 |
| scan_mode      | char8/<br>[nscans]   | sensor mode of each scan  | N/A/<br>[Day   Night  <br>Other]              | MISS_UI<br>NT8 |
| Mode           | uint8/ 1   | scan mode   | NA/ 0=night,<br>1=day,<br>2=mixed             | MISS_UI<br>NT8 |
| bgnTime        | int64/ 1   | begin boundary of the granule                                     | IET   | MISS_IN<br>T64 |
| endTime        | int64/ 1   | end boundary of the granule                                       | IET   | MISS_IN<br>T64 |
| first_scan     | int64/ 1   | IET of the first scan   | IET   | MISS_IN<br>T64 |
| last_scan      | int64/ 1   | IET of the last scan  | IET   | MISS_IN<br>T64 |
| sensor_softver | uint8/ [16]  | sensor software version   | N/A   | MISS_UI<br>NT8 |
| Sensor         | uint8/ [8]   | VIIRS sensor ID   | N/A   | MISS_UI<br>NT8 |
| sensor_model   | int32/ 1   | 1=EDU, 2=FU1 (Flight Unit),<br>FU2, FU3                           | N/A   | MISS_IN<br>T32 |
| dnb_sequence   | Uint8/<br>[nscans]   | DNB sequence number   | Unitless/<br>1 to 36                          | MISS_UI<br>NT8 |

<sup>1</sup> Note: The field is a digital count. Units/Valid Range are after polynomial conversion.

**Table 4 Verified VIIRS RDR Science Packet Data Inputs**

| Input             | Type<br>Dimensions       | Description            | Units<br>Range                    | Fill Value           |
|-------------------|--------------------------|------------------------|-----------------------------------|----------------------|
| <b>Image Band</b> |                          |                        |                                   |                      |
| IETusec           | Int64<br>[48]            | IET start of the scan  | Microseconds since<br>Jan 1, 1958 | MISS_INT64_FI<br>LL  |
| earthview         | UInt16 /<br>[1536][6400] | each pixel of the scan | 12 bit count<br>0 – 4095          | MISS_UINT16_<br>FILL |

| Input                            | Type<br>Dimensions    | Description             | Units<br>Range                    | Fill Value       |
|----------------------------------|-----------------------|-------------------------|-----------------------------------|------------------|
| <b>Single Gain Moderate Band</b> |                       |                         |                                   |                  |
| IETusec                          | Int64<br>[48]         | IET start of the scan   | Microseconds since<br>Jan 1, 1958 | MISS_INT64_FILL  |
| earthview                        | UINT16<br>[768][3200] | each pixel of the scan  | 12 bit count<br>0 – 4095          | MISS_UINT16_FILL |
| <b>Dual Gain</b>                 |                       |                         |                                   |                  |
| IETusec                          | Int64<br>[48]         | IET start of the scan   | Microseconds since<br>Jan 1, 1958 | MISS_INT64_FILL  |
| earthview                        | UInt16<br>[768][6304] | each pixel of the scan  | 12 bit count<br>0 – 4095          | MISS_UINT16_FILL |
| gain                             | UInt8<br>[768][6304]  | the gain for each pixel | 0 or 1                            | MISS_UINT8_FILL  |
| <b>DNB</b>                       |                       |                         |                                   |                  |
| IETusec                          | Int64<br>[48]         | IET start of the scan   | Microseconds since<br>Jan 1, 1958 | MISS_INT64_FILL  |
| earthview                        | UInt16<br>[768][4064] | each pixel of the scan  | 13 or 14 bit count<br>0 – 16383   | MISS_UINT16_FILL |
| gain                             | UInt8<br>[768][4064]  | the gain for each pixel | 0, 2, or 3                        | MISS_UINT8_FILL  |

**Table 5 Verified VIIRS RDR Calibration Packet Data Inputs**

| Input                            | Type<br>Dimensions   | Description                                   | Units<br>Range      | Fill Value       |
|----------------------------------|----------------------|---|---------------------|------------------|
| <b>Image Band</b>                |                      |   |                     |                  |
| sv_calib                         | UInt16<br>[1536][96] | space view calibration source                 | counts<br>0 – 32767 | MISS_UINT16_FILL |
| bb_calib                         | UInt16<br>[1536][96] | black body calibration source                 | counts<br>0 – 32767 | MISS_UINT16_FILL |
| sd_calib                         | UInt16<br>[1536][96] | solar diffuser calibration source             | counts<br>0 – 32767 | MISS_UINT16_FILL |
| <b>Single Gain Moderate Band</b> |                      |   |                     |                  |
| sv_calib                         | UInt16<br>[768][48]  | space view calibration source                 | counts<br>0 – 32767 | MISS_UINT16_FILL |
| bb_calib                         | UInt16<br>[768][48]  | black body calibration source                 | counts<br>0 – 32767 | MISS_UINT16_FILL |
| sd_calib                         | UInt16<br>[768][48]  | solar diffuser calibration source             | counts<br>0 – 32767 | MISS_UINT16_FILL |
| <b>Dual Gain / DN Bands</b>      |                      |   |                     |                  |
| sv_calib                         | UInt16<br>[768][48]  | space view calibration source                 | counts<br>0 – 32767 | MISS_UINT16_FILL |
| bb_calib                         | UInt16<br>[768][48]  | black body calibration source                 | counts<br>0 – 32767 | MISS_UINT16_FILL |
| sv_calib                         | UInt16<br>[768][48]  | solar diffuser calibration source             | counts<br>0 – 32767 | MISS_UINT16_FILL |
| sv_calib_gain                    | UInt8<br>[768][48]   | gain state for the space view calibration     | counts<br>0 – 1     | MISS_UINT8_FILL  |
| bb_calib_gain                    | UInt8<br>[768][48]   | gain state for the black body calibration     | counts<br>0 – 1     | MISS_UINT8_FILL  |
| sd_calib_gain                    | UInt8/<br>[768][48]  | gain state for the solar diffuser calibration | counts<br>0 – 1     | MISS_UINT8_FILL  |
| <b>DNB</b>                       |                      |   |                     |                  |
| sv_calib                         | UInt16<br>[768][64]  | space view calibration source                 | counts<br>0 – 32767 | MISS_UINT16_FILL |
| bb_calib                         | UInt16<br>[768][64]  | black body calibration source                 | counts<br>0 – 32767 | MISS_UINT16_FILL |
| sv_calib                         | UInt16<br>[768][64]  | solar diffuser calibration source             | counts<br>0 – 32767 | MISS_UINT16_FILL |

### 2.1.1.2 Outputs

The internal output of the VIIRS Verified RDR is a byte-aligned version of the VIIRS RDR.

### 2.1.2 Algorithm Processing

This is the derived algorithm for the VIIRS SDR Verified RDR algorithm and is a subclass of the `AutoGeneratedProSdrViirsVerifiedRdr` and `ProCmnAlgorithm` classes. The derived algorithm class creates a list of input data items read from DMS and passes required data into the algorithm. All output data items are written to DMS once the algorithm finishes processing this data.

VIIRS Science RDRs contain the science, CAL and engineering application packets that are required for SDR processing of a tasked granule. In addition to the tasked granule, the RDR information from the previous and following granule also need to be processed in order to accurately calibrate dual gain bands. Not all of the data in the RDRs are needed for SDR processing. A Verified RDR contains only the data from an RDR that is required for the SDR processing of a tasked granule. The data has been extracted, unpacked and byte aligned from the CCSDS application packets contained in the RDR. In other words, a Verified RDR is a byte-aligned RDR. This unpacked and byte-aligned data is assigned to the internal verified RDR structure, which is not in the same structure that the packet data came in (for efficiency reasons), and VIIRS SDR processing uses the data from that structure to do further processing. Figure 6 shows the Create Verified VIIRS RDR Flow.

The first sample from each of the 16 DNB detector outputs reported in the Earth View and the three calibration views (Space, Blackbody and Solar Diffuser) is anomalous for each VIIRS scan. The main cause for this anomaly was found to be due to a problem in the startup portion of the CCD timing. This timing problem may be fixed in the hardware for Flight Unit 2; however, for Flight Unit 1, this DNB anomaly should be removed during the VIIRS SDR process by placing fill integer 0 values in the RDR data for the DNB Earth View and the three calibration views. This VIIRS DNB First Frame anomaly was fixed per

NP-EMD-2007.510.0029\_NPP\_VIIRS\_SDR\_DNB\_FirstFrameAnomaly.

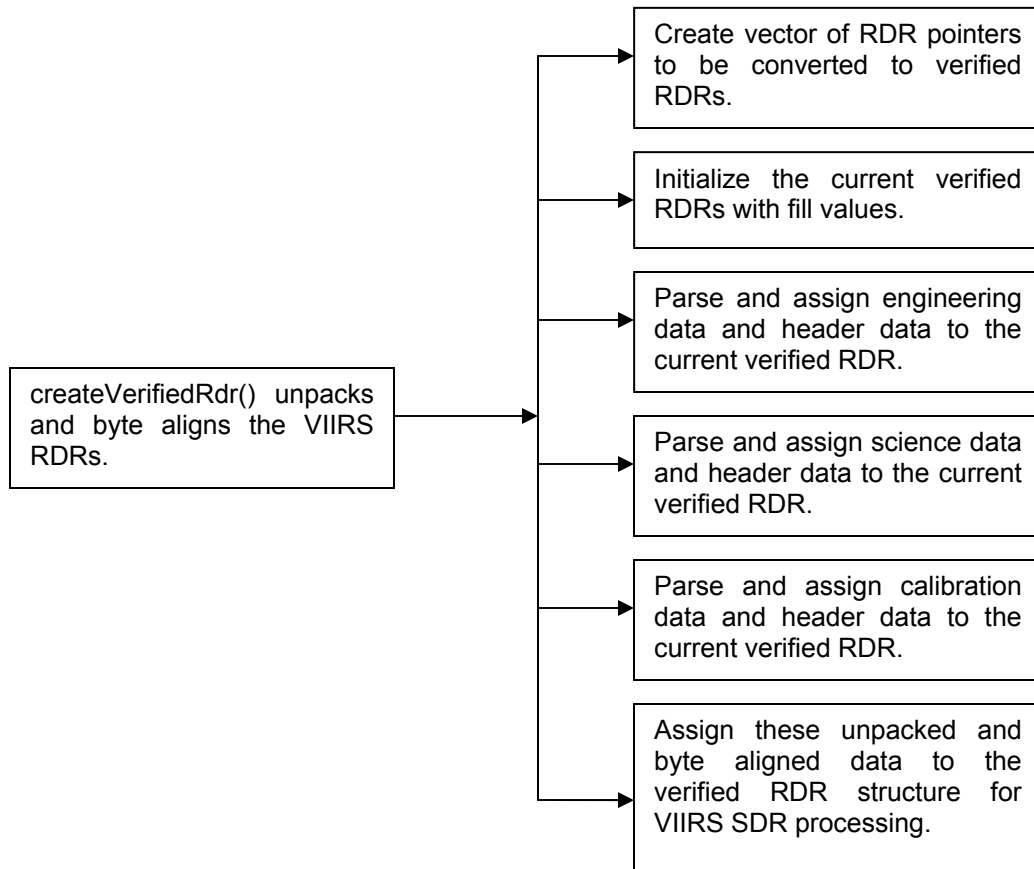


**Figure 6 Create Verified VIIRS RDR Flow Diagram**

### 2.1.2.1 createVerifiedRDR()

createVerifiedRDR() creates a VIIRS Verified RDR structure for the current, previous, and following granules and calls ProViirsVerifiedRDRConverter::convert() to fill the Verified RDRs with unpacked and byte-aligned engineering, science, and CAL data. The Verified RDR number of actual scans is validated and the granule mode (day, night, mixed) is determined.

### 2.1.2.2 ProViirsVerifiedRDRConverter()

ProViirsVerifiedRDRConverter() retrieves the engineering, science, and CAL packets by APID from the VIIRS RDRs and calls the appropriate methods (ViirsEngAppPacket::parsePkts(), ViirsSciAppPacket::parsePkts(), ViirsEngCalPacket::parsePkts()) to unpack and byte align the data which is stored in the VIIRS Verified RDR. To ensure that every granule starts at a scan 1 and that missing scans are treated appropriately, scan ids are turned into offsets from the minimum scan id in the granule.

### **2.1.2.3 ViirsCalAppPacket()**

The ViirsCalAppPacket class contains methods to retrieve and decompress the CAL packet data in the VIIRS RDR. It loops through the space view, black body, and solar diffuser CAL data and decompresses the views for each detector of each band. Universal Source Encoder for Space (USES) (viirs\_decmp()) is used for this purpose. This is also referred to Rice compression (after its creator or Modified NCSA (National Center for Supercomputing Applications) code. This class also converts the CCSDS time to IET time.

### **2.1.2.4 ViirsEngAppPacket()**

The ViirsEngAppPacket class contains methods to unpack and byte align engineering packet data in the VIIRS RDR. This class also retrieves and converts the CCSDS time to IET time.

### **2.1.2.5 ViirsHrdAppPacket()**

The ViirsHrdAppPacket class contains methods to retrieve and decompress the science packet data in the VIIRS RDR. This class also converts the CCSDS time to IET time and fills in the start of scan trigger time for the RDR.

## **2.1.3 Graceful Degradation**

The VIIRS Verified RDR procedure contains no graceful degradation.

### **2.1.3.1 Graceful Degradation Inputs**

None.

### **2.1.3.2 Graceful Degradation Processing**

None.

### **2.1.3.3 Graceful Degradation Outputs**

None.

## **2.1.4 Exception Handling**

No exception handling is performed in the VIIRS Verified RDR process.

## **2.1.5 Data Quality Monitoring**

No data quality monitoring is performed in the VIIRS Verified RDR process.

### **2.1.6 Computational Precision Requirements**

There are no computational precision requirements for the VIIRS Verified RDR process.

### **2.1.7 Algorithm Support Considerations**

The DMS and INF must be running before the algorithm is executed.

### **2.1.8 Assumptions and Limitations**

The VIIRS Verified RDR requires as input raw data packets transmitted from the satellite.

## **2.2 VIIRS SDR Geolocation Description**

The purpose of the VIIRS GEO software is to provide Earth location and related spatial information for each of the samples in the Raw Data Record (RDR) belonging to the moderate resolution radiometric bands (aggregated and unaggregated), the fine resolution imagery bands, and the Day/Night Band (DNB). The output GEO data fields include geodetic latitude, longitude and derived products such as satellite zenith and azimuth angles, range to the satellite, solar zenith and azimuth angles, and (for the DNB) both lunar zenith and azimuth angles. The VIIRS GEO algorithm processes the engineering VIIRS RDR and Spacecraft Ephemeris and Attitude (E&A) RDRs, as well as external support data sets to generate the GEO data fields. The Earth location fields, which include the geodetic latitude, longitude and height, are computed using rigorous models of the Earth and VIIRS instrument pointing. The algorithm computes the earth location by first determining each pixel's line-of-sight (LOS) vector by constructing dynamic models of the VIIRS instrument using the engineering and spacecraft RDR data. Each detector's LOS vector is then intersected with the rotating WGS84 ellipsoid to obtain geodetic latitude and longitude. If terrain correction is to be performed, then the LOS intersection with the terrain-adjusted surface (geoid plus height over the geoid) is computed to output a terrain corrected geodetic latitude, longitude and height. The GEO products are held in internal memory to be input to the radiometric CAL module before they are written out to the Data Management Subsystem (DMS). For a list of GEO products to be produced, please refer to Section 2.2.1.2. The Geolocation Processing Chain is shown in Figure 7.

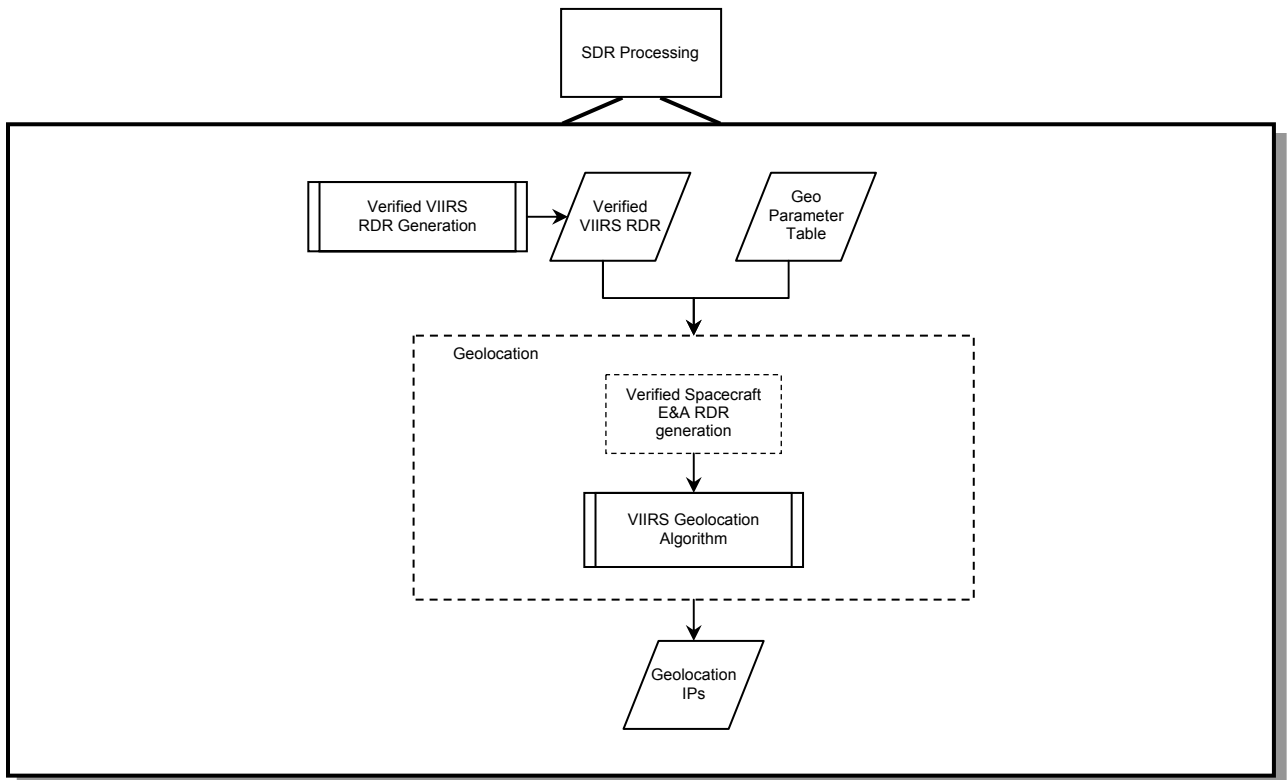


**Figure 7 Geolocation Processing Chain**

**2.2.1 Interfaces**

**2.2.1.1 Inputs**

Table 6 lists the VIIRS GEO SDR inputs which are further detailed within Tables 7, and 8. The rotating telescope assembly (RTA) encoder data and half angle mirror (HAM) encoder data is used by the Geolocation algorithm to construct models of the RTA and HAM rotation as a function of time. The scan timing information is used to relate the VIIRS spatial elements to the models of both the dynamic components of the instrument (RTA and HAM) and the S/C. Some parameters listed in this table are not used by GEO but must remain in the data structure for sizing purposes. Table 7 contains a list of the S/C ephemeris and attitude data used to construct a model of the platform position, velocity, and orientation as a function of time. Table 8, Geolocation Parameter Inputs, contains instrument constants that include focal plane, band, and detector locations which are used to generate corrections applicable to each detector (channel) in a spatial element.

**Table 6 VIIRS Geolocation Inputs**

| Input                       | Object/Format | Description   |
|-----------------------------|---------------|---|
| Verified VIIRS RDR          | Binary        | VIIRS Engineering RDR packets that have been byte aligned.      |
| Verified Spacecraft E&A RDR | Binary        | S/C Ephemeris and Attitude RDR data that has been byte aligned. |

| Input                       | Object/Format | Description  |
|-----------------------------|---------------|--|
| Geolocation Parameter Table | Binary        | File containing information specific for processing each resolution – 1 for each resolution. |

Table 7 S/C Ephemeris and Attitude Data

| Input   | Type/<br>Dimensions      | Description                                     | Units/<br>Valid Range           | Fill<br>Value |
|---------|--------------------------|---|---------------------------------|---------------|
| ietTime | Int64[NUM_EPH_RPTS]      | IET time of the ephemeris data                  | Microseconds since 1/1/1958     | None          |
| pos     | float32[NUM_EPH_RPTS][3] | ECEF (Earth Centered Earth Fixed)               | Meters<br>-7.25E6 to 7.25E6     | None          |
| vel     | float32[NUM_EPH_RPTS][3] | ECEF  | meters/sec<br>-7.55E3 to 7.55E3 | None          |
| ietTime | Int64[NUM_ATT_RPTS]      | IET time of the attitude data                   | Microseconds since 1/1/1958     | None          |
| quat    | float32[NUM_ATT_RPTS][4] | Quaternion of Control Frame relative to J2000.0 | Quaternion<br>[-1 to +1]        | None          |

Table 8 Geolocation Parameter Inputs

| Input           | Type/<br>Dimensions                  | Description  | Units/<br>Valid Range         | Fill<br>Value |
|-----------------|--------------------------------------|--|-------------------------------|---------------|
| revision        | UInt8/<br>(1,10)                     | Revision number for the parameter file (1-D array, 10 bytes in length).  | Unitless/<br>N/A              | None          |
| band_number     | Int32/<br>1                          | Band number to geolocate (0 is the ideal band). This parameter is used to index other band dependent parameters.   | Unitless/<br>[0 to 22]        | None          |
| latch_to_center | float64/<br>1                        | Used to calculate sample time from frame time. This specifies the fraction of the frame time that is used to compute the sample time, e.g., latch_to_center = 0.5 means that the sample time is computed at the center of the frame time.  | Unitless/<br>[0 – 1.0]        | None          |
| t_reset         | float64/<br>1                        | Time to reset the sample, otherwise called the readout time. This is computed by subtracting the integration time from the frame time. If the readout occurs at the beginning of the frame time (before the integration time), then a negative t_reset should be used in the parameter file to adjust the sample time equations appropriately. | Seconds<br>[-2.3e-5 - 2.3e-5] | None          |
| N_samp          | UInt16/<br>Max Band Number (MBN) + 1 | Factor used to determine the number of samples per frame for each band (0 is the ideal band).  | Unitless/<br>[1 – 2]          | None          |

| Input                  | Type/<br>Dimensions    | Description  | Units/<br>Valid Range  | Fill<br>Value |
|------------------------|------------------------|--|--|---------------|
| focal_length           | float64/<br>MBN+1      | Instrument focal length for each band. This parameter is tied to the Mag parameter. If the system Mag is used, then the system focal length should be used. Likewise, if the Mag of the Aft Optics is used, then the Aft Optics focal length should be used.       | Meters/<br>[0.270 - 1.15]  | None          |
| det_space_track        | float64/<br>MBN+1      | Detector center spacing in the track direction (0 is the ideal band)   | Meters/<br>Range for IMG:<br>[0.000508 – 0.000511]<br>Range for MOD:<br>[0.001016 – 0.001022]  | None          |
| det_space_scan         | float64/<br>MBN+1      | Detector center spacing in the scan direction (0 is the ideal band). This parameter currently set to zero for all bands since the scan offset is accounted for by a timing offset.   | Meters/<br>≥ 0   | None          |
| DNB_space_track        | float64/<br>32         | DNB detector center spacing in the track direction. Aggregation zone dependent, listed in order from Zone 0 to 31, where Aggregation Zone 0 is nadir.  | Meters/<br>[0.000484 - 0.001016]   | None          |
| DNB_space_scan         | float64/<br>32         | DNB detector center spacing in the scan direction. Aggregation zone dependent, listed in order from Zone 0 to 31, where aggregation Zone 0 is nadir. This parameter currently set to zero for all zones since the scan offset is accounted for by a timing offset. | Meters/<br>≥ 0   | None          |
| det_position           | float64/<br>(MBN+1, 2) | Band center x and y offset pairs with respect to the optical center (0 is the ideal band). This value is the average shift of all detector locations within the band from the nominal location (overall bias per band).  | Meters/<br>Range Dim 1 (scan):<br>[0 to 0.000177] IMG<br>[0 to 0.000354] MOD<br>[0 to 0.000015] DNB<br>Range Dim 2 (track):<br>[0 to 0.000508] IMG<br>[0 to 0.001016] MOD<br>[0 to 0.000024] DNB | None          |
| band_position          | float64/<br>MBN+1      | Scan IFOV offsets of band trailing edges with respect to the optical center (0 is the ideal band)  | MOD IFOV/<br>[-22 to 22]   | None          |
| earth_view_delay       | float64/<br>1          | The delay following the start of scan (referenced to the encoder clock reset) to the start of the first Earth View (EV) sample. This parameter specifies the dropped samples to allow for electronic settling before EV sampling.                                  | Seconds/<br>Real number  | None          |
| detector_sampling_rate | float64/<br>1          | Sampling rate for MOD, IMG and DNB resolution detectors.   | Seconds/<br>[0.000003 – 0.0009]  | None          |
| scan_length            | float64/<br>1          | Scan period (Length of VIIRS scan)   | Seconds/<br>[1.77 – 1.80]  | None          |

| Input              | Type/<br>Dimensions | Description   | Units/<br>Valid Range   | Fill<br>Value |
|--------------------|---------------------|---|---|---------------|
| agg_zone_bounds    | int32/<br>(1,5)     | Upper bounds for the MOD and IMG resolution along-scan aggregation zones. For the MOD res. case, specification of a Negative value for the first zone forces software to geolocate unaggregated MOD pixels. Capability required for CalVal. Note that N_frame should be consistent with choice made here.   | Frame number/<br>fixed set of values for<br>IMG and MOD   | None          |
| DNB_aggregation    | int32/<br>(32,2)    | The first column is the number of samples occurring in each DNB aggregation zone, and the second column is the number of along-scan photosites per pixel for that zone. Values are listed from aggregation zone 0 to 31, where Zone 0 is nadir.   | Unitless/<br>fixed set of values  | None          |
| DNB_ag_zone_bounds | Int32/<br>(64, 3)   | Frame number limits for the 32 DNB aggregation zones from start of scan through nadir to end of scan, and the associated DNB aggregation zone indices. Columns 0 & 1 are the lower and upper frame numbers per zone, respectively. Column 2 contains the associated aggregation zone index, where Index 0 corresponds to nadir and Index 31 the edge of scan. | <u>Units:</u><br>Col 0 & 1: Frame Num<br>Col 2: Agg Zone Index<br><u>Valid Range:</u><br>Col 0 & 1: [0 4063]<br>Col 2: [0 – 31] | None          |
| scan_ang_coef_tel  | float64/<br>1       | Scan angle coefficient for telescope  | Unitless/<br>Real number  | None          |
| scan_ang_coef_mirr | float64/<br>1       | Scan angle coefficient for HAM  | Unitless/<br>Real number  | None          |
| scan_ang_offsets   | float64/<br>(1,2)   | Scan angle offsets for computing the sample scan angle for mirror side 1 (element 0) and side 2 (element 1).  | Radians/<br>[0 - 2 $\pi$ ]  | None          |
| enc_scale          | float64/<br>1       | Scale factor for converting 14-bit encoders to 16-bit representation  | Unitless/<br>Fixed Value  | None          |
| mirr_abs_limit     | float64/<br>(1,2)   | Mirror encoder time stamp absolute limits in units of Scan-Time counter ticks. This parameter determines the valid range for the mirror encoder delta time stamp readings (specifies the acceptable stable scan rate range by limiting the delta timestamp readings).   | Scan-time counter<br>ticks/<br>[875 – 885]  | None          |
| mirr_del_limit     | float64/<br>1       | Mirror encoder time stamp delta limits in units of Scan-Time counter ticks. This parameter specifies the maximum allowable difference between adjacent mirror encoder delta time stamp readings (limits the instantaneous changes in scan rate).  | Scan-time counter<br>ticks/<br>$\leq 10$  | None          |

| Input               | Type/<br>Dimensions | Description   | Units/<br>Valid Range   | Fill<br>Value |
|---------------------|---------------------|---|---|---------------|
| tel_abs_limit       | float64/<br>(1,2)   | Telescope encoder time stamp absolute limits in units of Scan-Time counter ticks. This parameter determines the valid range for the telescope encoder delta time stamp readings (specifies the acceptable stable scan rate range by limiting the delta timestamp readings). | Scan-time counter ticks/<br>[875 – 885]                           | None          |
| tel_del_limit       | float64/<br>1       | Telescope encoder time stamp delta limits in units of Scan-Time counter ticks. This parameter specifies the maximum allowable difference between adjacent telescope encoder delta time stamp readings (limits the instantaneous changes in scan rate).                      | Scan-time counter ticks<br>≤10                                    | None          |
| sample_impulse_mirr | int32 /<br>1        | Mirror encoder pulses between each encoder sample (= 2)   | Encoder pulses/<br>Fixed Value                                    | None          |
| sample_impulse_tel  | int 32/<br>1        | Telescope encoder pulses between each encoder sample (= 4)  | Encoder pulses/<br>Fixed Value                                    | None          |
| A_bit_adj           | int32/<br>(1,2)     | Offset to convert from pseudo 15-bit to 16-bit encoders, depending on if the Start-of-Scan15-bit encoder is even or odd [even adjust / odd adjust]  | 16-bit encoder ticks/<br>[ 0 to 1]                                | None          |
| B_HAM_adj           | int32/<br>(1,2)     | Offset for converting HAM encoders to absolute encoders depending on the HAM side [HAM A adjust / HAM B adjust]   | 16-bit encoder ticks/<br>[ 0 to 2 <sup>16</sup> ]                 | None          |
| t_encoder           | float64/<br>1       | Encoder data scale factor to convert from scan time counter ticks to time.  | Microseconds per scan time counter tick/<br>[0.495624 – 0.495688] | None          |
| mirr_side1_range    | float64/<br>(1,2)   | Mirror side 1 angle range   | Radians/<br>[- $\pi$ – $\pi$ ]                                    | None          |
| alpha               | float64/<br>1       | Mirror wedge angle $\alpha$ is the non-parallelism of the HAM in the along-scan axis, and creates an along-scan offset between scans from mirror sides 1 and 2.   | Radians/<br>< 9.7e-5  | None          |
| beta                | float64/<br>1       | Mirror wedge angle $\beta$ is the non-parallelism of the HAM in the along-track axis, and creates an along-track offset.  | Radians/<br>< 9.7e-5  | None          |
| gammaa              | float64/<br>1       | Misalignment of the mirror plane-of-symmetry (defined as the plane midway between the two mirror surfaces) to the rotation axis (HAM motor axis)  | Radians/<br>[-4.85e-5 to 4.85e-5]                                 | None          |
| T_inst2sc           | float64/<br>(3,3)   | 3x3 Instrument to Spacecraft frame transformation matrix  | Unitless/<br>Real numbers   | None          |
| T_mirr2inst         | float64/<br>(3,3)   | 3x3 Mirror to Instrument frame transformation matrix  | Unitless/<br>Real numbers   | None          |

| Input            | Type/<br>Dimensions | Description   | Units/<br>Valid Range   | Fill<br>Value |
|------------------|---------------------|---|---|---------------|
| T_aft2inst       | float64/<br>(3,3)   | 3x3 AFT to Instrument frame transformation matrix (this matrix includes Focal plane to AFT frame transformation, which is a 3x3 rotation matrix with the scan velocity lag angle)   | Unitless/<br>[-1 to 1]  | None          |
| T_inst2SD        | float64/<br>(3,3)   | 3x3 Instrument to Solar Diffuser frame transformation matrix  | Unitless/<br>[-2 to 2]  | None          |
| T_tel2inst       | float64/<br>(3,3)   | 3x3 Telescope to Instrument frame transformation matrix   | Unitless/<br>Real numbers   | None          |
| num_thermistor   | int32/<br>1         | Number of thermistors currently used for thermal correction.  | N/A<br>[0 – 26]   | None          |
| thermistor_id    | Uint8/<br>(26,40)   | ID of thermistors used for temperature corrections. Each ID or name corresponds to a set of thermistor coefficients listed in the thermistor_coefs parameter. The number of items listed here should equal num_thermistor.  | Unitless/<br>N/A  | None          |
| thermistor_coefs | float64/<br>(26,6)  | Set of coefficients used in a conversion polynomial to derive a temperature from thermistor readings. Each set corresponds to a thermistor name (see thermistor_id). The number of items entered here should equal num_thermistor. (This parameter allows for 6 coefficients per thermistor). | Unitless/<br>Real numbers   | None          |
| Mag              | float64/<br>(3, 3)  | 3x3 telescope magnification matrix, where the matrix contains the term 1/m. This parameter is coupled with the focal_length parameter (see focal_length description).   | Unitless/<br>[0 – 1]  | None          |
| basis_in         | float64/<br>(3,3)   | 3x3 telescope entrance basis matrix   | Unitless/<br>[ 0 – 1]   | None          |
| basis_out        | float64/<br>(3,3)   | 3x3 telescope exit basis matrix   | Unitless/<br>[ 0 – 1]   | None          |
| poly_coef_mirr   | float64/<br>(1,5)   | Polynomial coefficients for mirror encoder-to-angle conversion. Assumes linear relationship, so only first two coefficients are populated.  | Elem. 0: Radians<br>Elem. 1: radians per<br>16-bit encoder ticks/<br>Real numbers | None          |
| poly_coef_tel    | float64/<br>(2,5)   | Polynomial coefficients for telescope encoder-to-angle conversion. Assumes linear relationship, so only first two coefficients are populated.   | Elem. 0: Radians<br>Elem. 1: radians per<br>16-bit encoder ticks/<br>Real numbers | None          |
| tel_ref          | float64/<br>1       | Telescope reference angle   | Radians/<br>[- $\pi$ to $\pi$ ]   | None          |
| band_type        | Int32               | Identifies band type: moderate (0), imagery (1), or DNB (2)   | Unitless/<br>[0 – 2]  | None          |
| num_detectors    | Int32               | Number of detectors per band (depends on band type).  | Unitless/<br>[16 – 32]  | None          |
| poly_degree      | int32/<br>1         | Degree of the polynomial for mirror encoder-to-angle conversion   | Unitless/<br>[1 – 4]  | None          |

| Input        | Type/<br>Dimensions | Description  | Units/<br>Valid Range      | Fill<br>Value |
|--------------|---------------------|--|----------------------------|---------------|
| N_frame      | Unit16              | Number of frames per scan<br>(depends on band type)  | Unitless/<br>[3200 – 6400] | None          |
| MIN_COS_VIEW | float64/<br>1       | This parameter specifies the sensor zenith angle limit used for flagging pixels as being near the limb. If the sensor zenith angle is greater than MIN_COS_VIEW, the pixels are flagged as being Near Limb | Unitless/<br>[0 – PI]      | None          |

### 2.2.1.2 Outputs

The VIIRS SDR GEO code produces six non-gridded GEO products (DNB, MOD, MOD Unagg, IMG, MOD terrain corrected, IMG terrain corrected) and two gridded GEO products (MOD and IMG). For the six non-gridded GEO products, the data is output in both radians and degrees. Either the radians geo product or the degrees geo product can be used by downstream algorithms. The two gridded GEO outputs are used for internal processing only. The default grid projection used by the Operational code is polar stereographic projection. The gridded GEO outputs are used for the remapping of Imagery EDRs and can be used for remapping from the VIIRS SDR to any map projection. See Sections 2.2.1.2.1 and 2.2.1.2.2 for associated geolocation output data. All relevant Metadata associated with these output items is defined in the CDFCB-X, Volume V.

Each non-gridded product contains the granule scan and pixel level data, as shown in Tables 9 through 12. Note that for MOD and IMG, the same structures are used for both terrain corrected and non-terrain corrected products. In the terrain corrected products, the latitude and longitude, and all of the pixel level products are adjusted for terrain.

Granule-Level quality flags (QF) (Automatic Quality and the Percent Missing) (note that these are two of the name/value pair metadata QFs) apply to IMG, MOD and DNB bands and are defined below: Automatic Quality QF:

- 1) HAM/RTA Encoder Flag: If the encoder flags are set to bad or degraded, Automatic QF should be triggered.
- 2) HAM/RTA Encoder Flag: If the encoder data is missing, Automatic QF should be triggered.
- 3) Missing E&A Flag: If E&A data is missing, Automatic QF should be triggered .
- 4) SAA flag - Automatic QF should NOT be triggered as this does not affect the geo quality,
- 5) Eclipse flag - Automatic QF should NOT be triggered as this does not affect the geo quality.
- 6) Bad pointing QF and Percent out of Bounds - if this is triggered Automatic QF should be triggered.
- 7) Bad terrain and invalid solar angles QF - if these are triggered; the Automatic QF should be triggered.

Percent Missing QF:

This quality flag is a percentage summary of:

- 1) geo Scan Quality=missing, OR
- 2) scan-level Missing ephemeris or attitude QF is anything other than nominal (there are 4 options)

**Table 9 DNB Geolocation Output Structure**

| Output          | Type/Dimensions                                     | Description   | Units/Valid Range  | Fill Value |
|-----------------|---|---|--|------------|
| Scan Start Time | Int64[VIIRS_RDR_SCANS]                              | Scan start time, defined at the leading edge of the first Earth View frame in IET               | Microseconds<br>0 <= scanStartTime <= 1.00E+38                               | -999       |
| Scan Mid Time   | Int64[VIIRS_RDR_SCANS]                              | Mid Time of Scan in IET   | Microseconds<br>0 <= scanMidTime <= 1.00E+38                                 | -999       |
| Latitude        | Float32[DNB_VIIRS_SDR_ROWS]<br>[DNB_VIIRS_SDR_COLS] | Geodetic latitude of the VIIRS pixels   | Degrees<br>-90° <= Latitude <= 90°<br>(positive to the North)                | -999.9     |
| Longitude       | Float32[DNB_VIIRS_SDR_ROWS]<br>[DNB_VIIRS_SDR_COLS] | Geodetic longitude of the VIIRS pixels  | Degrees<br>-180° <= Longitude <= 180°<br>(positive to the East of Greenwich) | -999.9     |
| SolarZenith     | Float32[DNB_VIIRS_SDR_ROWS]<br>[DNB_VIIRS_SDR_COLS] | Solar zenith angle relative to the VIIRS pixels measured from the local vertical                | Degrees<br>0° <= SolarZenith <= 180°   | -999.9     |
| SolarAzimuth    | Float32[DNB_VIIRS_SDR_ROWS]<br>[DNB_VIIRS_SDR_COLS] | solar azimuth angle relative to the VIIRS pixels and measured from the local North towards East | Degrees<br>-180° <= SolarAzimuth <= 180°                                     | -999.9     |
| satZen          | Float32[DNB_VIIRS_SDR_ROWS]<br>[DNB_VIIRS_SDR_COLS] | S/C zenith angle relative to the VIIRS pixels measured from the local vertical                  | Degrees<br>0° <= satZen <= 180°  | -999.9     |
| satAzm          | Float32[DNB_VIIRS_SDR_ROWS]<br>[DNB_VIIRS_SDR_COLS] | S/C azimuth angle relative to the VIIRS pixels and measured from the local North towards East   | Degrees<br>-180° <= satAzm <= 180°   | -999.9     |
| LunarZenith     | Float32[DNB_VIIRS_SDR_ROWS]<br>[DNB_VIIRS_SDR_COLS] | Lunar zenith angle relative to the VIIRS pixels measured from the local vertical                | Degrees<br>0° <= LunarZenith <= 180°   | -999.9     |
| LunarAzimuth    | Float32[DNB_VIIRS_SDR_ROWS]<br>[DNB_VIIRS_SDR_COLS] | Lunar azimuth angle relative to the VIIRS pixels and measured from the local North towards East | Degrees<br>-180° <= LunarAzimuth <= 180°                                     | -999.9     |
| Height          | Float32[DNB_VIIRS_SDR_ROWS]<br>[DNB_VIIRS_SDR_COLS] | Difference between ellipsoid and geoid heights  | Meters<br>-150 <= Height <= 150  | -999.9     |

| Output            | Type/Dimensions                                     | Description   | Units/Valid Range                                 | Fill Value |
|-------------------|---|---|---|------------|
| Range             | Float32[DNB_VIIRS_SDR_ROWS]<br>[DNB_VIIRS_SDR_COLS] | The distance from the ground position represented by the pixel to the S/C   | Meters<br>800000<=<br>Range<br><=2000000          | -999.9     |
| S/C Position      | Float32[VIIRS_RDR_SCANS][3]                         | S/C Position in ECR coordinates at mid-scan time  | Meters<br>-7.46E+06 <=<br>Position<br><=7.46E+06  | -999.9     |
| S/C Velocity      | Float32[VIIRS_RDR_SCANS][3]                         | S/C Velocity in ECR coordinates at mid-scan time  | Meters/sec<br>-6600<=<br>Velocity <=6600          | -999.9     |
| S/C Attitude      | Float32[VIIRS_RDR_SCANS][3]                         | S/C Attitude (roll, pitch, yaw) computed at mid-scan time. The roll, pitch, and yaw angles can be used to create a direction cosine matrix that rotates the S/C coordinates to the Orbit Frame coordinates <sup>1</sup> . | Arcseconds<br>-648000 <=<br>Attitude <=<br>648000 | -999.9     |
| S/C Solar Zenith  | Float32[VIIRS_RDR_SCANS]                            | Solar zenith angle with respect to the solar diffuser reference frame z-axis, where the SD z-axis is normal to the SD surface.  | Degrees<br>0 <= scSunZen<br><= 180                | -999.9     |
| S/C Solar Azimuth | Float32[VIIRS_RDR_SCANS]                            | Solar azimuth angle measured counterclockwise about the solar diffuser reference frame z-axis with respect to the solar diffuser x-axis (with positive z-axis towards the observer)                                       | Degrees<br>-180 <=<br>scSunZen <=<br>180          | -999.9     |
| moon_phase        | Float32   | Angle between ray vector from the moon to earth and ray vector of moon to sun.  | Degrees<br>0 <=<br>moon_phase <=<br>180           | -999.9     |
| mi_frac           | Float32   | Fraction of the moon illuminated (expressed as percent)   | No units<br>0.0 <= mi_frac<br><= 100              | -999.9     |
| scan_mode         | UInt8[VIIRS_RDR_SCANS]                              | The VIIRS operational mode, reported at the scan level. (Refer to Table 30.)  | None<br>0=Night; 1=Day;<br>2=Mixed                | 255        |
| mode              | UInt8   | The VIIRS operational mode, reported at the granule level. (Refer to Table 30.)   | None<br>0=Night; 1=Day;<br>2=Mixed                | 255        |
| act_scans         | Int32   | Actual number of VIIRS scans that were used to create this granule.   | 0 <= act_scans<br><= 48                           | -999       |
| scanQuality       | UInt8[VIIRS_RDR_SCANS]                              | Scan-level quality flags  | See QF1 in<br>Table 13                            | None       |
| Scan_Quality1     | UInt8[VIIRS_RDR_SCANS]                              | Scan-level quality flags  | See QF2 in<br>Table 13                            | None       |
| PixelQuality      | Int8[DNB_VIIRS_SDR_ROWS]<br>[DNB_VIIRS_SDR_COLS]    | Quality flags   | See Table 14                                      | None       |

<sup>1</sup> The Orbit Frame is defined as follows: the Orbit Frame z-axis is determined from the ECR position of the spacecraft. The initial vector is from the ECR position of the spacecraft to geodetic nadir. The ECR geodetic nadir vector is converted to ECI J2000 and converted to a unit vector. The ECR S/C velocity vector is converted to ECI J2000 coordinates, and the y-axis of the Orbit Frame is determined by calculating the following vector cross product: Orbit Frame z-axis X S/C velocity vector in ECI J2000. The result is then converted to a unit vector. The Orbit Frame x-axis is computed by taking the vector cross product of the y-axis and z-axis (y-axis X z-axis).

**Table 10 MOD Geolocation Output Structure**

| Output           | Type/Dimensions                                     | Description  | Units/Valid Range  | Fill Value |
|------------------|---|--|--|------------|
| Scan Start Time  | Int64[VIIRS_RDR_SCANS]                              | Scan start time, defined at the leading edge of the first Earth View frame in IET  | Microseconds<br>0 <= scanStartTime <= 1.00E+38                               | -999       |
| Scan Mid Time    | Int64[VIIRS_RDR_SCANS]                              | Mid Time of Scan in IET  | Microseconds<br>0 <= scanStartTime <= 1.00E+38                               | -999       |
| Latitude         | Float32[MOD_VIIRS_SDR_ROWS]<br>[MOD_VIIRS_SDR_COLS] | Geodetic latitude of the VIIRS pixels  | Degrees<br>-90° <= Latitude <= 90°<br>(positive to the North)                | -<br>999.9 |
| Longitude        | Float32[MOD_VIIRS_SDR_ROWS]<br>[MOD_VIIRS_SDR_COLS] | Geodetic longitude of the VIIRS pixels   | Degrees<br>-180° <= Longitude <= 180°<br>(positive to the East of Greenwich) | -<br>999.9 |
| SolarZenith      | Float32[MOD_VIIRS_SDR_ROWS]<br>[MOD_VIIRS_SDR_COLS] | Solar zenith angle relative to the VIIRS pixels measured from the local vertical   | Degrees<br>0 <= SolarZenith <= 180   | -<br>999.9 |
| SolarAzimuth     | Float32[MOD_VIIRS_SDR_ROWS]<br>[MOD_VIIRS_SDR_COLS] | solar azimuth angle relative to the VIIRS pixels and measured from the local North towards East  | Degrees<br>-180 <= SolarAzimuth <= 180                                       | -<br>999.9 |
| satZen           | Float32[MOD_VIIRS_SDR_ROWS]<br>[MOD_VIIRS_SDR_COLS] | S/C zenith angle relative to the VIIRS pixels measured from the local vertical   | Degrees<br>0° <= satZen <= 180°  | -<br>999.9 |
| satAzm           | Float32[MOD_VIIRS_SDR_ROWS]<br>[MOD_VIIRS_SDR_COLS] | S/C azimuth angle relative to the VIIRS pixels and measured from the local North towards East  | Degrees<br>-180 <= satAzm <= 180   | -<br>999.9 |
| Height           | Float32[MOD_VIIRS_SDR_ROWS]<br>[MOD_VIIRS_SDR_COLS] | Ellipsoid-geoid separation for non-terrain corrected Geo, and the height is the terrain height above the MSL for terrain corrected Geo   | Meters<br>-150 <= Height <= 150  | -<br>999.9 |
| Range            | Float32[MOD_VIIRS_SDR_ROWS]<br>[MOD_VIIRS_SDR_COLS] | The distance from the ground position represented by the pixel to the S/C  | Meters<br>800000 <= Range <= 2000000   | -<br>999.9 |
| S/C Position     | Float32[VIIRS_RDR_SCANS][3]                         | S/C Position in ECR coordinates at mid-scan time   | Meters<br>-7.46E+06 <= Position <= 7.46E+06                                  | -<br>999.9 |
| S/C Velocity     | Float32[VIIRS_RDR_SCANS][3]                         | S/C Velocity in ECR coordinates at mid-scan time   | Meters/sec<br>-6600 <= Velocity <= 6600                                      | -<br>999.9 |
| S/C Attitude     | Float32[VIIRS_RDR_SCANS][3]                         | S/C Attitude (roll, pitch, yaw) computed at mid-scan time. The roll, pitch, and yaw angles can be used to create a direction cosine matrix that rotates the S/C coordinates to the Orbit Frame coordinates (see Footnote 1). | Arcseconds<br>-648000 <= Attitude <= 648000                                  | -<br>999.9 |
| S/C Solar Zenith | Float32[VIIRS_RDR_SCANS]                            | Solar zenith angle with respect to the solar diffuser reference frame z-axis, where the SD z-axis is normal to the SD surface.   | Degrees<br>0 <= scSunZen <= 180  | -<br>999.9 |

| Output            | Type/Dimensions                              | Description   | Units/Valid Range                  | Fill Value |
|-------------------|--|---|------------------------------------|------------|
| S/C Solar Azimuth | Float32[VIIRS_RDR_SCANS]                     | Solar azimuth angle measured counterclockwise about the solar diffuser reference frame z-axis with respect to the solar diffuser x-axis (with positive z-axis towards the observer) | Degrees<br>-180 <= scSunZen <= 180 | -<br>999.9 |
| scan_mode         | Uint8[VIIRS_RDR_SCANS]                       | The VIIRS operational mode, reported at the scan level. (Refer to Table 30.)  | None<br>0=Night; 1=Day; 2=Mixed    | 255        |
| mode              | Uint8  | The VIIRS operational mode, reported at the granule level. (Refer to Table 30.)   | None<br>0=Night; 1=Day; 2=Mixed    | 255        |
| act_scans         | Int32  | Actual number of VIIRS scans that were used to create this granule.   | 0 <= act_scans <= 48               | -999       |
| scanQuality       | Uint8[VIIRS_RDR_SCANS]                       | Scan-level quality flags  | See QF1 in Table 13                | none       |
| Scan_Quality1     | Uint8[VIIRS_RDR_SCANS]                       | Scan-level quality flags  | See QF2 in Table 13                | None       |
| pixelQuality      | Int8[MOD_VIIRS_SDR_ROWS][MOD_VIIRS_SDR_COLS] | Pixel-level quality flags   | See Table 14                       | none       |

**Table 11 Unaggregated MOD Geolocation Output Structure**

| Output          | Type/Dimensions                                    | Description   | Units/Valid Range  | Fill Value |
|-----------------|--|---|--|------------|
| Scan Start Time | Int64[VIIRS_RDR_SCANS]                             | Scan start time, defined at the leading edge of the first Earth View frame in IET               | Microseconds<br>0 <= scanStartTime <= 1.00E+38                               | -999       |
| Scan Mid Time   | Int64[VIIRS_RDR_SCANS]                             | Mid Time of Scan in IET   | Microseconds<br>0 <= scanStartTime <= 1.00E+38                               | -999       |
| Latitude        | Float32[MOD_VIIRS_SDR_ROWS][MOD_UA_VIIRS_SDR_COLS] | Geodetic latitude of the VIIRS pixels   | Degrees<br>-90° <= Latitude <= 90°<br>(positive to the North)                | -<br>999.9 |
| Longitude       | Float32[MOD_VIIRS_SDR_ROWS][MOD_UA_VIIRS_SDR_COLS] | Geodetic longitude of the VIIRS pixels  | Degrees<br>-180° <= Longitude <= 180°<br>(positive to the East of Greenwich) | -<br>999.9 |
| SolarZenith     | Float32[MOD_VIIRS_SDR_ROWS][MOD_UA_VIIRS_SDR_COLS] | Solar zenith angle relative to the VIIRS pixels measured from the local vertical                | Degrees<br>0 <= SolarZenith <= 180   | -<br>999.9 |
| SolarAzimuth    | Float32[MOD_VIIRS_SDR_ROWS][MOD_UA_VIIRS_SDR_COLS] | solar azimuth angle relative to the VIIRS pixels and measured from the local North towards East | Degrees<br>-180 <= SolarAzimuth <= 180                                       | -<br>999.9 |
| satZen          | Float32[MOD_VIIRS_SDR_ROWS][MOD_UA_VIIRS_SDR_COLS] | S/C zenith angle relative to the VIIRS pixels measured from the local vertical                  | Degrees<br>0° <= satZen <= 180°  | -<br>999.9 |
| satAzm          | Float32[MOD_VIIRS_SDR_ROWS][MOD_UA_VIIRS_SDR_COLS] | S/C azimuth angle relative to the VIIRS pixels and measured from the local North towards East   | Degrees<br>-180 <= satAzm <= 180   | -<br>999.9 |

| Output            | Type/Dimensions  | Description  | Units/Valid Range                          | Fill Value |
|-------------------|--|--|--|------------|
| Height            | Float32[MOD_VIIRS_SDR_ROWS]<br>[MOD_UA_VIIRS_SDR_COLS] | Difference between ellipsoid and geoid heights   | Meters<br>-150 <= Height <= 150            | -<br>999.9 |
| Range             | Float32[MOD_VIIRS_SDR_ROWS]<br>[MOD_UA_VIIRS_SDR_COLS] | The distance from the ground position represented by the pixel to the S/C  | Meters<br>800000<= Range <=2000000         | -<br>999.9 |
| S/C Position      | Float32[VIIRS_RDR_SCANS][3]                            | S/C Position in ECR coordinates at mid-scan time   | Meters<br>-7.46E+06 <= Position <=7.46E+06 | -<br>999.9 |
| S/C Velocity      | Float32[VIIRS_RDR_SCANS][3]                            | S/C Velocity in ECR coordinates at mid-scan time   | Meters/sec<br>-6600<= Velocity <=6600      | -<br>999.9 |
| S/C Attitude      | Float32[VIIRS_RDR_SCANS][3]                            | S/C Attitude (roll, pitch, yaw) computed at mid-scan time. The roll, pitch, and yaw angles can be used to create a direction cosine matrix that rotates the S/C coordinates to the Orbit Frame coordinates (see Footnote 1). | -648000 <= Attitude <= 648000              | -<br>999.9 |
| S/C Solar Zenith  | Float32[VIIRS_RDR_SCANS]                               | Solar zenith angle with respect to the solar diffuser reference frame z-axis, where the SD z-axis is normal to the SD surface.   | Degrees<br>0 <= scSunZen <= 180            | -<br>999.9 |
| S/C Solar Azimuth | Float32[VIIRS_RDR_SCANS]                               | Solar azimuth angle measured counterclockwise about the solar diffuser reference frame z-axis with respect to the solar diffuser x-axis (with positive z-axis towards the observer)  | Degrees<br>-180 <= scSunZen <= 180         | -<br>999.9 |
| scan_mode         | Uint8[VIIRS_RDR_SCANS]                                 | The VIIRS operational mode, reported at the scan level. (Refer to Table 30.)   | None<br>0=Night; 1=Day; 2=Mixed            | 255        |
| mode              | Uint8  | The VIIRS operational mode, reported at the granule level. (Refer to Table 30)   | None<br>0=Night; 1=Day; 2=Mixed            | 255        |
| act_scans         | Int32  | Actual number of VIIRS scans that were used to create this granule.  | 0 <= act_scans <= 48                       | -999       |
| scanQuality       | Uint8[VIIRS_RDR_SCANS]                                 | Scan-level quality flags   | See QF1 in Table 13                        | none       |
| Scan_Quality1     | Uint8[VIIRS_RDR_SCANS]                                 | Scan-level quality flags   | See QF2 in Table 13                        | None       |
| pixelQuality      | Int8[MOD_VIIRS_SDR_ROWS]<br>[MOD_UA_VIIRS_SDR_COLS]    | Pixel-level quality flags  | See Table 14                               | none       |

**Table 12 IMG Geolocation Output Structure**

| Output          | Type/Dimensions        | Description   | Units/Valid Range                              | Fill Value |
|-----------------|------------------------|---|--|------------|
| Scan Start Time | Int64[VIIRS_RDR_SCANS] | Scan start time, defined at the leading edge of the first Earth View frame in IET | Microseconds<br>0 <= scanStartTime <= 1.00E+38 | -999       |
| Scan Mid Time   | Int64[VIIRS_RDR_SCANS] | Starting Time of Scan in IET  | Microseconds<br>0 <= scanStartTime <= 1.00E+38 | -999       |

| Output            | Type/Dimensions                                     | Description  | Units/Valid Range  | Fill Value |
|-------------------|---|--|--|------------|
| Latitude          | Float32[IMG_VIIRS_SDR_ROWS]<br>[IMG_VIIRS_SDR_COLS] | Geodetic latitude of the VIIRS pixels  | Degrees<br>-90° <= Latitude<br><= 90°<br>(positive to the North)             | -999.9     |
| Longitude         | Float32[IMG_VIIRS_SDR_ROWS]<br>[IMG_VIIRS_SDR_COLS] | Geodetic longitude of the VIIRS pixels   | Degrees<br>-180° <= Longitude <= 180°<br>(positive to the East of Greenwich) | -999.9     |
| SolarZenith       | Float32[IMG_VIIRS_SDR_ROWS]<br>[IMG_VIIRS_SDR_COLS] | Solar zenith angle relative to the VIIRS pixels measured from the local vertical   | Degrees<br>0 <= SolarZenith <= 180   | -999.9     |
| SolarAzimuth      | Float32[IMG_VIIRS_SDR_ROWS]<br>[IMG_VIIRS_SDR_COLS] | solar azimuth angle relative to the VIIRS pixels and measured from the local North towards East  | Degrees<br>-180 <= SolarAzimuth <= 180                                       | -999.9     |
| satZen            | Float32[IMG_VIIRS_SDR_ROWS]<br>[IMG_VIIRS_SDR_COLS] | S/C zenith angle relative to the VIIRS pixels measured from the local vertical   | Degrees<br>0° <= satZen <= 180°  | -999.9     |
| satAzm            | Float32[IMG_VIIRS_SDR_ROWS]<br>[IMG_VIIRS_SDR_COLS] | S/C azimuth angle relative to the VIIRS pixels and measured from the local North towards East  | Degrees<br>-180 <= satAzm <= 180   | -999.9     |
| Height            | Float32[IMG_VIIRS_SDR_ROWS]<br>[IMG_VIIRS_SDR_COLS] | Ellipsoid-geoid separation for non-terrain corrected Geo, and the height is the terrain height above the MSL for terrain corrected Geo   | Meters<br>-150 <= Height <= 150  | -999.9     |
| Range             | Float32[IMG_VIIRS_SDR_ROWS]<br>[IMG_VIIRS_SDR_COLS] | The distance from the ground position represented by the pixel to the S/C  | Meters<br>800000 <= Range <= 2000000   | -999.9     |
| S/C Position      | Float32[VIIRS_RDR_SCANS][3]                         | S/C Position in ECR coordinates at mid-scan time   | Meters<br>-7.46E+06 <= Position <= 7.46E+06                                  | -999.9     |
| S/C Velocity      | Float32[VIIRS_RDR_SCANS][3]                         | S/C Velocity in ECR coordinates at mid-scan time   | Meters/sec<br>-6600 <= Velocity <= 6600                                      | -999.9     |
| S/C Attitude      | Float32[VIIRS_RDR_SCANS][3]                         | S/C Attitude (roll, pitch, yaw) computed at mid-scan time. The roll, pitch, and yaw angles can be used to create a direction cosine matrix that rotates the S/C coordinates to the Orbit Frame coordinates (see Footnote 1). | Arcseconds<br>-648000 <= Attitude <= 648000                                  | -999.9     |
| S/C Solar Zenith  | Float32[VIIRS_RDR_SCANS]                            | Solar zenith angle with respect to the solar diffuser reference frame z-axis, where the SD z-axis is normal to the SD surface.   | Degrees<br>0 <= scSunZen <= 180  | -999.9     |
| S/C Solar Azimuth | Float32[VIIRS_RDR_SCANS]                            | Solar azimuth angle measured counterclockwise about the solar diffuser reference frame z-axis with respect to the solar diffuser x-axis (with positive z-axis towards the observer)  | Degrees<br>-180 <= scSunZen <= 180   | -999.9     |
| scan_mode         | Uint8[VIIRS_RDR_SCANS]                              | The VIIRS operational mode, reported at the scan level. (Refer to Table 30.)   | None<br>0=Night; 1=Day; 2=Mixed  | 255        |

| Output        | Type/Dimensions                              | Description  | Units/Valid Range               | Fill Value |
|---------------|--|--|---------------------------------|------------|
| mode          | UInt8  | The VIIRS operational mode, reported at the granule level. (Refer to Table 30) | None<br>0=Night; 1=Day; 2=Mixed | 255        |
| act_scans     | Int32  | Actual number of VIIRS scans that were used to create this granule.            | 0 <= act_scans <= 48            | -999       |
| scanQuality   | UInt8[VIIRS_RDR_SCANS]                       | Scan-level quality flags   | See QF1 in Table 13             | None       |
| Scan_Quality1 | UInt8[VIIRS_RDR_SCANS]                       | Scan-level quality flags   | See QF2 in Table 13             | None       |
| pixelQuality  | Int8[IMG_VIIRS_SDR_ROWS][IMG_VIIRS_SDR_COLS] | Pixel-level quality flags  | See Table 14                    | None       |

**Table 13 Scan Level Geolocation Quality Bytes**

| Byte | Bit | Flag Description                       | Result  |
|------|-----|--|---|
| QF1  | 0-1 | Interpolation Stage                    | 0: Nominal – E&A data available<br>1: Missing data <= Small gap<br>2: Small gap < Missing data <= Granule boundary<br>3: Missing data > Granule boundary  |
|      | 2-3 | HAM/RTA Encoder Flag                   | 0: Good data – all encoder data is valid<br>1: Bad data – either HAM encoders, RTA encoders or both corrupted for the entire scan<br>2: Degraded data – either HAM encoders, RTA encoders or both are corrupted within the scan.<br>3: Missing data – Missing encoder data for the scan (dropped engineering packets) |
|      | 4   | Above South Atlantic Anomaly           | 0: False<br>1: True   |
|      | 5   | Solar Eclipse                          | 0: False<br>1: True   |
|      | 6   | Lunar Eclipse (DNB only)               | 0: False<br>1: True   |
|      | 7   | HAM Side                               | 0: Mirror Side A<br>1: Mirror Side B  |
| QF2  | 0-1 | Scan Controller Electronics (SCE) Side | 0: Both sides powered off<br>1: Side A power on<br>2: Side B power on<br>3: Invalid side (this should never occur)  |
|      | 4-7 | Spare                                  |   |

**Table 14 Pixel Level Geolocation Quality Byte**

| Bit | Flag Description   | Result                              |
|-----|--|-------------------------------------|
| 0   | Input Quality indicates whether any of the S/C ephemeris or attitude data is invalid or the encoder data is invalid            | 0: Input valid<br>1: Input invalid  |
| 1   | Pointing indicates that the sensor Line of Sight does not intersect the geoid, is near the limb, or has invalid sensor angles. | 0: Pointing good<br>1: Pointing bad |

|   |  |   |
|---|--|---|
| 2 | Terrain indicates that the algorithm could not obtain a valid terrain value. | 0: Terrain good<br>1: Terrain bad         |
| 3 | Solar Angle indicates that the solar angles are good or bad.                 | 0: Solar angle good<br>1: Solar angle bad |

### 2.2.1.2.1 Geolocation Gridded Outputs

In addition to the Granule and Scan level data specified in Tables 9 – 12, each gridded product contains map data defined in Table 15, plus the pixel level data listed in Table 16 and Table 17.

**Table 15 Map Data Set (mds\_type) (Geolocation)**

| Output            | Type/Dimensions | Description  | Units/Valid Range   | Fill Value |
|-------------------|-----------------|--|---|------------|
| grid_type         | Int16           | identifies which map projection is being used  | 11=std Mercator, cylindrical, coaxial<br>21=Polar Stereographic, Northern Hemisphere<br>25=Polar Stereographic, Southern Hemisphere<br>31=Lambert Conformal Conic, Tangent cone, Northern Hemisphere<br>35=Lambert Conformal Conic, Tangent cone, Southern Hemisphere<br>41=Lambert Conformal Conic, Secant cone, Northern Hemisphere<br>45=Lambert Conformal Conic, Secant cone, Southern Hemisphere<br>51=Cylindrical Equidistant<br>61=Northern Polar Azimuthal Equidistant<br>65=Southern Polar Azimuthal Equidistant | none       |
| wedge_rotation    | Int16           | used for Lambert Conformal Conic, position of the empty wedge                              | 1=up,2=left,3=down,4=right  | none       |
| mds_num           | Int32           | id number of mds, not used by NPOESS system  | unitless  | none       |
| stan_lat1         | Float64         | first std latitude   | radians/-pi/2 to +pi/2  | none       |
| stan_lat2         | Float64         | 2 <sup>nd</sup> std latitude, needed for Lambert Conformal Conics, secant cone projections | radians/-pi/2 to +pi/2  | none       |
| base_lon          | Float64         | base longitude of the X-Y coordinate system  | radians/-pi to +pi  | none       |
| grid_inc_constant | Float64         | determines scaling and grid sizes  | unitless  | none       |
| grid_inc_c2       | Float64         | 2 <sup>nd</sup> constant of same purpose, needed in cylindrical equidistant                | unitless  | none       |
| grid_exponent     | Float64         | needed for Lambert projections   | unitless  | none       |
| grid_constant_A   | Float64         | needed for Lambert   | unitless  | none       |

| Output        | Type/Dimensions | Description   | Units/Valid Range                  | Fill Value |
|---------------|-----------------|---|------------------------------------|------------|
|               |                 | projections   |                                    |            |
| max_row       | Float64         | max grid row number   | established at time MDS is created | none       |
| max_col       | Float64         | max grid column number  | established at time MDS is created | none       |
| upr_left_lat  | Float64         | latitude of grid upper left corner  | radians/-pi/2 to +pi/2             | none       |
| upr_left_lon  | Float64         | longitude of grid upper left corner   | radians/-pi to +pi                 | none       |
| lwr_right_lat | Float64         | latitude of grid lower right corner   | radians/-pi/2 to +pi/2             | none       |
| lwr_right_lon | Float64         | longitude of grid lower right corner  | radians/-pi to +pi                 | none       |
| upr_left_x    | Float64         | x coordinate of upper left corner   | established at time MDS is created | none       |
| upr_left_y    | Float64         | y coordinate of upper left corner   | established at time MDS is created | none       |
| lwr_right_x   | Float64         | x coordinate of lower right corner  | established at time MDS is created | none       |
| lwr_right_y   | Float64         | y coordinate of lower right corner  | established at time MDS is created | none       |
| split_lon     | Float64         | longitude on both sides of empty sector for all lamberts  | radians/-pi to +pi                 | none       |
| costanlat     | Float64         | cosine tangent of latitude  | unitless                           | none       |
| latsml        | Float64         | smallest latitude in the MDS  | radians/-pi/2 to +pi/2             | none       |
| latbig        | Float64         | largest latitude in the MDS   | radians/-pi/2 to +pi/2             | none       |
| lonqml        | Float64/[2]     | smallest longitude in the MDS (need 2 because there might be 2 longitude ranges in the MDS, which happens when the MDS spans 180 degrees longitude) | radians/-pi to +pi                 | none       |
| lonbig        | Float64/[2]     | biggest longitude in the MDS, need 2 for the same reason as lonqml  | radians/-pi to +pi                 | none       |
| num_lonrange  | Int16           | number of longitude ranges in MDS   | always either 1 or 2               | none       |

Table 16 Gridded Geolocation Moderate Output (Geolocation)

| Output   | Type/Dimensions                                  | Description                                  | Units/Valid Range | Fill Value       |
|----------|--|--|-------------------|------------------|
| grow     | Float64/<br>[M_VIIRS_SDR_ROWS][M_VIIRS_SDR_COLS] | row location in grid                         | unitless          | ERR_FLOAT64_FILL |
| gcol     | Float64/<br>[M_VIIRS_SDR_ROWS][M_VIIRS_SDR_COLS] | column location in grid                      | unitless          | ERR_FLOAT64_FILL |
| ctr_grow | Float64/<br>[MOD_GEOLOC_ROWS][MOD_GEOLOC_COLS]   | center coordinate of interpolation rectangle | unitless          | ERR_FLOAT64_FILL |
| ctr_gcol | Float64/<br>[MOD_GEOLOC_ROWS][MOD_GEOLOC_COLS]   | center coordinate of interpolation rectangle | unitless          | ERR_FLOAT64_FILL |

| Output | Type/Dimensions | Description            | Units/Valid Range | Fill Value |
|--------|-----------------|------------------------|-------------------|------------|
| gmds   | mds_type        | map data set structure | N/A               | N/A        |

**Table 17 Gridded Geolocation Imagery Output (Geolocation)**

| Output   | Type/Dimensions                                  | Description                                  | Units/Valid Range | Fill Value       |
|----------|--|--|-------------------|------------------|
| grow     | Float64/<br>[I_VIIRS_SDR_ROWS][I_VIIRS_SDR_COLS] | row location in grid                         | unitless          | ERR_FLOAT64_FILL |
| gcol     | Float64/<br>[I_VIIRS_SDR_ROWS][I_VIIRS_SDR_COLS] | column location in grid                      | unitless          | ERR_FLOAT64_FILL |
| ctr_grow | Float64<br>[IMG_GEOLOC_ROWS][IMG_GEOLOC_COLS]    | center coordinate of interpolation rectangle | unitless          | ERR_FLOAT64_FILL |
| ctr_gcol | Float64/<br>[IMG_GEOLOC_ROWS][IMG_GEOLOC_COLS]   | center coordinate of interpolation rectangle | unitless          | ERR_FLOAT64_FILL |
| gmds     | mds_type   | map data set structure                       | N/A               | N/A              |

**2.2.2 Algorithm Processing**

IDPS designed and developed a library of functions called common GEO that are used by all of the SDRs to calculate geodetic latitude and longitude as well as solar and lunar geometries. ProSdrCmnGeo methods are to: retrieve attitude and ephemeris information; retrieve moon vectors; determine the nadir latitude and longitude values of the scan; determine the ellipsoid intersect and satellite angles for each pixel and get terrain correction GEO values for each pixel. For more details regarding the common GEO library of functions, please refer to the ProSdrCmnGeo OAD, D41869.

Geolocation is performed using a combination of sensor specific functions and the Common Geolocation library of functions. The main driver for the geolocation algorithm is called geolocateGranule(). Consecutive calls to this driver are issued for each band type: DNB, Imagery, and Moderate. The Day/Night Band is processed first, followed by Imagery (ellipsoid and terrain corrected), and Moderate (ellipsoid and terrain corrected, and unaggregated Moderate). In order to meet latency requirements, the operational Geolocation code has implemented an interpolation scheme for computing ellipsoid geolocation. For DNB and Imagery resolution, ellipsoid geolocation is determined by performing full geolocation on a subset of pixels. The lat/long values for this subset of points are converted to a polar stereographic grid, and then quadratic interpolation is used to determine the geolocation for the remaining pixels. The results from the interpolation are then converted back to lat/long values. The terrain corrected product for Imagery is generated from the ellipsoid product for each lat/long pixel. The Moderate resolution ellipsoid product is created from the Imagery ellipsoid product by averaging four imagery pixels that surround each Moderate pixel. This averaging is done to compute the MOD ellipsoid geo for all pixels except for a subset of pixels near nadir, where full geolocation is performed (see Section 2.2.2.19 for more details). The resulting Moderate geolocation is then used to generate the terrain corrected product, as well as the unaggregated Moderate product. The unaggregated product is produced by a quadratic interpolation scheme that has been implemented as part of the code optimization for latency improvement.

### 2.2.2.1 Main driver for Geolocation ( geolocateGranule() )

The main driver for geolocation is called `geolocateGranule()`. It calls the function `initGeoDataStructs()` to initialize the processing parameters, validate the scan encoder data, determine the thermal correction matrix, and to determine the band type dependent sample times. The next step in the `geolocateGranule()` function is to check the band type setting. If band type is set to Moderate resolution, then the function `calcModFromImg()` is called to calculate the Moderate geolocation products (ellipsoid, terrain corrected and unaggregated). If the band type is set to DNB or Imagery, the function `createInterpRctngls()` is called to define a subset of pixels based on rectangles that span across the scan and do not cross the aggregation zone boundaries. Next, `geolocateDecim()` is called to perform the full geolocation on the decimated set of points, and then `geolocateFullFromDecim()` is called to calculate the geolocation of the remaining pixels using quadratic interpolation. The final step of the `geolocateGranule()` function is to store the geolocation data to memory using the function called `storeGranule()`. If the band type is Imagery, the terrain corrected product is produced in `storeGranule()`, and then saved to memory. The flow diagram for `geolocateGranule()` is shown in Figure 8.

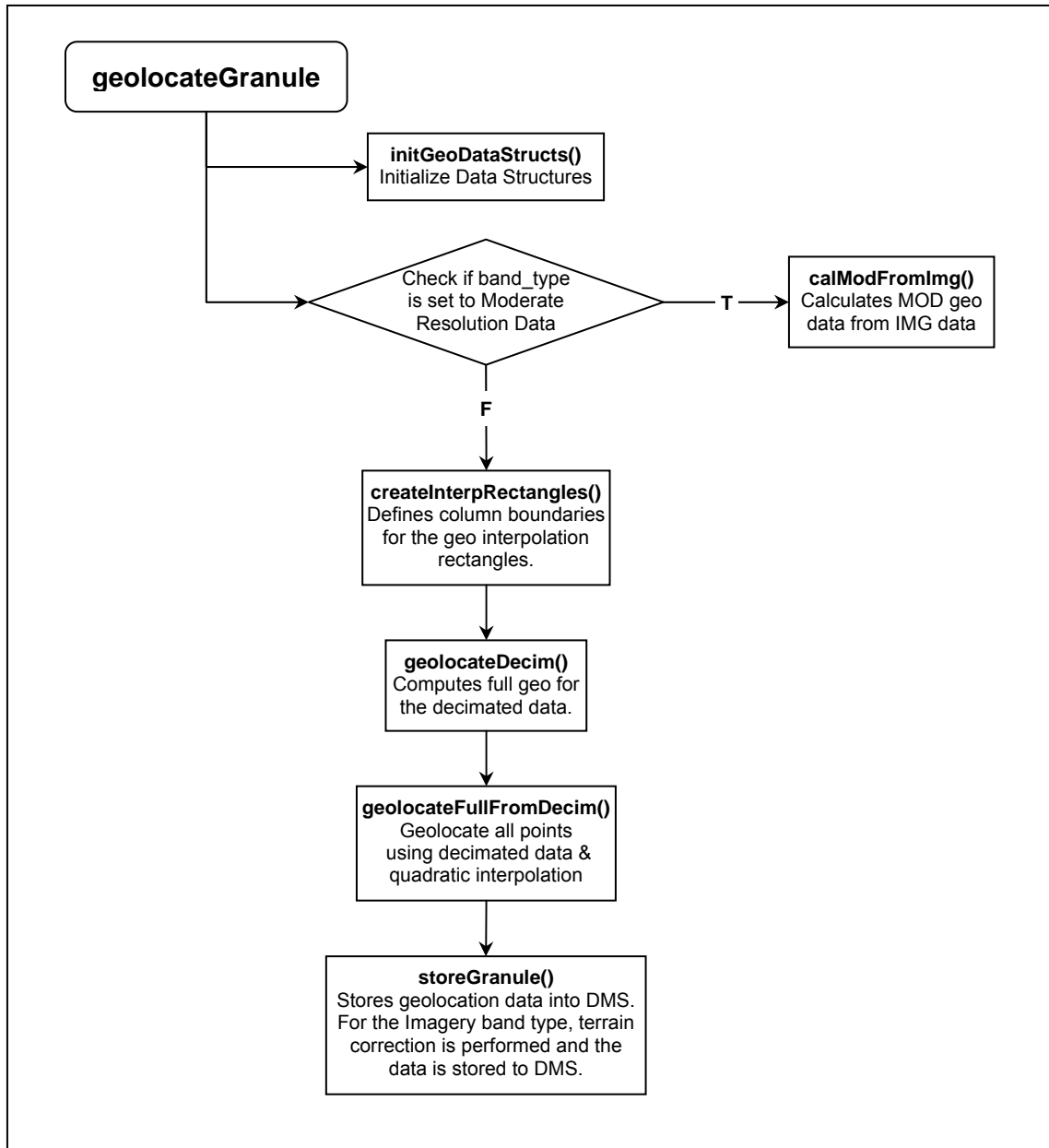


Figure 8 geolocateGranule() Flow Diagram

2.2.2.2 GEO\_absolute\_limit\_check()

GEO\_absolute\_limit\_check() validates a set of input data samples against absolute limits. Flags are set to BAD\_DATA for all samples that are not within limits.

### **2.2.2.3 GEO\_determine\_DNB\_sample\_time\_offsets()**

`GEO_determine_DNB_sample_time_offsets()` determines the set of relative sample times for all pixels for the DNB. It uses the sample index range to determine the aggregation zone and the number of samples and photosites per zone.

The scan starts at DNB aggregation zone 32, moves through the decreasing side of nadir from zone 32 through to zone 1, crosses nadir, and continues through the increasing side of nadir from zone 1 through to zone 32 where it ends. (i.e. 32, 3, ..., 2, 1, 1, 2, ..., 31, 32).

The sample time determined is the time relative to the scan start. The scan start time is not added, as the GEO software already does this. The relative time is also used independently in several locations.

### **2.2.2.4 GEO\_determine\_sample\_time\_offsets()**

`GEO_determine_sample_time_offsets()` determines the set of relative sample times for all pixels for the requested resolution. It uses the sample index range to determine the aggregation zone and the number of samples (or observations) to be aggregated into a pixel.

The sample time for the first pixel is determined using the latch-to-center time and a time factor for the appropriate resolution. Subsequent sample times use the preceding sample time.

The sample time determined is the time relative to the scan start. The scan start time is not added, as the GEO software already does this. The relative time is also used independently in several locations.

### **2.2.2.5 GEO\_determine\_thermal\_corrections()**

`GEO_determine_thermal_corrections()` determines the temperature dependent corrections to apply to the granule's geolocation.

Note: The delivered routine of the science VIIRS geolocation code contained an untested or unverified version of temperature correction. All of the delivered test data had the routine 'turned off' by an indicator flag in the test data set. Rather than commenting out the sections of unverified code, it was determined to be better to replace the routine with a stubbed version that was always 'turned on' and returned zero correction for temperature. It is recognized that this routine is to be replaced once actual thermal correction testing verification has occurred. As the routine is currently implemented it should be easy to plug in a new routine into the existing code.

### **2.2.2.6 GEO\_determine\_view\_vectors()**

`GEO_determine_view_vectors()` calculates object space view vectors in the instrument coordinate system for each along-track detector in a sample. See Figure 9 below.

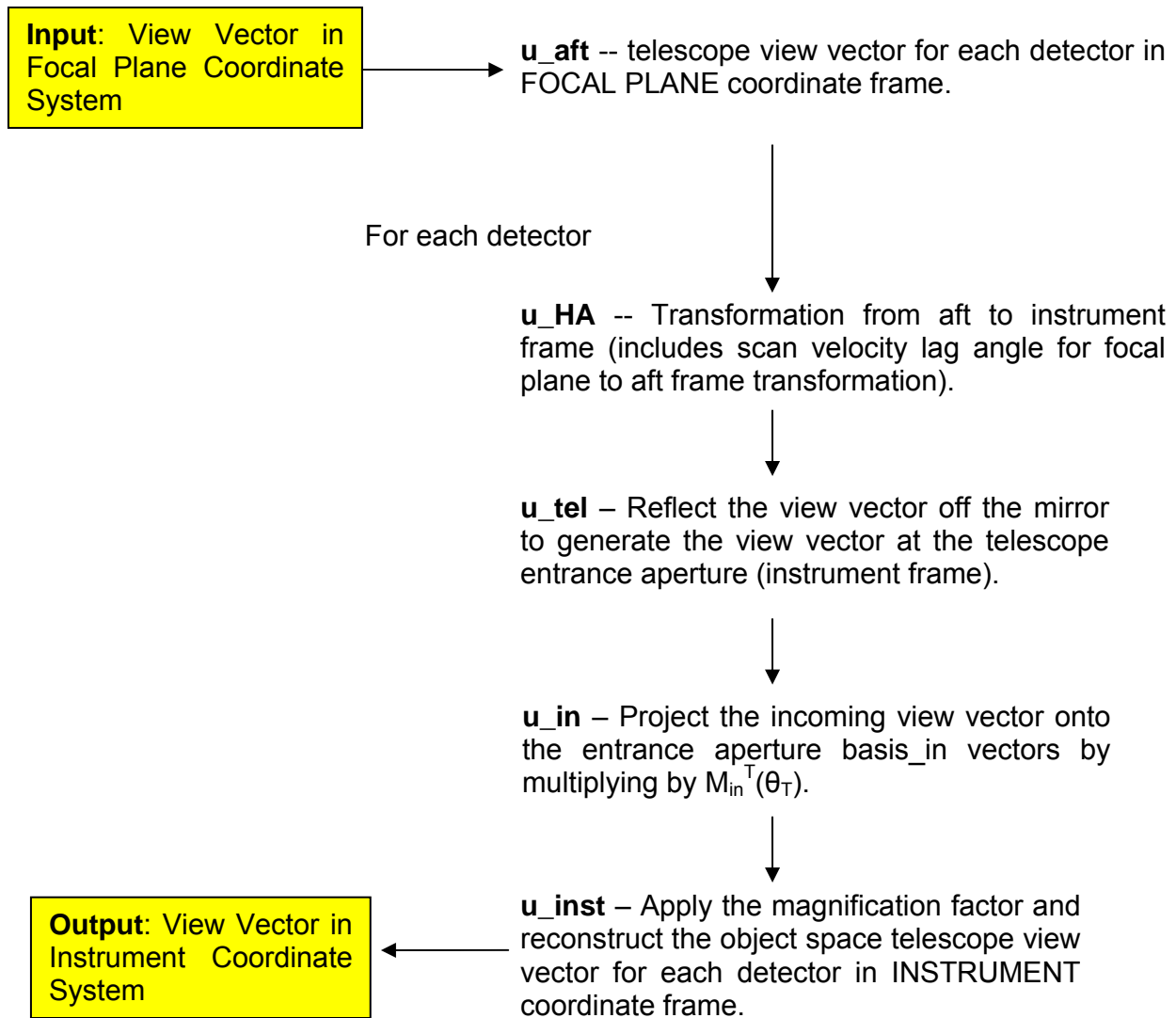


Figure 9 GEO\_determine\_view\_vectors() Block Diagram (Geolocation)

### 2.2.2.7 GEO\_evaluate\_polynomial()

GEO\_evaluate\_polynomial() uses the input parameters to evaluate a polynomial.

### 2.2.2.8 GEO\_find\_next\_flag()

GEO\_find\_next\_flag() finds the next unflagged sample in a flag array.

### 2.2.2.9 GEO\_get\_grid()

GEO\_get\_grid() generates a grid product.

**2.2.2.10 GEO\_interp\_mod\_unagg()**

GEO\_interp\_mod\_unagg() uses a quadratic interpolation method to calculate GEO from the values already calculated for the aggregated Moderate resolution, then stores per scan data into output structures based on resolution.

**2.2.2.11 GEO\_interpolate\_mirror\_encoder()**

GEO\_interpolate\_mirror\_encoder() interpolates the mirror encoder number using a linear interpolation method to interpolate the encoder data to the sample time, using the identified encoder times as bounding variables.

**2.2.2.12 GEO\_interpolate\_telescope\_encoder()**

GEO\_interpolate\_telescope\_encoder() interpolates the telescope encoder number using a linear interpolation method to interpolate the encoder data to the sample time, using the encoder times as bounding variables.

**2.2.2.13 GEO\_process\_parameters()**

GEO\_process\_parameters() processes input parameter files to extract key values used in GEO processing.

**2.2.2.14 GEO\_relative\_limit\_check()**

GEO\_relative limit check() validates a set of data samples by comparing differences between successive samples against a limit. Previously flagged values are not checked. Flags are set to BAD\_DATA for all samples not within limits.

**2.2.2.15 GEO\_validate\_scan\_encoder\_data()**

GEO\_validate\_scan\_encoder\_data() unpacks the telescope and mirror encoder data from the encoder and sector start segments. For each scan, it unpacks mirror encoder times from the encoder data, computes encoder values from the sector start and mirror side, and validates the data.

**2.2.2.16 geolocatePixel()**

This function performs full geolocation for a specific pixel. It uses the ProSdrCmnGeo class to calculate the ellipsoid intersection latitude, longitude and the azimuth, zenith angles to the spacecraft, sun, and moon.

**2.2.2.17 geolocateDecim()**

This function generates geolocation data for the subset of points that define the interpolation rectangles.

**2.2.2.18 geolocateFullFromDecim()**

This function uses quadratic interpolation to provide geolocation data for all pixels in the interpolation rectangles.

**2.2.2.19 calcModFromImg()**

This function calculates the geolocation data for the aggregated Moderate band type by averaging the four Imagery pixels that surround each Moderate pixel. The Imagery pixels are still in the default projection. Due to small satellite zenith values, the code performs full geolocation for pixels that are near nadir. This region is defined by pixel column (1531 through 1670 zero based). The function also generates the terrain corrected product from the ellipsoid for each lat/long pixel.

**2.2.2.20 createInterpRctngls()**

This function defines the start, middle, and end row/column numbers for each interpolation rectangle.

**2.2.2.21 initGeoDataStructs()**

This function initializes structures and setup data necessary for geolocation.

**2.2.2.22 storeGranule()**

This function copies the geolocation data for each band type into DMS. For the Imagery band type, terrain correction occurs here.

**2.2.2.23 fixSatAngles()**

This function corrects satellite azimuth angles. When the satellite zenith angle gets very small, the satellite azimuth angle changes rapidly. Because quadratic interpolation was used, the satellite azimuth angles need to be recalculated.

**2.2.2.24 quadInterp()**

This function performs quadratic interpolation.

### **2.2.2.25 geolocateAllRecPix()**

This function performs full geolocation calculations for every pixel in an interpolation rectangle. These calculations are done only if an error does not occur in any of the nine points in the interpolation rectangle.

### **2.2.2.26 interpLocations()**

This function interpolates the latitude and longitude values. The function converts the lat/long values to polar stereographic projection and performs the quadInterp function. The results of this are then converted back to lat/long values.

### **2.2.2.27 interpAngles()**

This function interpolates the satellite, sun, and moon azimuth and zenith angles.

### **2.2.2.28 Geolocation Quality Flag Logic**

Every output product has one pixel level quality flag. The pixel quality flag is an eight-bit field for each pixel indicating the status of the invalid input, bad pointing, bad terrain, invalid solar angles, and a spare unused bit. See Table 14. Any pixel level quality flag with a value of zero contains good data and a pixel level quality flag value other than zero contains anomalous data.

Each output also has two scan level quality flags. The first scan quality flag is an 8-bit field representing the Interpolation Stage, HAM impulse flag, SAA, Solar Eclipse, Lunar Eclipse flags and HAM side. The second quality flag is an 8-bit field representing the Scan Encoder Electronics side. See Table 13. Details of the logic used to set these quality flags can be learned by examining the geolocation functions along with the geolocatePixel() and geolocateGranule() functions.

### **2.2.2.29 Create Degree GEO Products**

After geolocation and calibration processing have been completed then the delivered GEO products, with angles in degrees, are created by calling createDegreeProducts() and convertToDegrees(). This process is performed for all six non-gridded geolocation products.

Angle-values such as latitude, longitude, and satellite and solar azimuth and zenith angles are stored as radians for the internal GEO products and as degrees for the delivered GEO products. The DNB output GEO has no corresponding radian (internal) form, and reports all of the angle-values previously mentioned, with the addition of lunar azimuth and zenith angles and moon phase, in degrees.

## **2.2.3 Graceful Degradation**

The VIIRS SDR Geolocation procedure contains no graceful degradation.

### 2.2.3.1 Graceful Degradation Inputs

None.

### 2.2.3.2 Graceful Degradation Processing

None.

### 2.2.3.3 Graceful Degradation Outputs

None.

## 2.2.4 Exception Handling

The error handling concept used produces a product if at all possible. This is accomplished by using error fill values to fill data structures at the scan and pixel levels, setting flags and continuing with processing to recover from minor errors and still be able to produce a product. Error handling has been implemented at the granule, scan, and pixel levels of the code.

At the granule level, invalid function arguments, out-of-bound arrays, and failed function calls result in error messages being sent via the INF log mechanism and exiting the function by returning a fail value (with the exception of a failed call to `GEO_get_Gring_points()` which causes an error message to be sent and fill values to be used). When this occurs, no GEO product for that granule is produced. If missing scans are detected, an error message is sent, the scans are filled with fill values, and processing continues.

At the scan level, invalid function arguments and out-of-bound arrays result in error messages being sent via the infrastructure log mechanism and exiting the function by returning a fail value to the granule level function. For invalid IET time, invalid satellite attitude and ephemeris, or invalid mirror side, a flag is set, the entire scan is filled with the appropriate fill values and processing continues with the next scan. For invalid satellite ephemeris and attitude data, invalid sun or moon angles, no ellipse intersect, failed terrain correction, or failure in determining view vectors, a flag is set, the sample is filled with the appropriate fill values, and processing continues with the next sample in the scan.

At the pixel level, invalid function arguments, out-of-bound arrays, and failed function calls result in error messages being sent via the infrastructure log mechanism and exiting the function by returning a fail value. The returned "fail values" are caught by the scan level calling functions resulting in the pixel being filled with the error fill value, a flag being set, and processing continuing with the next pixel.

## 2.2.5 Data Quality Monitoring

No data quality monitoring is performed by the VIIRS SDR Geolocation procedure.

## 2.2.6 Computational Precision Requirements

All internal calculations are done at double precision, and they need to be done this way as small scan angle errors lead to large GEO errors. The geodetic Latitude and Longitude fields are output

as floats, which can introduce an uncertainty no larger than two meters in Earth location. Sensor, sun and lunar angles are output as floats.

## 2.2.7 Algorithm Support Considerations

The DMS and INF must be running before the algorithm is executed.

## 2.2.8 Assumptions and Limitations

### 2.2.8.1 Sci2Ops Issues

From the examination and exercising of the accompanying code, several considerations about possible implementation modifications have been identified. Some of the following comments incorporate insights provided by one of the code developers, Mark Kowitt.

- Thermal correction from S/C attitude to mounting matrix.
- The thermal compensation mechanism for the VIIRS sensor has been implemented as an error in effective attitude (roll, pitch and yaw) of the spacecraft. If a common module is implemented, the thermal “error” term should be used to modify the instrument-to-spacecraft effective alignment, rather than the spacecraft attitude.

Note: The delivered routine of the science VIIRS GEO code contained an untested or unverified version of temperature correction. All of the delivered test data had the routine ‘turned off’ by an indicator flag in the test data set. Rather than commenting out the sections of unverified code, it was determined to be better to replace the routine with a stubbed version that was always ‘turned on’ and returned zero correction for temperature. It is recognized that this routine is to be replaced once actual thermal correction testing verification has occurred. As the routine is currently implemented it should be easy to plug in a new routine into the existing code.

### 2.2.8.2 Numerical Computation Considerations

Several of the inputs in the parameters LUT have to be updated when results from SBRS testing become available and during CalVal. These values are modified to eliminate most of the static and slowly varying biases affecting GEO uncertainty. The methodology to determine these changes has been developed for other sensors, but it has not yet been adapted to VIIRS and no software in its support has been written.

### 2.2.8.3 Additional Assumptions

It is assumed that the Verified VIIRS RDR and the Verified spacecraft E&A RDR is available for processing. The VIIRS flight model identifier and the RTA and HAM encoder data are assumed to be present in the RDR and of good quality.

#### 2.2.8.4 Additional Limitations

Refer to Section 4.2 of the Geolocation Algorithm Theoretical Basis Document, D43776, for the limitations associated with the algorithm.

### 2.3 VIIRS SDR Calibration Description

The purpose of the Radiometric CAL Component is to convert the VIIRS digital counts to radiance fields at the top of atmosphere (TOA), as well as brightness temperature and reflectance values. The algorithm used for radiometric CAL has been derived from first principles and then simplified through judicious specifications of algorithm input parameters. The Radiometric CAL Component processes the Verified VIIRS Raw Data Records (RDRs) to produce VIIRS SDRs, VIIRS On-board Calibrator (OBC) Intermediate Product (IP), and VIIRS Calibrated Dual Gain IP<sup>2</sup>. The output SDR data fields include TOA radiances, reflectances, and brightness temperature fields, in addition to quality information. The prototype science code consists of two independent, executable units: Earth View (EV) Radiometric CAL Unit and a Solar Diffuser (SD) View Data Processing Unit. The EV Radiometric CAL Unit is executed on a near real-time basis, whereas the SD View Processing Unit is executed once per orbit. Outputs from the EV Radiometric CAL Unit are the VIIRS SDRs for each resolution, the Dual Gain IP, and the OBC IP. The SD View Data Processing Unit produces scale factors, F, that are used as a multiplier to the CAL lookup tables (LUTs) used by the EV Radiometric CAL Unit. Refer to Section 2.3.1.2 for details on output SDRs and Ips. The Calibration Processing Chain is shown in

Figure 10.

---

<sup>2</sup> For dual gain bands only: M1 – M5, M7 and M13.

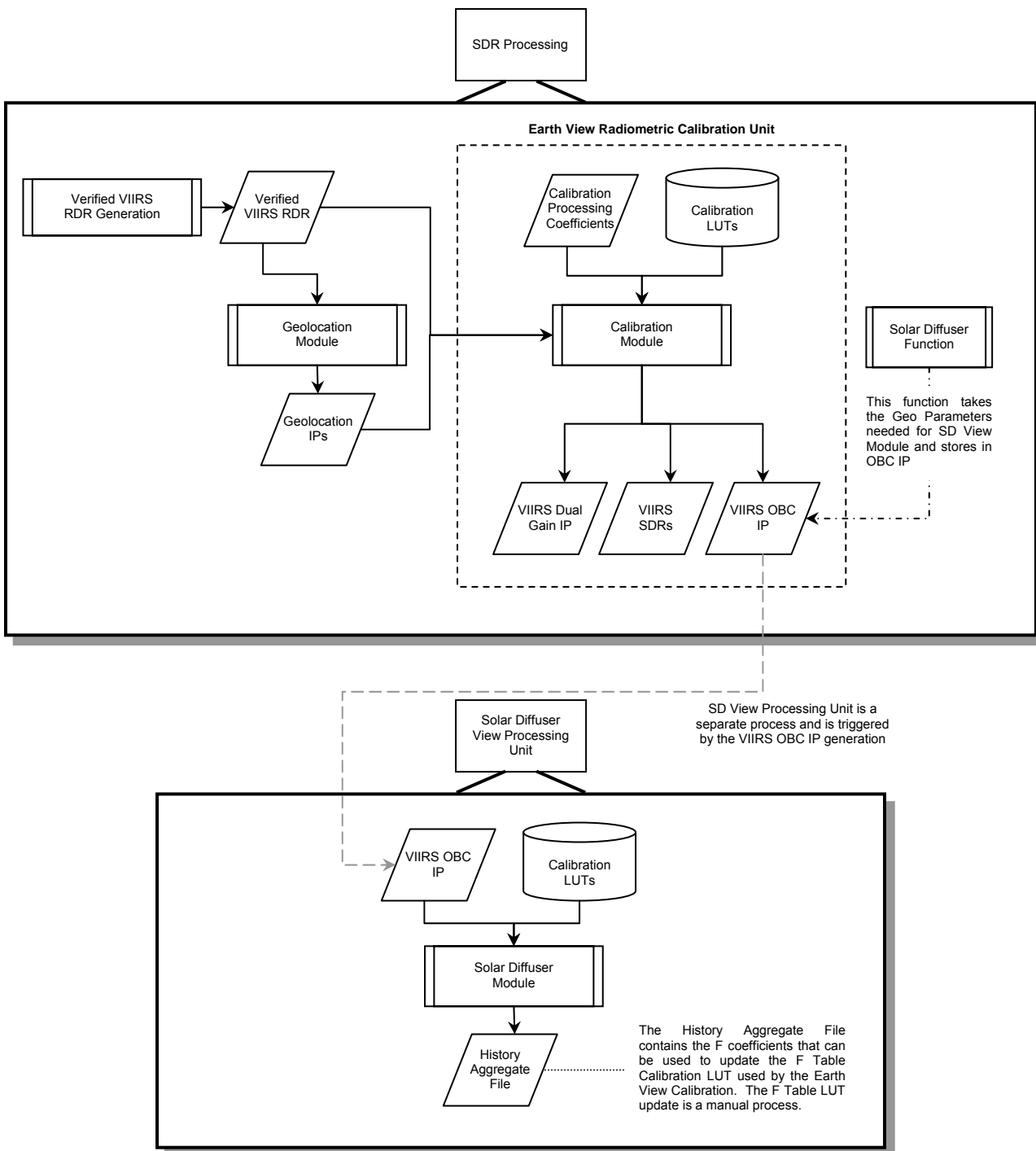


Figure 10 Calibration Processing Chain

**2.3.1 Interfaces**

**2.3.1.1 Inputs**

The inputs to the Earth View Radiometric Calibration Unit of the VIIRS Radiometric CAL Component are the Verified VIIRS RDRs, the VIIRS GEO Ips, and a suite of CAL parameter files that include LUTs, CAL coefficients and CAL run-time parameters. The input files are summarized in Tables 18 and 19.

Several of the LUT input items contain platform dependant values. Each platform must have a separate LUT associated with that specific sensor. During the input phase of the algorithms IPO processing model, the spacecraft ID provided in the tasking information is used as search metadata in order to ensure the correct LUT is retrieved from DMS.

**Table 18 Earth View Radiometric Calibration Unit Inputs**

| Input   | Description  |
|---|--|
| Verified VIIRS RDR                            | Data containing digital numbers for earth view, onboard calibrator view and space view data, as well as engineering data, health and safety data. This is raw satellite data that has been reformatted, pre-processed, and verified prior to processing.   |
| VIIRS Geolocation Ips                         | Data containing terrain corrected solar zenith and azimuth angles, satellite zenith and azimuth angles, as well as latitudes and longitudes for each VIIRS grid point for each of the three VIIRS resolutions. ( 375m, 750m, and DNB )   |
| VIIRS Geolocation OBC-IP                      | The VIIRS On Board Calibrator IP file contains solar diffuser observations, the associated gain state and HAM side information, and all engineering and housekeeping data, including unscaled data from the Solar Diffuser Stability Monitor (SDSM)/VIIRS Earth View Radiometric Calibration Unit and the Solar Diffuser GEO angles. |
| VIIRS SDR Calibration Processing Coefficients | Configurable coefficients required for processing. (Scale and Offset Values etc.)  |
| VIIRS SDR Calibration LUTs                    | Look up tables required for VIIRS SDR Calibration processing.  |

**Table 19 Earth View Radiometric Calibration Parameter & LUT Inputs**

| Input                  | Description/Source   |
|------------------------|--|
| DeltaCTempLUT          | Contains Delta C Temperature response values.  |
| DetectorResponseLUT    | VIIRS Detector Response Coefficient LUT.   |
| DnbCCoeffLUT           | DayNight Band C coefficients.  |
| DnbDN0LUT              | Contains DN (Digital count) 0 values for DNB calibration.  |
| DnbFPredictedTableLUT  | Time-dependent F Coefficients for DNB calibration as calculated from Solar Diffuser data                       |
| DnbFrameToZoneLUT      | DayNight Band Frame to Zone LUT.   |
| RvfDnbLUT              | Day Night Band response versus frame LUT   |
| EmissiveLUT            | This file contains various LUTs for emissive band calibration.   |
| FPredictedTableLUT     | Time-dependent F Coefficients as calculated from Solar Diffuser data   |
| GainTableLUT           | Table containing gain values for each of the bands.  |
| HAMERLUT               | Contains the LUT for calculating the emitted radiance of the half angle mirror (HAM) based on its temperature. |
| ElectronicsResponseLUT | VIIRS Electronics Response LUT.  |
| LtoEBBTLUT             | Contains the LUTs for converting radiance to brightness temperature.   |

| Input                           | Description/Source  |
|---------------------------------|---|
| OBCERLUT                        | Contains LUTs for calculating the emitted radiance of the blackbody based on the temperature.   |
| OBCRRLUT                        | Contains LUTs for calculating the reflected radiance of the blackbody based on the temperature.   |
| ObsToPixelsLUT                  | Contains the dual gain band along-scan samples to aggregated pixel frame number mapping table.  |
| QALUT                           | Contains LUTs related to quality assurance. Consists of the following SDSs: Detector Quality Flags, Moon Offset Limits.   |
| RMPParametersLUT                | Radiometric Parameters LUT.   |
| RSRLUT                          | Relative Spectral Response table for reflective bands (M1-M11 and I1-I3).   |
| RTAERLUT                        | Rotating telescope assembly emissive radiance tables for each VIIRS emissive band (I4-I5), (M12-M16).   |
| RVFLUT                          | Response Vs. Frame LUT for all imagery and moderate resolution bands.   |
| ReflectiveLUT                   | Contains values for calibrating reflective bands. Values include: first frame to use for OBC average, number of frames to use for OBC average and RSB moon include. |
| SolarIradLUT                    | Solar power table needed for calculation of d coefficients, which are used in reflectance algorithm.  |
| TeleCoeffLUT                    | Calibration coefficients for VIIRS thermistors as provided by Raytheon SBRS. Default values for thermistors.  |
| SDSM Volt                       | Volt Scale values   |
| VIIRS Imagery Even/Odd Parity   | Array of Boolean values for setting whether first, second sub-frame calibration averages are swapped to correct sub-frame timing offset.                            |
| DNB Stray Light Radiance Levels | List of radiance levels below which the DNB stray light quality flag may set.   |
| DG anomaly DN limits            | List of min/max DN values for which the DG anomaly quality flag will be set   |

### 2.3.1.2 Outputs

The VIIRS EV Radiometric CAL Unit produces 22 SDRs and two Ips, as shown in Table 20. A separate SDR is output for each band in each resolution: Imagery (I1-I5), Moderate (M1-M16), and DNB. All Imagery resolution SDRs and Moderate resolution SDRs contain the full resolution geolocated calibrated TOA radiances. In addition, reflective band SDRs (bands I1-I3 and M1-M11) contain full resolution calibrated reflectances and emissive band SDRs (bands I4-I5 and M12-M16) contain full resolution calibrated TOA brightness temperatures. The DNB SDR contains the full resolution geolocated calibrated TOA radiances for the DNB. The OBC IP contains sensor calibrator view data (space view, blackbody, and solar diffuser) from all VIIRS bands arranged by scan and unprocessed engineering and housekeeping data. The OBC IP is the input to the Solar Diffuser View Processing Unit and is also the primary input to offline Cal/Val analysis. The Calibrated Dual Gain IP contains unaggregated TOA radiances for each dual gain band for the nadir (aggregation by three) and the near-nadir (aggregation by two) aggregation zones.

**Table 20 Outputs from the Earth View Radiometric Calibration Unit (Calibration)**

| Output       | Description   |
|--------------|---|
| VIIRS_I1_SDR | The VIIRS 375m I1 band SDR contains TOA radiances, reflectances for each VIIRS pixel.     |
| VIIRS_I2_SDR | The VIIRS 375m I2 band SDR contains TOA radiances, and reflectances for each VIIRS pixel. |

| Output                        | Description  |
|-------------------------------|--|
| VIIRS_I3_SDR                  | The VIIRS 375m I3 band SDR contains TOA radiances, and reflectances for each VIIRS pixel.  |
| VIIRS_I4_SDR                  | The VIIRS 375m I4 band SDR contains TOA radiances, and brightness temperatures for each VIIRS pixel.   |
| VIIRS_I5_SDR                  | The VIIRS 375m I5 band SDR contains TOA radiances, and brightness temperatures for each VIIRS pixel.   |
| VIIRS_M1_SDR                  | The VIIRS 750m M1 band SDR contains TOA radiances, reflectances for each VIIRS pixel.  |
| VIIRS_M2_SDR                  | The VIIRS 750m M2 band SDR contains TOA radiances, reflectances for each VIIRS pixel.  |
| VIIRS_M3_SDR                  | The VIIRS 750m M3 band SDR contains TOA radiances, reflectances for each VIIRS pixel.  |
| VIIRS_M4_SDR                  | The VIIRS 750m M4 band SDR contains TOA radiances, reflectances for each VIIRS pixel.  |
| VIIRS_M5_SDR                  | The VIIRS 750m M5 band SDR contains TOA radiances, reflectances for each VIIRS pixel.  |
| VIIRS_M6_SDR                  | The VIIRS 750m M6 band SDR contains TOA radiances, reflectances for each VIIRS pixel.  |
| VIIRS_M7_SDR                  | The VIIRS 750m M7 band SDR contains TOA radiances, reflectances for each VIIRS pixel.  |
| VIIRS_M8_SDR                  | The VIIRS 750m M8 band SDR contains TOA radiances, reflectances for each VIIRS pixel.  |
| VIIRS_M9_SDR                  | The VIIRS 750m M9 band SDR contains TOA radiances, reflectances for each VIIRS pixel.  |
| VIIRS_M10_SDR                 | The VIIRS 750m M10 band SDR contains TOA radiances, reflectances for each VIIRS pixel.   |
| VIIRS_M11_SDR                 | The VIIRS 750m M11 band SDR contains TOA radiances, reflectances for each VIIRS pixel.   |
| VIIRS_M12_SDR                 | The VIIRS 750m M12 band SDR contains TOA radiances, brightness temperatures for each VIIRS pixel.  |
| VIIRS_M13_SDR                 | The VIIRS 750m M13 band SDR contains TOA radiances, brightness temperatures for each VIIRS pixel.  |
| VIIRS_M14_SDR                 | The VIIRS 750m M14 band SDR contains TOA radiances, brightness temperatures for each VIIRS pixel.  |
| VIIRS_M15_SDR                 | The VIIRS 750m M15 band SDR contains TOA radiances, brightness temperatures for each VIIRS pixel.  |
| VIIRS_M16_SDR                 | The VIIRS 750m M16 band SDR contains TOA radiances, brightness temperatures for each VIIRS pixel.  |
| VIIRS_DNB_SDR                 | The VIIRS Day/Night Band SDR contains TOA radiances for each VIIRS pixel.  |
| VIIRS OBC IP                  | The VIIRS On Board Calibrator IP file contains space view, solar diffuser, on-board calibrator blackbody (OBCBB) view observations, the associated gain state and HAM side information, and all engineering and housekeeping data, including unscaled data from the Solar Diffuser Stability Monitor (SDSM)/VIIRS Earth View Radiometric Calibration Unit and the Solar Diffuser GEO angles.   |
| VIIRS Calibrated Dual Gain IP | The Calibrated Dual Gain IP file contains unaggregated, calibrated TOA radiances for those VIIRS sub-pixel samples that are aggregated along-scan during post-calibration ground processing. In other words, this file contains the calibrated M1 – M5, M7 and M13 dual gain band data from the nadir and near-nadir zones that would otherwise be discarded following post-calibration aggregation/Earth View Radiometric Calibration Unit. |

### 2.3.1.2.1 Definitions of the Calibration VIIRS SDR Outputs

The contents of the VIIRS SDR outputs are described in Tables 18 through 24. The fields specific to a given resolution SDR are indicated in the Description column. The VIIRS SDR CAL routine outputs two structures for each band in the Moderate (750m) resolution, and Imagery (375m) resolution: a scaled version and an unscaled version of the SDR. The scaled versions of the bands are identified for long term storage, and the non scaled full floating point versions are used

for immediate processing of EDRs and IPs. These full floating point versions are removed by the storage system after an amount of time, post creation. All relevant Metadata associated with these output items is defined in the CDFCB-X, Volume IV.

**Table 21 Imagery Resolution SDR**

| Field                                   | Type           | Dimensions                          | Description   | Units   |
|---|----------------|-------------------------------------|---|---|
| Radiance                                | Float32        | VIIRS_IMG_COLS x<br>VIIRS_IMG_ROWS  | TOA radiances   | W/(m <sup>2</sup> -sr-μm)                             |
| Reflectance or<br>BrightnessTemperature | Float32        | VIIRS_IMG_COLS x<br>VIIRS_IMG_ROWS  | Reflectances or<br>brightness<br>temperatures<br>determined by band | NA for reflectance<br>K for brightness<br>temperature |
| Header                                  | VIIRS_HDR_TYPE | NA                                  | VIIRS SDR HDR<br>Type   | See Table 30  |
| Actual Scan Count                       | Int            | NA                                  | Number of actual<br>scans in granule                                | Unitless  |
| numOfMissingPkts                        | Int32          | VIIRS_RDR_SCANS                     | Missing Packets in<br>Scan  | Count   |
| numOfBadChecksum                        | Int32          | VIIRS_RDR_SCANS                     | Packets with bad<br>CRC in Scan                                     | Count   |
| numOfDiscardedPkts                      | Int32          | VIIRS_RDR_SCANS                     | Discarded Packets<br>in Scan  | Count   |
| Scan Quality                            | UInt8          | VIIRS_RDR_SCANS                     | Scan level quality<br>information                                   | See Table 26  |
| Pixel Quality                           | UInt8          | VIIRS_IMG_COLS x<br>VIIRS_IMG_ROWS  | Pixel level quality<br>Information                                  | See Table 27  |
| RDR Scan Quality                        | Int            | VIIRS_RDR_SCANS x<br>RDR_SCAN_FLAGS | Scan level rdr<br>quality information                               | See Table 28  |
| Reduced Quality Flag                    | UInt8          | VIIRS_IMG_ROWS                      | Detector x scan<br>level quality flag                               | See Table 29  |
| Bad Detector                            | Int            | NA                                  | 1 bit per scan<br>0 = detector good<br>1 = detector bad             | Unitless  |

**Table 22 Moderate Resolution SDR**

| Field                                   | Type           | Dimensions                          | Description   | Units  |
|---|----------------|-------------------------------------|---|--|
| Radiance                                | Float32        | VIIRS_MOD_COLS x<br>VIIRS_MOD_ROWS  | TOA radiances   | W/(m <sup>2</sup> -sr-μm)                                |
| Reflectance or<br>BrightnessTemperature | Float32        | VIIRS_MOD_COLS x<br>VIIRS_MOD_ROWS  | Reflectances or<br>brightness<br>temperatures<br>determined by band | NA for<br>reflectance K for<br>brightness<br>temperature |
| Header                                  | VIIRS_HDR_TYPE | NA                                  | VIIRS SDR HDR<br>Type   | See Table 30   |
| numOfMissingPkts                        | Int32          | VIIRS_RDR_SCANS                     | Missing Packets in<br>Scan  | Count  |
| numOfBadChecksum                        | Int32          | VIIRS_RDR_SCANS                     | Packets with bad<br>CRC in Scan                                     | Count  |
| numOfDiscardedPkts                      | Int32          | VIIRS_RDR_SCANS                     | Discarded Packets in<br>Scan  | Count  |
| Actual Scan Count                       | Int            | NA                                  | Number of actual<br>scans in granule                                | Unitless   |
| Scan Quality                            | UInt8          | VIIRS_RDR_SCANS                     | Scan level quality<br>information                                   | See Table 26   |
| Pixel Quality                           | UInt8          | VIIRS_MOD_COLS x<br>VIIRS_MOD_ROWS  | Pixel level quality<br>Information                                  | See Table 27   |
| RDR Scan Quality                        | Int            | VIIRS_RDR_SCANS x<br>RDR_SCAN_FLAGS | Scan level rdr<br>quality information                               | See Table 28   |

| Field                | Type  | Dimensions     | Description   | Units        |
|----------------------|-------|----------------|---|--------------|
| Reduced Quality Flag | UInt8 | VIIRS_MOD_ROWS | Detector x scan level quality flag                      | See Table 29 |
| Bad Detector         | Int   | NA             | 1 bit per scan<br>0 = detector good<br>1 = detector bad | Unitless     |

Table 23 Day/Night Band SDR

| Field                | Type           | Dimensions                          | Description                        | Units                   |
|----------------------|----------------|-------------------------------------|------------------------------------|-------------------------|
| Radiance             | Float32        | VIIRS_DNB_COLS x<br>VIIRS_DNB_ROWS  | TOA radiances                      | W/(cm <sup>2</sup> -sr) |
| Header               | VIIRS_HDR_TYPE | NA                                  | VIIRS SDR HDR Type                 | See Table 30            |
| Actual Scan Count    | Int            | NA                                  | Number of actual scans in granule  | Unitless                |
| Scan Quality         | UInt8          | VIIRS_RDR_SCANS                     | Scan level quality information     | See Table 26            |
| Pixel Quality        | UInt8          | VIIRS_DNB_COLS x<br>VIIRS_DNB_ROWS  | Pixel level quality Information    | See Table 27            |
| RDR Scan Quality     | Int            | VIIRS_RDR_SCANS x<br>RDR_SCAN_FLAGS | Scan level rdr quality information | See Table 28            |
| Reduced Quality Flag | UInt8          | VIIRS_DNB_ROWS                      | Detector x scan level quality flag | See Table 30            |

Table 24 Imagery Resolution Scaled SDR

| Field                                     | Type           | Dimensions                         | Description   | Units  |
|---|----------------|------------------------------------|---|--|
| Radiance                                  | UInt16         | VIIRS_IMG_COLS x<br>VIIRS_IMG_ROWS | Scaled TOA radiances  | W/(m <sup>2</sup> -sr-μm <sup>4</sup> )            |
| Reflectance or BrightnessTemperature      | UInt16         | VIIRS_IMG_COLS x<br>VIIRS_IMG_ROWS | Reflectances or brightness temperatures determined by band                              | NA for reflectance<br>K for brightness temperature |
| RadianceOffset                            | Float32        | NA                                 | Offset value of the scaled Radiances  | W/(m <sup>2</sup> -sr-μm <sup>4</sup> )            |
| RadianceScale                             | Float32        | NA                                 | Scaling factor for the scaled Radiances   | NA   |
| ReflectanceOffset or BrightnessTempOffset | Float32        | NA                                 | Offset value of the scaled Reflectances or Brightness Temperatures depending on band    | NA / K   |
| ReflectanceScale or BrightnessTempScale   | Float32        | NA                                 | Scaling factor for the scaled Reflectances or Brightness Temperatures depending on band | NA   |
| Header                                    | VIIRS_HDR_TYPE | NA                                 | VIIRS SDR HDR Type  | See Table 31                                       |
| Actual Scan Count                         | Int            | NA                                 | Number of actual scans in granule   | Unitless   |
| numOfMissingPkts                          | Int32          | VIIRS_RDR_SCANS                    | Missing Packets in Scan   | Count  |
| numOfBadChecksum                          | Int32          | VIIRS_RDR_SCANS                    | Packets with bad CRC in Scan  | Count  |
| numOfDiscardedPkts                        | Int32          | VIIRS_RDR_SCANS                    | Discarded Packets in Scan   | Count  |
| Scan Quality                              | UInt8          | VIIRS_RDR_SCANS                    | Scan level quality information  | See Table 26                                       |
| Pixel Quality                             | UInt8          | VIIRS_IMG_COLS x<br>VIIRS_IMG_ROWS | Pixel level quality Information   | See Table 27                                       |

| Field                | Type  | Dimensions                          | Description   | Units        |
|----------------------|-------|-------------------------------------|---|--------------|
| RDR Scan Quality     | Int   | VIIRS_RDR_SCANS x<br>RDR_SCAN_FLAGS | Scan level rdr quality<br>information                   | See Table 28 |
| Reduced Quality Flag | UInt8 | VIIRS_IMG_ROWS                      | Detector x scan level<br>quality flag                   | See Table 29 |
| Bad Detector         | Int   | NA                                  | 1 bit per scan<br>0 = detector good<br>1 = detector bad | Unitless     |

Table 25 Moderate Resolution Scaled SDR

| Field  | Type           | Dimensions                          | Description   | Units   |
|--|----------------|-------------------------------------|---|---|
| Radiance                                     | UInt16         | VIIRS_MOD_COLS x<br>VIIRS_MOD_ROWS  | Scaled TOA<br>radiances   | W/(m <sup>2</sup> -sr-μm)                             |
| Reflectance or<br>BrightnessTemperature      | UInt16         | VIIRS_MOD_COLS x<br>VIIRS_MOD_ROWS  | Reflectances or<br>brightness<br>temperatures<br>determined by band                                 | NA for reflectance<br>K for brightness<br>temperature |
| RadianceOffset                               | Float32        | NA                                  | Offset value of the<br>scaled Radiances   | W/(m <sup>2</sup> -sr-μm)                             |
| RadianceScale                                | Float32        | NA                                  | Scaling factor for the<br>scaled Radiances  | NA  |
| ReflectanceOffset or<br>BrightnessTempOffset | Float32        | NA                                  | Offset value of the<br>scaled Reflectances<br>or Brightness<br>Temperatures<br>depending on band    | NA / K  |
| ReflectanceScale or<br>BrightnessTempScale   | Float32        | NA                                  | Scaling factor for the<br>scaled Reflectances<br>or Brightness<br>Temperatures<br>depending on band | NA  |
| Header                                       | VIIRS_HDR_TYPE | NA                                  | VIIRS SDR HDR<br>Type   | See Table 30  |
| Actual Scan Count                            | Int32          | NA                                  | Number of actual<br>scans in granule  | Unitless  |
| numOfMissingPkts                             | Int32          | VIIRS_RDR_SCANS                     | Missing Packets in<br>Scan  | Count   |
| numOfBadChecksum                             | Int32          | VIIRS_RDR_SCANS                     | Packets with bad<br>CRC in Scan   | Count   |
| numOfDiscardedPkts                           | Int32          | VIIRS_RDR_SCANS                     | Discarded Packets<br>in Scan  | Count   |
| Scan Quality                                 | UInt8          | VIIRS_RDR_SCANS                     | Scan level quality<br>information   | See Table 26  |
| Pixel Quality                                | UInt8          | VIIRS_MOD_COLS x<br>VIIRS_MOD_ROWS  | Pixel level quality<br>Information  | See Table 27  |
| RDR Scan Quality                             | Int            | VIIRS_RDR_SCANS x<br>RDR_SCAN_FLAGS | Scan level rdr quality<br>information   | See Table 28  |
| Reduced Quality Flag                         | UInt8          | VIIRS_MOD_ROWS                      | Detector x scan level<br>quality flag   | See Table 29  |
| Bad Detector                                 | Int            | NA                                  | 1 bit per scan<br>0 = detector good<br>1 = detector bad   | Unitless  |

Table 26 Scan Quality Byte

| Bit | Flag Description       | Result   |
|-----|------------------------|--|
| 0   | Half Angle Mirror Side | 0: A-side<br>1: B-side                             |
| 1   | Moon in Keep-out-box   | 0: Moon not in space view<br>1: Moon in space view |

**Table 27 Pixel Quality Byte**

| Bit | Flag Description | Result  |
|-----|------------------|---|
| 0-1 | SDR Quality      | 0: Good<br>1: Poor<br>2: No calibration   |
| 2-3 | Saturated Pixel  | 0: None saturated<br>1: Some saturated<br>2: All saturated  |
| 4-5 | Missing Data     | 0: All data present<br>1: EV RDR data missing<br>2: Cal data missing<br>3: Thermistor data missing                  |
| 6-7 | Out of Range     | 0: All data within range<br>1: Radiance out of range<br>2: Reflectance or EBBT out of range<br>3: Both out of range |

**Table 28 RDR Scan Quality Int**

| Bit | Flag Description  | Result   |
|-----|-------------------|--|
| 0-5 | Checksum          | 0: Did verify<br>1: Did not verify             |
| 6   | Scan Data Present | 2.4 0: Some valid data<br>2.5 1: No valid data |

**Table 29 Reduced Quality Flag Byte**

| Bit   | Flag Description               | Result                               |
|-------|--------------------------------|--------------------------------------|
| 0-255 | Detector per band quality flag | 0: Good<br>255: Reduced quality flag |

**Table 30 VIIRS SDR Header**

| Field    | Type   | Dimensions | Description                             | Units |
|----------|--------|------------|---|-------|
| numScans | Int32  | NA         | Number of complete scans in the granule | NA    |
| scanMode | UInt8* | 16         | Day/night indicator per scan            | NA    |
| mode     | UInt8  | NA         | Day/night indicator per granule         | NA    |

**2.3.1.2.2 VIIRS On-Board Calibrator Intermediate Product**

Table 31 summarizes the contents of the VIIRS OBC IP output. The OBC IP contains the same granule metadata as the output SDR.

Table 31 OBC IP Output

| Output                          | Type/<br>Dimensions               | Description  | Units/<br>Valid<br>Range  | Fill Value                |
|---------------------------------|-----------------------------------|--|---------------------------|---------------------------|
| Scan Number                     | int32/<br>(nscans)                | VIIRS RDR scan number  | Unitless/<br>[1 – nscans] | -999                      |
| SD_375m                         | Float32/<br>(nscans*32,5,96)      | Digital counts from the Solar Diffuser for imagery resolution bands. Table Note 1                                | Counts/<br>[0 – 4095]     | MISS_FL<br>OAT32_FI<br>LL |
| SD_750m_SG                      | Float32/<br>(nscans*16,11,48)     | Digital counts from the Solar Diffuser for single gain moderate resolution bands. Table Note 1                   | Counts/<br>[0 – 4095]     | MISS_FL<br>OAT32_FI<br>LL |
| SD_750m_DG                      | Float32/<br>(nscans*16,7,48)      | Digital counts from the Solar Diffuser for dual gain moderate resolution bands. Table Note 1                     | Counts/<br>[0 – 4095]     | MISS_FL<br>OAT32_FI<br>LL |
| SD_DNB                          | Float32/<br>(nscans*16,64)        | Digital counts from the Solar Diffuser for Day/Night band.   | Counts/<br>[0 – 4095]     | MISS_FL<br>OAT32_FI<br>LL |
| BB_375m                         | Float32/<br>(nscans*32,5,96)      | Digital counts from the Blackbody for imagery resolution bands. Table Note 1                                     | Counts/<br>[0 – 4095]     | MISS_FL<br>OAT32_FI<br>LL |
| BB_750m_SG                      | Float32/<br>(nscans*16,11,48)     | Digital counts from the Blackbody for single gain moderate resolution bands. Table Note 1                        | Counts/<br>[0 – 4095]     | MISS_FL<br>OAT32_FI<br>LL |
| BB_750m_DG                      | Float32/<br>(nscans*16,7,48)      | Digital counts from the Blackbody for dual gain moderate resolution bands. Table Note 1                          | Counts/<br>[0 – 4095]     | MISS_FL<br>OAT32_FI<br>LL |
| BB_DNB                          | Float32/<br>(nscans*16,64)        | Digital counts from the Blackbody for Day/Night band.  | Counts/<br>[0 – 4095]     | MISS_FL<br>OAT32_FI<br>LL |
| SV_375m                         | Float32/<br>(nscans*32,5,2*48)    | Digital counts from the Space View for imagery resolution bands. Table Note 1                                    | Counts/<br>[0 – 4095]     | MISS_FL<br>OAT32_FI<br>LL |
| SV_750m_SG                      | Float32/<br>(nscans*16,<br>11,48) | Digital counts from the Space View for single gain moderate resolution bands. Table Note 1                       | Counts/<br>[0 – 4095]     | MISS_FL<br>OAT32_FI<br>LL |
| SV_750m_DG                      | Float32/<br>(nscans*16,7,48)      | Digital counts from the Space View for dual gain moderate resolution bands. Table Note 1                         | Counts/<br>[0 – 4095]     | MISS_FL<br>OAT32_FI<br>LL |
| SV_DNB                          | Float32/<br>(nscans*16,64)        | Digital counts from the Space View for Day/Night band.   | Counts/<br>[0 – 4095]     | MISS_FL<br>OAT32_FI<br>LL |
| DN_obc_avg_375m                 | float32<br>(nscans*32,5,2)        | Average digital counts from the Blackbody for imagery resolution bands.  | Counts                    | FLOAT32<br>_FILL          |
| DN_obc_avg_750m_s<br>g          | float32<br>(nscans*16,9)          | Average digital counts from the Blackbody for single gain moderate resolution bands.                             | Counts                    | FLOAT32<br>_FILL          |
| DN_obc_avg_750m_d<br>g          | float32<br>(nscans*16,7)          | Average digital counts from the Blackbody for dual gain moderate resolution bands.                               | Counts                    | FLOAT32<br>_FILL          |
| DN_obc_375M_outlier<br>_mask    | uint64/<br>(nscans*32,5,2)        | Number of pixels rejected in calculating the average Blackbody counts for imagery resolution bands.              | Counts                    | MISS_64_<br>FILL          |
| DN_obc_750M_SG_ou<br>tlier_mask | uint64/<br>(nscans*16,9,2)        | Number of pixels rejected in calculating the average Blackbody counts for single gain moderate resolution bands. | Counts                    | MISS_64_<br>FILL          |
| DN_obc_750M_DG_ou<br>tlier_mask | uint64/<br>(nscans*16,7,2)        | Number of pixels rejected in calculating the average Blackbody counts for dual gain moderate resolution bands.   | Counts                    | MISS_64_<br>FILL          |

| Output                             | Type/<br>Dimensions       | Description  | Units/<br>Valid<br>Range | Fill Value      |
|------------------------------------|---------------------------|--|--------------------------|-----------------|
| DN_obc_avg_first_frame_to_use      | Int32                     | Average First Frame to Use Digital Number  | Unitless                 | MISS_INT32_FILL |
| DN_obc_avg_number_of_frames_to_use | Int32                     | Average Number of Frames to Use Digital Number   | Unitless                 | MISS_INT32_FILL |
| OBC Gain States                    | UInt16 / (7*16 * nscans ) | Gain States for the Dual Gain Moderate bands for each calibrator view, for each detectors for each scan.   | 0 or 1                   | 0               |
| Moon in keep-out-box               | Int8<br>(nscans,22)       | Indicates if the moon was found in the keep-out-box for each scan and each band. The keep-out-box is a region including and near to the SV port. | Unitless/<br>[0 – 1]     | -999            |
| dp_reg_tbl_rev                     | UInt8 / nscans            | Indicates which table revision you are on for the DPP register table.  | Counts / [0-255]         | NONE            |
| dp_state_tran_tbl_rev              | UInt8 / nscans            | Indicates which table revision you are on for the DPP state transition table.  | Counts / [0-255]         | NONE            |
| dp_band_proc_tbl_rev               | UInt8 / nscans            | Indicates which table revision you are on for the DPP band processing table.   | Counts / [0-255]         | NONE            |
| dp_heat_ctrl_tbl_rev               | UInt8 / nscans            | Indicates which table revision you are on for the PWM heater control table.  | Counts / [0-255]         | NONE            |
| dp_macro_cmd_tbl_rev               | UInt8 / nscans            | Indicates which table revision you are on for the macro command table.   | Counts / [0-255]         | NONE            |
| dp_crit_tele_tbl_rev               | UInt8 / nscans            | Indicates which table revision you are on for the critical telemetry table.  | Counts / [0-255]         | NONE            |
| dp_stor_cmd_tbl_rev                | UInt16 / nscans           | Indicates which table revision you are on for the stored command table.  | Counts / [0-65535]       | NONE            |
| dp_dn_m_l_gain_pkt                 | UInt8 / nscans            | Indicates occasional selection to 0=NOT_SEND, 1=SEND DNB Middle Gain Stage (MGS) and Low Gain Stage (LGS) Pkts                                   | Unitless/<br>[0 – 1]     | MISS_UINT8_FILL |
| dp_hrd_pkt_norm_test               | UInt8 / nscans            | PKT_Norm_Test state 0=NORMAL, 1= TEST unique value for all FPA channels except DNB. Valid in Oper and Diag modes.                                | Unitless/<br>[0 – 1]     | MISS_UINT8_FILL |
| dp_nonrdt_fpie_pwr                 | UInt8 / nscans            | 0=PS1, 1=PS2; If FPIE Ok connect to active PS. If fault condition, connect to inactive PS  | Unitless/<br>[0 – 1]     | MISS_UINT8_FILL |
| dp_servo_in_use                    | UInt8 / nscans            | FSW echo of C_DP04, 0=SERVO_A, 1=SERVO_B   | Unitless/<br>[0 – 1]     | MISS_UINT8_FILL |
| ps_sec_b_apfp_on                   | UInt8 / nscans            | PS_SEC_B 0=OFF, 1=ON   | Unitless/<br>[0 – 1]     | MISS_UINT8_FILL |
| ps_sec_c_se_on                     | UInt8 / nscans            | PS_SEC_C 0=OFF, 1=ON   | Unitless/<br>[0 – 1]     | MISS_UINT8_FILL |
| ps_sec_d_csog_on                   | UInt8 / nscans            | PS_SEC_D 0=OFF, 1=ON   | Unitless/<br>[0 – 1]     | MISS_UINT8_FILL |
| ps_sec_e_isog_on                   | UInt8 / nscans            | PS_SEC_E 0=OFF, 1=ON   | Unitless/<br>[0 – 1]     | MISS_UINT8_FILL |
| se_a_anlg_pwr_on                   | UInt8 / nscans            | Analog Pwr present on SE_A   | Unitless/<br>[0 – 1]     | MISS_UINT8_FILL |
| se_a_mtr_coil_driver               | UInt8 / nscans            | Driver source for SE_A Mtr Coil.   | Unitless/<br>[0 – 1]     | MISS_UINT8_FILL |
| se_a_mtrs_stopped                  | UInt8 / nscans            | SE_A Motor state   | Unitless/<br>[0 – 1]     | MISS_UINT8_FILL |

| Output                | Type/<br>Dimensions | Description   | Units/<br>Valid<br>Range  | Fill Value           |
|-----------------------|---------------------|---|---------------------------|----------------------|
| se_a_tele_pos_known   | Uint8 / nscans      | Telescope position_A, Known covers Static Case (Stowed) and Dynamic Case (Servo up to speed and controlled)   | Unitless/<br>[0 – 1]      | MISS_UIN<br>T8_FILL  |
| se_b_anlg_pwr_on      | Uint8 / nscans      | Analog Pwr present on SE_B  | Unitless/<br>[0 – 1]      | MISS_UIN<br>T8_FILL  |
| se_b_mtr_coil_driver  | Uint8 / nscans      | Driver source for SE_B Mtr Coil   | Unitless/<br>[0 – 1]      | MISS_UIN<br>T8_FILL  |
| se_b_mtrs_stopped     | Uint8 / nscans      | SE_B Motor state  | Unitless/<br>[0 – 1]      | MISS_UIN<br>T8_FILL  |
| se_b_tele_pos_known   | Uint8 / nscans      | Telescope position_B, Known covers Static Case (Stowed) and Dynamic Case (Servo up to speed and controlled),  | Unitless/<br>[0 – 1]      | MISS_UIN<br>T8_FILL  |
| dp_dn_aggreg_mod      | Uint8 / nscans      | Earth view DNB Aggregation Mode   | Unitless/<br>[0 – 36]     | MISS_UIN<br>T8_FILL  |
| cp_blk_pwr_sel        | Uint8 / nscans      | 1=XSTRAP, 0=NORMAL; XS1 NORMAL connects PS1_A_PWR to CP_BLK_A (CP, DP, CT and SI) and PS2_A_PWR to CP_BLK_B; XSTRAP connects PS2_A_PWR to CP_BLK_A and PS1_A_PWR to CP_BLK_B; also by SC pt-pt T_SC02                                 | Unitless/<br>[0 – 1]      | MISS_UIN<br>T8_FILL  |
| dp_ap_m16_tdi_on      | Uint8 / nscans      | Indicates ASP M16 TDI state   | Unitless/<br>[0 – 1]      | MISS_UIN<br>T8_FILL  |
| dp_scan_encdr_delta   | Uint16 / nscans     | Scan Encoder Delta shift from normal value  | Counts / [0-32767]        | MISS_UIN<br>T16_FILL |
| dp_ap_self_test       | Uint8 / nscans      | DP_AP Self Test State   | Unitless/<br>[0 – 1]      | MISS_UIN<br>T8_FILL  |
| se_servo_pwr_sel      | Uint8 / nscans      | 1=XSTRAP, 0=NORMAL. XS2 NORMAL connects PS1_A_PWR and PS1_C_PWR to Servo_A; and PS2_A_PWR and PS2_C_PWR to Servo_B. XS2 XSTRAP connects PS2_A_PWR and PS1_C_PWR to Servo_A; and PS1_A_PWR and PS1_C_PWR to Servo_B; also by SC pt-pt. | Unitless/<br>[0 – 1]      | MISS_UIN<br>T8_FILL  |
| dp_dnb_1a_1b_stage    | Uint8 / nscans      | What DNB stage 1 data is sent   | Unitless/<br>[0 – 2]      | MISS_UIN<br>T8_FILL  |
| dp_dnb_tmng_mode      | Uint8 / nscans      | DNB Timing mode   | Unitless/<br>[0 – 1]      | MISS_UIN<br>T8_FILL  |
| dp_dnb_dark_sub_cal   | Uint8 / nscans      | Dark pixel subtraction for cal views  | Unitless/<br>[0 – 1]      | MISS_UIN<br>T8_FILL  |
| dp_dnb_dark_sub_earth | Uint8 / nscans      | Dark pixel subtraction for Earth views  | Unitless/<br>[0 – 1]      | MISS_UIN<br>T8_FILL  |
| ap_dc_fast_restor     | Uint8 / nscans      | 1 = Fast_Low_Resolution Restore Algorithm<br>0 = Slow_High_Resolution Algorithm   | Unitless/<br>[0 – 1]      | MISS_UIN<br>T8_FILL  |
| se_a_ham_mir_side     | Uint8 / nscans      | SE_A Mirror Side  | Unitless/<br>[0 – 1]      | MISS_UIN<br>T8_FILL  |
| se_b_ham_mir_side     | Uint8 / nscans      | SE_B Mirror Side  | Unitless/<br>[0 – 1]      | MISS_UIN<br>T8_FILL  |
| se_a_ham_mtr_curr     | Int16 / nscans      | SE_A Half Angle Mirror Motor Current  | Unitless/<br>[-8192–8191] | NONE                 |
| se_a_tele_mtr_curr    | Int16 / nscans      | SE_A Telescope Motor Current  | Unitless/<br>[-8192–8191] | NONE                 |

| Output               | Type/<br>Dimensions  | Description   | Units/<br>Valid<br>Range  | Fill Value       |
|----------------------|--|---|---------------------------|------------------|
| se_b_ham_mtr_curr    | Int16 / nscans   | SE_B Half Angle Mirror Motor Current  | Unitless/<br>[-8192–8191] | NONE             |
| se_b_tele_mtr_curr   | Int16 / nscans   | SE_B Telescope Motor Current  | Unitless/<br>[-8192–8191] | NONE             |
| ct_prec_tref_mux1ca1 | Int16 / nscans   | Precision Thermistor Cal Ref Resistor = 4.42Kohm  | Unitless/<br>[-8192–8191] | NONE             |
| ct_prec_tref_mux1ca2 | Int16 / nscans   | Precision Thermistor Cal Ref Resistor =2.87Kohm   | Unitless/<br>[-8192–8191] | NONE             |
| ct_prec_tref_mux1ca3 | Int16 / nscans   | Precision Thermistor Cal Ref Resistor =1.47Kohm   | Unitless/<br>[-8192–8191] | NONE             |
| ft_adc_ref           | Int16 / nscans   | FT ADC Ref 5V   | Unitless/<br>[-8192–8191] | NONE             |
| ft_adc_ref_lw_stpt   | Int16 / nscans   | FT ADC Ref LW Setpoint Volt Ref   | Unitless/<br>[-8192–8191] | NONE             |
| ft_ckt_gnd           | Int16 / nscans   | FT Circuit Gnd  | Unitless/<br>[-8192–8191] | NONE             |
| ft_lw_cfpa_htr_pwr   | Int16 / nscans   | FT LW Heater volts  | Unitless/<br>[-8192–8191] | NONE             |
| ft_lw_setpt_ref      | Int16 / nscans   | FT LW SETPT Ref   | Unitless/<br>[-8192–8191] | NONE             |
| ft_sm_cfpa_htr_pwr   | Int16 / nscans   | FT SM Heater volts  | Unitless/<br>[-8192–8191] | NONE             |
| ft_sm_setpt_ref      | Int16 / nscans   | FT SM SETPT Ref   | Unitless/<br>[-8192–8191] | NONE             |
| se_a_ham_rate_error  | Int16 / nscans   | SE_A Half Angle Mirror Rate Error   | Unitless/<br>[-8192–8191] | NONE             |
| se_a_tele_rate_error | Int16 / nscans   | SE_A Telescope Rate Error   | Unitless/<br>[-8192–8191] | NONE             |
| se_b_ham_rate_error  | Int16 / nscans   | SE_B Half Angle Mirror Rate Error   | Unitless/<br>[-8192–8191] | NONE             |
| se_b_tele_rate_error | Int16 / nscans   | SE_Btelescope Rate Error  | Unitless/<br>[-8192–8191] | NONE             |
| EV start time        | float64/<br>(nscans)   | The Earth View start of scan trigger time in IET  | Seconds/<br>[min-max]     | NONE             |
| HAM side             | int16/<br>(nscans)   | Mirror side in optical path – “0” for side 1 and “1” for side 2.                              | Unitless<br>[0 1]         | NONE             |
| SDSM – position data | Uint8/(nscans)   | Solar Diffuser sensor monitor (SDSM) data of the ENG packet. 0=home, 1=SD view and 2=sun view | Unitless<br>[0 2]         | NONE             |
| SDSM – sample data   | Float32/(nscans,<br>n_sdsm_detectors(8),<br>n_sdsm_samples(5)) | Solar Diffuser sensor monitor (SDSM) data of the ENG packet.                                  | Volts<br>[-2.5 to 2.5]    | FLOAT32<br>_FILL |
| BB Temps             | Int16/ (nscans,6)  | Black Body Temperatures   | Counts                    | -999             |

| Output                   | Type/<br>Dimensions | Description   | Units/<br>Valid<br>Range | Fill Value |
|--------------------------|---------------------|---|--------------------------|------------|
| ap_lw_cca                | int16/<br>(nscans)  | Long wave IR CCA Information stored in the Engineering packet.                    | Counts                   | -999       |
| ap_sm_cca                | int16/<br>(nscans)  | Short/Med wave IR CCA information stored in the Engineering packet.               | Counts                   | -999       |
| ap_vn_cca                | int16/<br>(nscans)  | Visible/Near IR CCA information stored in the Engineering packet                  | Counts                   | -999       |
| mf_scan_cavity_nxp       | int16/              | Mainframe Scan Cavity NX PZ Thermistor 46   | Counts                   | -999       |
| mf_scan_cavity_baf_nz    | (nscans)            | Mainframe Scan Cavity Baffle NZ Precision Thermistor 10                           | Counts                   | -999       |
| mf_scan_cavity_baf_pz    | int16/<br>(nscans)  | Mainframe Scan Cavity Baffle PZ Precision Thermistor 9                            | Counts                   | -999       |
| dp_dnb_cca               | int16/<br>(nscans)  | Digital Preprocessor DNB Circuit Card Assembly Thermistor 60                      | Counts                   | -999       |
| ft_lw_cfpa_hi_rsl        | int16/<br>(nscans)  | FT LW CFPA high resolution temperature  | Counts                   | -999       |
| ft_lw_cfpa_lo_rsl        | int16/<br>(nscans)  | FT LW CFPA wide range temperature   | Counts                   | -999       |
| ft_sm_cfpa_hi_rsl        | int16/<br>(nscans)  | Focal Plane Array Temperature Controller Long Wave IR High Resolution Temperature | Counts                   | -999       |
| ft_sm_cfpa_lo_rsl        | int16/<br>(nscans)  | Focal Plane Array Long Wave Wide Range Temperature                                | Counts                   | -999       |
| ft_vis_nir_fpa           | int16/<br>(nscans)  | Focal Plane Temperature Controller Visual/Near IR FPA Temperature                 | Counts                   | -999       |
| ham_tmp1                 | int16/<br>(nscans)  | Half Angle Mirror T1 Precision Thermistor 07, Radiatively Coupled Temperature     | Counts                   | -999       |
| ham_tmp2                 | int16/<br>(nscans)  | Half Angle Mirror T2 Precision Thermistor 08, Radiatively Coupled Temperature     | Counts                   | -999       |
| mf_tel_blkhd_py          | int16/<br>(nscans)  | Mainframe Telescope Bulkhead Therm 33, RT16 (Node 1022 in Radiometry Model)       | NONE                     | -999       |
| mf_ao_blkhd_px_nz        | int16/<br>(nscans)  | MF_AO_BLKHD_PX_NZ Therm 44  | NONE                     | -999       |
| mf_ao_blkhd_nx_pz        | int16/<br>(nscans)  | MF_AO_BLKHD_NX_PZ Therm 45  | NONE                     | -999       |
| mf_stopassy_baff_nz      | int16/<br>(nscans)  | On Baffle NZ of Apert Stop Assy between HAM and FM2 Therm 14                      | NONE                     | -999       |
| mf_fold_mir_blkhd_ct     | int16/<br>(nscans)  | MF_FOLD MIRROR BLKHD Center Therm 6   | NONE                     | -999       |
| mf_ham_blkhd             | int16/<br>(nscans)  | MF HAM Bulkhead Therm 43  | NONE                     | -999       |
| ev_ct_prec_tref_mux1c a1 | int16/<br>(nscans)  | Precision Thermistor Cal Ref Resistor 1   | NONE                     | -999       |
| ev_ct_prec_tref_mux1c a2 | int16/<br>(nscans)  | Precision Thermistor Cal Ref Resistor 2   | NONE                     | -999       |
| ev_ct_prec_tref_mux1c a3 | int16/<br>(nscans)  | Precision Thermistor Cal Ref Resistor 3   | NONE                     | -999       |
| DNB_sequence             | Uint8/<br>(nscans)  | DNB Sequence number   | Unitless/<br>1 to 36     | 255        |
| dp_dnb_ccd               | int16/<br>(nscans)  | DNB CCD Temperature   | Counts                   | -999       |
| mf_tel_blkhd_nypz        | int16/<br>(nscans)  | On Tel Blkhd NYPZ Therm 11  | Counts                   | -999       |

| Output                                  | Type/<br>Dimensions                | Description   | Units/<br>Valid<br>Range  | Fill Value |
|---|------------------------------------|---|---|------------|
| sdsm_preamp                             | int16/<br>(nscans)                 | SDSM Preamp Thermistor 57   | Counts  | -999       |
| South Atlantic Anomaly<br>Flag          | Uint8/<br>(nscans)                 | Lowest 48 bits, one bit for each scan, set to 1 if scan is over the South Atlantic Anomaly  | Unitless  | None       |
| x_Detector Offsets<br>x = [1 to nbands] | Int16/(nscans,nham,<br>ndetectors) | Detector offsets for each scans for each band for each mirror side for each detector.   | Unitless  | -999       |
| Solar                                   | float32<br>(nscans x 3)            | The solar vector in instrument coordinates, computed at the center time of the Solar Diffuser View sector.  | Meters/<br>Range for<br>each<br>component:<br>[-1.53E11 –<br>1.53E11];<br>Range for<br>vector<br>magnitude:<br>[1.46E11 –<br>1.53E11] | -999       |
| Lunar                                   | float32<br>(nscans x 3)            | Moon unit vector in instrument centered coordinates at center of space view sector.   | Unitless/<br>-1<= Moon<br>Vector <= 1   | -999       |
| sunZen                                  | Float32/(nscans)                   | The S/C sun zenith angle with respect to the Solar Diffuser (SD) Reference Frame z-axis, where the positive SD z-axis is defined as the normal to the SD surface. | Radians/<br>[0 – $\pi$ ]  | -999.9     |
| earthSunDistance                        | Float32/nscans)                    | Earth sun distance calculated from the Solar Vector at center of Space View scan.   | Meters/1.35<br>E11 –<br>1.65E11   | -999.9     |

<sup>1</sup> Note: The field is divide by 4 and truncated.

### 2.3.2 Algorithm Processing

This is the derived algorithm for the Earth View Radiometric CAL Unit algorithm and is a subclass of the AutoGeneratedProSdrViirsCal and ProCmnAlgorithm classes. The derived algorithm class creates a list of input data items read from DMS and passes required data into the algorithm. All output data items are written to DMS once the algorithm finishes processing this data.

The objective of the Radiometric CAL algorithm is to produce TOA radiances, reflectances (reflective bands only), and brightness temperatures (emissive bands only) for each pixel in an imagery, ideal moderate or day/night band. The radiometric CAL equations are derived from first principles. The equations that are implemented in the code have been simplified through extensive modeling and analysis and careful specification of the algorithm input parameters.

The Earth View Radiometric CAL Unit plus 21 functions for the Solar Diffuser View Processing Unit are described functionally in the following sections. Figure 11 shows the Earth View Radiometric Calibration Flow. Figure 12 shows the Solar Diffuser View processing flow. For details on the structure of the various functions, please refer to embedded code comments and the function descriptions located in Section 2.2.2. For variable and structure definitions please refer to embedded code comments and the data dictionary in Rose.

The logic flow of the main program for the Earth View Radiometric CAL algorithm is provided in Figure 11. The core of the CAL algorithm occurs in the functions:

Calibrate\_Emissive\_Bands(), Calibrate\_Reflective\_Bands(), and Calibrate\_DayNight\_Band(). Core equations for the reflective and emissive radiometric CAL algorithms are specified in Table throughTable . A summary of the symbols and units used in these equations can be found in Table . For a complete derivation of the radiometric CAL equations used in the science code and used for generating the CAL LUTs and coefficients, refer to the VIIRS Radiometric Calibration Equations Document, D36966, and the Radiometric Calibration ATBD, 474-00027.

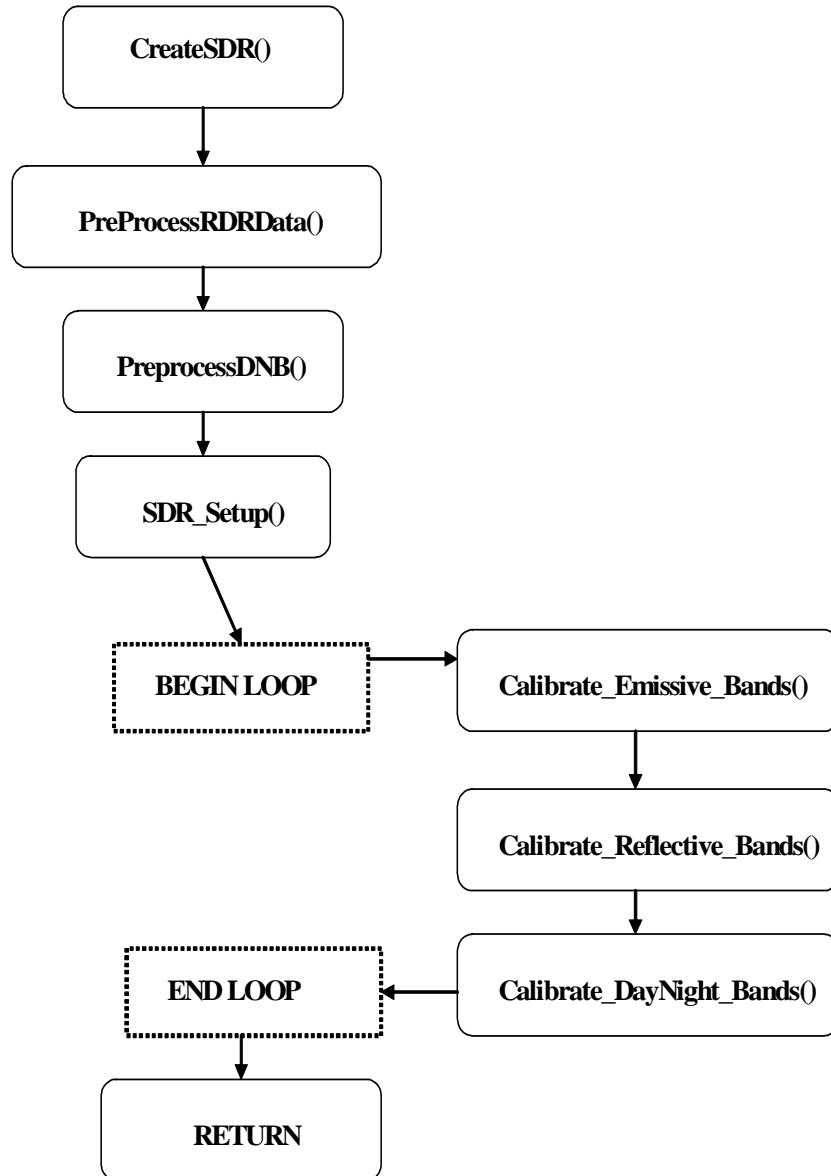


**Figure 11 Radiometric Calibration Main Program Flow**

### 2.3.2.1 Sub-frame Offset Compensation

It has been determined that in imagery band samples there is a consistent offset difference between the 1<sup>st</sup> (odd) and 2<sup>nd</sup> sub-frames (even). This anomaly is apparent in both space view and black body samples. In order to compensate for this difference, averages are computed for each sub-frame of each offset type, space view or black body. These subframe averages are then swapped per even/odd detector according to the swapEvenOdd arrays and are then used in calibration. Note that this swapping does not occur for the data written out to the OBC IP. For a complete description of the offset difference anomaly see NP-EMD-2007.510.0009\_VIIRS\_Even\_odd\_subframe\_design and NP-EMD-2009.510.0041 SDR Calibration Imagery Even Odd Parity Fix Code Update.

### 2.3.2.2 Robust Algorithm Design

Each scan contains data from four views: earth, solar diffuser, space, and black body. In addition each scan contains data regarding DC restore voltage for each detector and thermistor temperatures. These data are used in the calibration algorithm. Since calibration is dependent on all of these inputs, when any input is invalid then an alternate data source is used to replace the invalid data and calibration continues. For a listing of alternate data sources see NP-EDM.2007.510.0010\_VIIRS\_SDR\_Robust\_Alg\_design. Scans calibrated using an alternate data source are indicated by a non-zero value in the SDR reduced quality flag field. See Table 29.

### 2.3.2.3 Earth View Radiometric Calibration Error Handling

When the radiometric metrics cannot be computed due to missing input data, dead detectors, invalid electronic background digital numbers, invalid computed CAL coefficients, saturated earth view pixels, or a solar zenith angle greater than 89 degrees (reflectance values only) then the pixel quality flag is set to the appropriate value. The dual gain band pixel quality flags are set according to the convention outlined in Table 27.

### 2.3.2.4 calibrateSDR()

This is the main driver for the science processing of the EV Radiometric CAL algorithm. It controls each of the calls to the separate modules described below, and is responsible for handling stop calls and processing failures.

### 2.3.2.5 PreprocessRDR() and PreprocessDNB()

These routines are pre-process parameters needed for scan by scan calibration. Temperatures are determined from VIIRS engineering data. These functions calculate frame-averaged SV counts and standard deviation with outlier rejection for reflective bands. Calibrator gain states are extracted and telemetry and calibrator data are copied to the OBC\_IP output item.

### **2.3.2.6 SDRSetup()**

This routine performs a variety of functions in preparation for EV calibration. It calculates radiance and reflectance coefficients, sets up data structures used by CAL routines, as well as initializes QA parameters.

### **2.3.2.7 Combine\_Reduced\_Quality\_Flags()**

This routine calculates and stores the SDR reduced quality flag data in the SDR.

### **2.3.2.8 Calibrate\_Emissive\_Bands()**

This function calculates emissive band calibrated TOA radiance and brightness temperature for a scan.

### **2.3.2.9 Find\_SV\_Scan\_Index()**

When a dual gain band undergoes either emissive or reflective calibration, the space view with corresponding mirror side and gain state to the current pixel must be used to correctly calibrate the dn value. Due to a dcr state change every four scans, only the space view with the corresponding parameters that is also within the dcr grouping should be used for calibration. At the beginning and end of a granule, it is possible the space view scan required is located within the previous or following granule. This routine determines the correct granule and scan number to use for accurate dual gain calibration.

### **2.3.2.10 Calibrate\_Reflective\_Bands()**

This function calculates reflective band calibrated TOA radiance and reflectance for a scan.

### **2.3.2.11 Calibrate\_DayNight\_Bands()**

This function calculates DNB calibrated TOA radiance for a scan. The first frame of a scan line for each of the 16 DNB detectors is filled with zero integer for the Earth View and the three calibration views (Space View, Blackbody View and Solar Diffuser View) in the RDR. This process of zeroing out the first frame for the DNB scan lines is implemented for sensor FU1 to fix an anomaly with hardware.

### **2.3.2.12 Aggregate\_750M\_DG()**

This function aggregates the dual bands into the single gain resolution. It is responsible for storing the aggregated values in the SDR outputs and the unaggregated values in the Dual Gain IP product.

### 2.3.2.13 viirs\_decmp()

This code decompresses VIIRS earth view packet data. See code headers for copyright and redistribution restrictions.

## 2.3.3 Graceful Degradation

The VIIRS SDR Calibration procedure contains no graceful degradation.

### 2.3.3.1 Graceful Degradation Inputs

None.

### 2.3.3.2 Graceful Degradation Processing

None.

### 2.3.3.3 Graceful Degradation Outputs

None.

## 2.3.4 Exception Handling

The code primarily checks for invalid reference values for input and output structures, division by epsilon, and invalid array indexes. These conditions are handled on a case by case basis depending on the purpose of the function they are located within. In all cases an error or debug message is logged. For the dual-gain bands, multiple RDR pixels are aggregated (two or three) together to produce a single output SDR pixel. This creates the possibility of an SDR output pixel where there is a mix of good and bad quality RDR pixels. The dual-gain SDR products therefore have a special quality flag that indicates an aggregated mix of good and bad quality identified as NON\_NOMINAL (see Table 11). Problems with CAL cause quality flags to be applied to all SDR pixels that derive from the CAL computation. If CAL source data is missing (space view, solar diffuser, or OBC BB) then a CAL exception occurs and this is applied as a quality flag to all earth view SDR output pixels that require that calibration. Since CAL applies over a whole scan or over multiple scans, this causes a quality flag to be issued for the entire scan.

## 2.3.5 Data Quality Monitoring

Table 32 shows the VIIRS SDR Calibration data quality monitoring.

**Table 32 VIIRS SDR Calibration Data Quality Monitoring**

| Name                      | Value     | Description   |
|---------------------------|-----------|---|
| Summary VIIRS SDR Quality | 0 – 100 % | Percentage of good quality pixels in granule                                  |
| Scan Quality Exclusion    | 0 – 48    | Number of scans in granule excluded from processing (including partial scans) |

### **2.3.6 Computational Precision Requirements**

The VIIRS SDR CAL routine outputs two structures for each band in the Moderate (750m) resolution, and Imagery (375m) resolution: a scaled version and a non-scaled version of the SDR. The scaled versions of the bands are identified for long term storage, and the non-scaled full floating point versions are used for immediate processing of EDRs and Ips. These full floating point versions are removed by the storage system after an amount of time, post creation.

### **2.3.7 Algorithm Support Considerations**

The DMS and INF must be running before the algorithm is executed.

### **2.3.8 Assumptions and Limitations**

#### **2.3.8.1 I/O Timeliness**

Dual gain bands require calibration space view data from the previous granule and next granule. From this, one-granule latency occurs for the dual gain bands.

#### **2.3.8.2 Sci2Ops Issues**

The CAL code expects that the Verified VIIRS RDR data follows the “product order” convention for detector numbering, which requires that the highest number detector in scan N lies adjacent to detector number 1 in scan N+1 (see Section 2.2.2.3 of the ATBD, 474-00027).

#### **2.3.8.3 Numerical Computation Considerations**

The scientific SDR and EDR algorithms must be convertible into operational code that is compatible with data latency requirements. This essentially means that most EDRs must be completely processed from VIIRS raw data, including CAL and georeferencing, within 28 minutes from the time the raw data are available. The complexity of the calculations used for VIIRS radiometric CAL is similar to those in routine MODIS processing and are therefore expected to perform within a reasonable allocation of the operational timeline.

Here are optimization considerations. The current version of the operational algorithm is deemed to fall within acceptable processing timeline. Should it become necessary then additional optimization can be achieved by threading the algorithm to multiprocess each scan, or multiprocess each CAL step (Reflective, Emissive, DayNight).

#### **2.3.8.4 Additional Assumptions**

It is assumed that Verified RDR data are provided in correct time sequence and that complete scans are provided (missing data within a scan is to be filled). It is also assumed that RDR data are reconstructed to remove any coding, compression, and band referencing that was performed on-board.

It is assumed that the time and spacecraft parameters provided in the downlinked data and extracted by the VIIRS Build RDR module are present and correct unless a quality flag is set.

It is assumed that the VIIRS GEO Ips are available at the time of execution of the science code.

It is assumed that sufficient resources are available to support operational processing using the VIIRS Build SDR radiometric CAL algorithm.

It is assumed that the required coefficients and look up tables are complete and provided in the correct format.

Refer to Section 4.0 of the Calibration Algorithm Theoretical Basis Document, D43777, for assumptions made with respect to the on-board processing, input data content, and inputs from pre-launch CAL testing.

### **2.3.8.5 Additional Limitations**

Refer to Section 4.0 of the VIIRS Radiometric Calibration Algorithm Theoretical Basis Document ATBD, 474-00027.

## **2.4 VIIRS SDR Solar Diffuser Description**

### **2.4.1 Interfaces**

#### **2.4.1.1 Inputs**

The inputs for the Solar Diffuser View Data Processing Unit are the VIIRS OBC IP and a suite of Calibration parameter files that include LUTs and CAL coefficients. The input files are summarized in Table 33 and Table 34.

**Table 33 Solar Diffuser View Data Processing Unit Inputs (Calibration)**

| Input                        | Description/Source  |
|------------------------------|---|
| VIIRS OBC IP Equivalent Data | The VIIRS On Board Calibrator IP file contains space view, solar diffuser, on-board calibrator blackbody (OBCBB) view observations, the associated gain state and HAM side information, and all engineering and housekeeping data, including raw data from the Solar Diffuser Stability Monitor (SDSM)/VIIRS Earth View Radiometric Calibration Unit. The OBC IP also includes geolocation outputs such as the S/C solar and lunar vectors, the S/C solar zenith angle, and the earth-to-sun distance needed by the SD View Data Processing Unit. |

**Table 34 SD View Data Processing Unit Calibration Parameter Input Files**

| Input                           | Description   | Units | Valid Range |
|---------------------------------|---|-------|-------------|
| VIIRS-SDR-SOLAR-IRAD-LUT        | See CDFCB-X VIII  |       |             |
| VIIRS-SDR-RSR-LUT               | Relative spectral response table for moderate and imagery resolution bands, containing wavelengths and corresponding response values.<br>See CDFCB-X VIII   |       |             |
| VIIRS-SDR-GAIN-LUT              | This file contains the gain value for each VIIRS band.<br>See CDFCB-X VIII  |       |             |
| VIIRS-SOLAR-DIFF-RVF-LUT        | Response versus frame at the solar diffuser angle.<br>See CDFCB-X VIII  |       |             |
| VIIRS-SDR-COEFF-A-LUT           | VIIRS Detector Response Coefficients.<br>See CDFCB-X VIII   |       |             |
| VIIRS-SDR-COEFF-B-LUT           | VIIRS Instrument Electronics Response Coefficients.<br>See CDFCB-X VIII   |       |             |
| VIIRS-SDR-DELTA-C-LUT           | See CDFCB-X VIII  |       |             |
| VIIRS-SOLAR-DIFF-REFL-LUT       | Binary file containing the solar diffuser BRDF LUT by wavelength, horizontal and vertical angles.<br>For more details see CDFCB-X VIII.   |       |             |
| VIIRS-SDR-TELE-COEFFS-LUT       | Thermistor coefficients used to convert thermistor counts to temperature.<br>For more details see CDFCB-X VIII.   |       |             |
| VIIRS-SDR-RADIOMETRIC-PARAM-LUT | Thermistor weights used for computing the temperatures for the 2 focal planes and Telec.<br>Telect_Therm_Weights[5]<br>Tfpm_Weights<br>Tfplw_Weights<br>For more details see CDFCB-X VIII.  |       |             |
| VIIRS-SOLAR-DIFF-REFL-LUT       | Binary file containing the solar diffuser transmittance LUT for imagery bands by detector, wavelength, horizontal and vertical angles. The transmittance also vary by detector so the format is repeated for each detector.<br>For more details see CDFCB-X VIII. |       |             |

| Input                                   | Description   | Units   | Valid Range  |
|---|---|---|--|
| VIIRS-SOLAR-DIFF-REFL-LUT               | Binary file containing the solar diffuser transmittance LUT for moderate bands by detector, wavelength, horizontal and vertical angles. The transmittance also vary by detector so the format is repeated for each detector. For more details see CDFCB-X VIII.                         |   |  |
| VIIRS-SOLAR-DIFF-PROC-COEFFS-LUT        | See CDFCB-X VIII  |   |  |
| VIIRS-SOLAR-DIFF-AGG-HISTORY-AUX-AC-Int | This file contains frame and scan aggregation parameters. Included are frame limits, orbits to aggregate, min/max DN values and sigmas, and min SNRs. For more details see CDFCB-X VIII.  |   |  |
| VIIRS-SOLAR-DIFF-AGG-LUT                | See CDFCB-X VIII  |   |  |
| VIIRS-SOLAR-DIFF-SDSM-BRDF-LUT          | Solar diffuser BRDF as observed by the SDSM. There are 8 x 46 elevation, There are 8 x 12 azimuth angle and 8 x 12 x 46 factors.  | elevation and azimuth degrees<br>All others: 1/sr     | elevation 14 to 18.5<br>azimuth 14 to 45<br>All others: Real, 0 to 1   |
| VIIRS-SOLAR-DIFF-SDSM-TIME-LUT          | Scan fractions of SDSM sample times, array of 5 floats  | Fraction of scan                                      | Real, 0 to 1   |
| VIIRS-SOLAR-DIFF-SDSM-TRANS-SCREEN-LUT  | Solar diffuser stability monitor screen transmittivity. There are 8 x 25 elevation. There are 8 x 19 azimuth. There are 8 x 19 x 25 factors.  | elevation and azimuth degrees<br>All others: unitless | elevation -1.8 to 1.8<br>azimuth -18 to 18<br>All others: Real, 0 to 1 |
| VIIRS-SOLAR-DIFF-TRANS-SCREEN-LUT       | The transmittance screen coefficients for the Solar Diffuser. There are 8 x 46 elevation, There are 8 x 12 azimuth angle and 8 x 12 x 46 factors.   | elevation and azimuth degrees<br>All others: unitless | elevation 14 to 18.5<br>azimuth 14 to 45<br>All others: Real, 0 to 1   |
| VIIRS-SOLAR-DIFF-ROT-MATRIX-LUT         | Solar diffuser rotation matrix, 3x3 array of floats and Solar diffuser stability monitor screen rotation matrix, 3x3 array of floats  | None  | Real, 0 to 1   |
| VIIRS SDSM Acceptance Angles            | Array of float values for minimum elevation, maximum elevation, minimum azimuth, maximum azimuth in SDSM screen coordinates (0 deg elevation and azimuth is perpendicular to SDSM attenuation screen, positive elevation is towards negative Z, positive azimuth is towards negative Y) | degrees   | -180 to 180  |

#### 2.4.1.2 Outputs for Solar Diffuser View Data Processing Unit

The Solar Diffuser View Data Processing Unit has one output file, as described in Table . This file contains the VIIRS reflective bands F coefficient gain data, which is used to build the Ftable LUT used by the Earth View Radiometric CAL Unit. The Ftable LUT used by CAL is not automatically updated every time the SD Processing Unit outputs a History Aggregate File. An initial FTable

LUT will be generated pre-launch with ground measurements, and the Ftable LUT will be updated through a manual process.

**Table 35 Solar Diffuser: Table Output**

Note - This is broken out by Static and Dynamic Section for the same output.

| Output   | Type              | Description/Source  | Units   | Valid Range  |
|--|-------------------|---|---|--|
| History Aggregate Output<br>(Static Size Section)  | Binary            | This file contains statistical data on the confidence level in the computed F values. Listed are time, band, detector, mirror side, gain state, number of valid scans per estimate, F, dF/dt, F sigma, dF/dt sigma, Chi squared, and goodness of fit [6].<br>Field 1: numScans<br>Field 2: sdsCount<br>Field 3: F<br>Field 4: nScans<br>Field 5: dF_dt, rate of change in F<br>Field 6: F_error<br>Field 7: dF_dt_error<br>Field 8: chisqr<br>Field 9: confidence, goodness of fit<br>Probability   | Field 1&2: counter<br>Field 3: 1/sec<br>Field 4: counter<br>Field 5: 1/sec<br>Field 6: Unitless<br>Field 7: 1/sec<br>Field 8: Unitless<br>Field 9: Unitless   | Field 1: int >=0<br>Field 2: int >=0<br>Field 3: real number<br>Field 4: int >=0<br>Field 5-7: real number<br>Field 8: real, between 0 and 1.<br>Field 9: real   |
| History Aggregate Output<br>(Dynamic size section) | Binary<br>(Cont.) | The following items in the History Aggregate output have a dynamic size in that there are "numScans" entries for each of these values.<br><br>Col 1: SDStartTime<br>Col 2: Band<br>Col 3: Detector<br>Col 4: GainState<br>Col 5: HAMside<br>Col 6 – 9: Temperatures<br>Col 10-11: Phi angles<br>Col 12: sun-earth distance<br>Col 13: cos theta<br>Col 14: SD radiance<br>Col 15: BRDF<br>Col 16: Transmittance<br>Col 17: Ave. DN_SV<br>Col 18: Variance DN_SV<br>Col 19: Samples DN_SV<br>Col 20-21: min/max DN_SV<br>Col 22-26: same as 17-21 for DN_SD<br>Col 27: Vdcr<br>Col 28-31: coefficients<br>Col 32: rvsSD<br>Col 33: measRadiance<br>Col 34: Fscan<br>Col 35: scan Signal to Noise | Col 1: secs (from 1/1/1993)<br>Col 2: index<br>Col 3: index<br>Col 4: index<br>Col 5: index<br>Col 6-9: Kelvin<br>Col 10-11: degrees<br>Col 12: meters<br>Col 13: unitless<br>Col 14: W/(m <sup>2</sup> µm sr)<br>Col 15: 1/sr<br>Col 16: unitless<br>Col 17: Counts<br>Col 18: Counts<br>Col 19: Index<br>Col 20-21: Counts<br>Col 22-26: same as 17-21<br>Col 27: Volts<br>Col 28: W/(m <sup>2</sup> µm sr)<br>Col 29: W/(m <sup>2</sup> µm sr cnts)<br>Col 30: W/(m <sup>2</sup> µm sr cnts <sup>2</sup> )<br>Col 31: unitless<br>Col 32: W/(m <sup>2</sup> µm sr)<br>Col 33: unitless<br>Col 34: unitless | Col 1: real<br>Col 2: [0-13]<br>Col 3: [0-31]<br>Col 4: [0 or 1]<br>Col 5: [0 or 1]<br>Col 6-9: real >0<br>Col 10-11: real<br>Col 12: real >0<br>Col 13: real [0-1]<br>Col 14: real<br>Col 15: real<br>Col 16: [0 – 1]<br>Col 17: real >=0<br>Col 18: real >=0<br>Col 19: int >=0<br>Col 20-21: int>=0<br>Col 22-26: same as 17-21<br>Col 27: real >=0<br>Col 28: real<br>Col 29: real<br>Col 30: real<br>Col 31: real [0-2]<br>Col 32: real<br>Col 33: real<br>Col 34: real |

| Output       | Type          | Description/Source   | Units                                | Valid Range                                   |
|--------------|---------------|--|--------------------------------------|---|
| SDSM H Table | Binary (Cont) | The following items in the History Aggregate output have a dynamic size in that there are "sdsmCount" entries for each of these values.<br><br>Col1: EVStartTime<br>Col2 H Factor<br>Col3 Standard Dev | Microseconds<br>Unitless<br>Unitless | Col1: Integer > 0<br>Col2: Real<br>Col3: Real |

**2.4.2 Algorithm Processing**

This is the derived algorithm for the Solar Diffuser Unit algorithm and is a subclass of the ProCmnAlgorithm class. The derived algorithm class creates a list of input data items read from DMS and passes required data into the algorithm. All output data items are written to DMS once the algorithm finishes processing this data.

**2.4.2.1 Solar Diffuser View Data Processing Logic**

The logic flow of the main program for the Solar Diffuser View Data Processing algorithm is provided in Figure 12. The core of the Solar Diffuser View Data Processing occurs in the function Calibrate(), where the F scale factors are computed for the reflective bands. The output item F\_coefficients is generated and combined with an aggregate for future processing.

Core equations used for the Solar Diffuser View Data Processing algorithm are specified in Table 18. For a complete derivation of the radiometric calibration equations used in the science code for generating the F Scale Factors, refer to the VIIRS Radiometric Calibration Equations document, D36966, and the Radiometric Calibration ATBD, 474-00027.

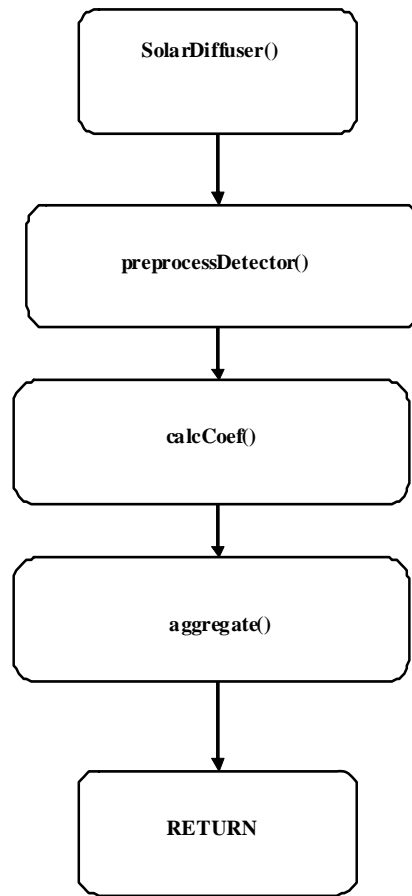


Figure 12 Solar Diffuser View Data Processing Main Program Flow

2.4.2.2 Calibration Symbols and Units

Table 36 Calibration Symbols and Units

| Symbol         | Un-notated Indices <sup>3</sup> | Description   | Units                         |
|----------------|---------------------------------|---|-------------------------------|
| $a_1(T_{det})$ | B, d, g, m                      | Temperature dependent first order (linear) coefficient of the response function of a detector circuit. This is the effective capacitance of the detector circuit. | Photoelectrons/V              |
| $a_2(T_{det})$ | B, d, g, m                      | Temperature dependent second order coefficient of the response function of a detector circuit.  | Photoelectrons/V <sup>2</sup> |
| $agg(N_F)$     | N/A                             | Along-scan aggregation zone for DNB.  | Unitless                      |
| $B$            | N/A                             | Band number.  | Unitless                      |

<sup>3</sup> In order to reduce complexity of the notation some indices are dropped in the equations in this document. The following abbreviations are used in this column. B=band number; d=detector number; g=gain state; m=mirror side; n=cross-track pixel number

| Symbol  | Un-notated Indices <sup>3</sup> | Description   | Units                                       |
|---|---------------------------------|---|---|
| $b_1(T_{elec})$                                 | B, d, m                         | Temperature dependent first order (linear) coefficient of the response function of electronics. This is the inverse of the gain of the combined ADC & ASP circuits. | V/count                                     |
| $b_2(T_{elec})$                                 | B, d, m                         | Temperature dependent second order coefficient of the response function of electronics.   | V/count <sup>2</sup>                        |
| $BRDF(\phi_h, \phi_v, \lambda, t)$              | B, d                            | Bi-directional reflectance distribution function of solar diffuser expressed in terms of lab angles.  | 1/sr  |
| $c_0$   | B, d, g, m                      | 0 order coefficient of the radiance response function.  | W/(m <sup>2</sup> μm sr)                    |
| $c_1(T_{det}, T_{elec})$                        | B, d, g, m                      | Temperature dependent first order (linear) coefficient of the response function for radiance.   | W/(m <sup>2</sup> μm sr cnts)               |
| $c_2(T_{det}, T_{elec})$                        | B, d, g, m                      | Temperature dependent second order coefficient of the response function for radiance.   | W/(m <sup>2</sup> μm sr cnts <sup>2</sup> ) |
| $c_j(T_{det}, T_{elec})$                        | B, d, g, m                      | Temperature dependent jth order coefficient of the response function after calibration update.  | W/(m <sup>2</sup> μm sr cnts <sup>j</sup> ) |
| $c[\text{agg}(N_F, N_P, N_G)]$                  |                                 | Pre-determined DNB calibration coefficients, dependent on $N_F$ , $N_P$ , and $N_G$ .   | W/(m <sup>2</sup> μm sr cnts <sup>j</sup> ) |
| $\Delta C_j$                                    | B, d, g, m                      | Adjustment to coefficient of the response function.   | W/(m <sup>2</sup> μm sr cnts <sup>j</sup> ) |
| $d_j(T_{det}, T_{elec})$                        | B, d, g, m                      | Temperature dependent jth order coefficient of the response function for reflectance.   | 1/counts <sup>j</sup>                       |
| $d_{se}(t)$                                     |                                 | Distance from sun to earth at time $t$ .  | Meter                                       |
| $\overline{d_{se}}$                             |                                 | Distance from sun to earth averaged over a year.  | Meter                                       |
| $dn_{sd}(t)$                                    | B, d, g, m, n                   | Differential detector counts at solar diffuser with space view subtracted.  | Counts                                      |
| $\overline{dn_{sd}(t_n)}$                       | B, d, g, m                      | Differential detector counts at solar diffuser averaged over the acquisition at time $t_n$ .  | Counts                                      |
| $dn_{obc}(t)$                                   | B, d, g, m, n                   | Differential detector counts at OBCBB with space view subtracted at time $t$ .  | Counts                                      |
| $\overline{dn_{obc}(t_n)}$                      | B, d, g, m                      | Differential detector counts at OBCBB averaged over the acquisition at time $t_n$ .   | Counts                                      |
| $DN$  | B, d, g, m, n                   | Total detector counts.  | Counts                                      |
| $DN_{DNB}$                                      |                                 | Total DNB detector counts.  | Counts                                      |
| $DN_{SV\_DNB}[N_F, N_P, N_G]$                   |                                 | DNB space view offset LUT, as a function of $N_F$ , $N_P$ , and $N_G$ .   | Counts                                      |
| $dn_{ev}$                                       | B, d, g, m, n                   | Differential detector earth view counts with space view subtracted.   | Counts                                      |
| $dn_{DNB}$                                      |                                 | Differential DNB detector counts with space view subtracted.  | Counts                                      |
| $\overline{DN_{sv}}$                            | B, d, g, m                      | Total detector counts per frame averaged over space view.   | Counts                                      |
| $E_{sun}(\lambda, t), E_{sun}(\lambda, d_{se})$ |                                 | Irradiance from the sun upon a surface with normal pointing toward the sun.   | W/(m <sup>2</sup> μm)                       |
| $F$   | B, d, g, m                      | Factor for update of the radiance coefficients.   | Unitless                                    |
| $F_{cav}$                                       | B                               | Factor describing the effective solid angle of the cavity as seen by the OBD BB.  | sr  |
| $F_{sh}$  | B                               | Factor describing the effective solid angle of the shield as seen by the OBD BB.  | sr  |
| $F_{tele}$                                      | B                               | Factor describing the effective solid angle of the telescope as seen by the OBD BB.   | sr  |
| $G$   | B                               | Gain converting detector electron counts to radiance.   | W/(m <sup>2</sup> μm sr) /photoelectron     |
| $\overline{\Delta L_{det}(\theta, B)}$          | d, m                            | Differential band-averaged detected spectral radiance at field stop for angle $\theta$ relative to space view.  | W/(m <sup>2</sup> μm sr)                    |
| $\overline{L_{ap}(\theta, B)}$                  | d                               | Band-averaged spectral radiance at the aperture for scan angle $\theta$ .   | W/(m <sup>2</sup> μm sr)                    |
| $\overline{L_{nsd}(\phi_h, \phi_v, B)}$         | d                               | Band-averaged normalized solar diffuser spectral radiance.  | W/(m <sup>2</sup> μm sr)                    |

| Symbol   | Un-notated Indices <sup>3</sup> | Description   | Units                    |
|--|---------------------------------|---|--------------------------|
| $\overline{L}_{DNB}$                               |                                 | Band-averaged spectral radiance at the aperture for Day Night Band.                                   | W/(m <sup>2</sup> μm sr) |
| $L(T, \lambda)$                                    |                                 | Blackbody spectral radiance according to Planck's function.   | W/(m <sup>2</sup> μm sr) |
| $L_{obc\_rfl}(T_{sh}, T_{cav}, T_{tele}, \lambda)$ | B, d, n                         | Spectral radiance emissive background from shield, cavity and telescope, and reflected off the OBCBB. | W/(m <sup>2</sup> μm sr) |
| $N_{acq}$  |                                 | Number of scans over which solar diffuser is observed   | Unitless                 |
| $N_{cal}$  | B                               | Number of frames per scan while observing OBCBB.  | Unitless                 |
| $N_F$  |                                 | Along-scan frame number.  | Unitless                 |
| $N_G$  |                                 | DNB Gain stage.   | Unitless                 |
| $N_H$  |                                 | HAM side index.   | Unitless                 |
| $N_P$  |                                 | Along-track pixel.  | Unitless                 |
| $N_{SDfrm}$  | B                               | The number of frames per scan over which the solar diffuser calibration counts are recorded.          | Unitless                 |
| $RVS(\theta, B)$                                   | d, m                            | Response Versus Scan function at scan angle $\theta$ for band $B$ .                                   | Unitless                 |
| $RVS[N_F, N_P, N_H]$                               |                                 | Pre-determined Response Versus Scan for DNB, as a function of $N_F$ , $N_P$ , and $N_H$ .             | Unitless                 |
| $t$  |                                 | Time.   | Seconds                  |
| $t_n$  |                                 | Time of scan n of an acquisition.   | Seconds                  |
| $\Delta t_{frame}$                                 | B                               | Time between frames or samples for detectors.   | Seconds                  |
| $T_{cav}$  |                                 | Temperature of cavity contributing to reflection off OBCBB.   | K                        |
| $T_{det}$  |                                 | Temperature of FPA detector circuits.   | K                        |
| $T_{elec}$   |                                 | Temperature of electronics module.  | K                        |
| $T_{ham}$  |                                 | Temperature of HAM.   | K                        |
| $T_{obc}$  |                                 | Temperature of OBCBB.   | K                        |
| $T_{rta}$  |                                 | Temperature of RTA.   | K                        |
| $T_{sh}$   |                                 | Temperature of shield contributing to reflection off OBCBB.   | K                        |
| $T_{tele}$   |                                 | Temperature of telescope contributing to reflection off OBCBB.  | K                        |
| $V_{dcr}$  | B, d                            | Analog DC restore voltage signal with respect to some nominal dark condition.                         | V                        |
| $\varepsilon_{obc}(\lambda)$                       |                                 | Spectral emissivity of the OBCBB  | Unitless                 |
| $\theta_{inc}$                                     |                                 | Incidence angle onto solar diffuser relative to normal.   | Radians                  |
| $\theta_{obc}$                                     |                                 | Scan angle of OBCBB.  | Radians                  |
| $\theta_{sd}$                                      |                                 | Scan angle at solar diffuser.   | Radians                  |
| $\theta_{ev}$                                      |                                 | Scan angle at earth view.   | Radians                  |
| $\theta_{sun\_earth}$                              |                                 | Solar incidence angle of the sun on the earth.  | Radians                  |
| $\lambda$  |                                 | Wavelength.   | μm                       |
| $\overline{\rho}_{ev}(\theta_{ev}, B)$             |                                 | Band-averaged earth view spectral reflectance.  | Unitless                 |
| $\rho_{rta}(\lambda)$                              |                                 | Spectral reflectance of RTA.  | Unitless                 |
| $\tau_{sds}(\phi_h, \phi_v, \lambda)$              | d                               | Spectral transmittance of solar diffuser screen.  | Unitless                 |
| $\phi_v(t)$  |                                 | Vertical incidence angle of solar illumination upon SD in laboratory coordinates.                     | Radians                  |
| $\phi_h(t)$  |                                 | Horizontal incidence angle of solar illumination upon SD in laboratory coordinates.                   | Radians                  |
| $\phi_{inc}$                                       |                                 | Azimuthal incidence angle onto solar diffuser relative to x-axis.                                     | Radians                  |
| $\Phi_{sun}(\lambda, t)$                           |                                 | Spectral output power of the sun.   | W/μm                     |

2.4.2.3 Reflective Calibration Core Equations

Table 37 Reflective Calibration Core Equations (Calibration)

| Equations   | ATBD Eqn |
|---|----------|
| $\overline{L_{ap}}(\theta_{ev}, B) = \frac{\overline{\Delta L_{det}}(\theta_{ev}, B)}{RVS(\theta_{ev}, B)} = \frac{F \cdot \sum_{j=0}^2 c_j \cdot dn_{ev}^j}{RVS(\theta_{ev}, B)} = \frac{\sum_{j=0}^2 c'_j \cdot dn_{ev}^j}{RVS(\theta_{ev}, B)}$  | 70       |
| $\overline{\rho_{ev}}(\theta_{ev}, B) = \frac{\pi \cdot \sum_{j=0}^2 c'_j \cdot dn_{ev}^j}{RVS(\theta_{ev}, B) \cdot \cos(\theta_{sun\_earth}) \cdot \overline{E_{sun}}(\lambda, d_{se})}$ $= \frac{\sum_{j=0}^2 d_j \cdot dn_{ev}^j}{RVS(\theta_{ev}, B) \cdot \cos(\theta_{sun\_earth})}$ | 81       |
| $dn_{ev} = DN - DN_{sv}$  | 28       |
| $c'_j = F \cdot c_j$  | 65       |
| $d_j = \frac{\pi}{\overline{E_{sun}}(\lambda, d_{se})} \cdot c'_j$  | 76       |
| $C_0(T_{det}, T_{elec}) = \Delta C_0(T_{det}, T_{elec})$  | Table 18 |
| $C_1(T_{det}, T_{elec}, V_{dcr}) = G \cdot b_1(T_{elec}) \cdot [a_1(T_{det}) + 2a_2(T_{det}) \cdot V_{dcr}] + \Delta C_1(T_{det}, T_{elec})$  | Table 18 |
| $C_2(T_{det}, T_{elec}, V_{dcr}) = G \cdot [a_1(T_{det}) + 2a_2(T_{det}) \cdot V_{dcr}] \cdot b_2(T_{elec}) + a_2(T_{det}) \cdot b_1(T_{elec})^2 + \Delta C_2(T_{det}, T_{elec})$   | Table 18 |

2.4.2.4 Emissive Calibration Core Equations

Table 38 Emissive Calibration Core Equations (Calibration)

| Equations  | ATBD Eqn |
|--|----------|
| $\overline{L_{ap}}(\theta_{ev}, B) = \frac{(1 - RVS(\theta_{ev}, B)) \cdot \left[ \left( \frac{1}{\rho_{rta}(\lambda)} - 1 \right) \cdot \overline{L(T_{rta}, \lambda)} - \frac{\overline{L(T_{ham}, \lambda)}}{\rho_{rta}(\lambda)} \right] + F \cdot \sum_{j=0}^2 c_j(T_{det}, T_{elec}) \cdot dn_{ev}^j}{RVS(\theta_{ev}, B)}$  | 115      |
| $F = RVS(\theta_{obc}) \cdot \frac{\left\{ \left( 1 - \frac{1}{RVS(\theta_{obc})} \right) \cdot \left[ \left( \frac{1}{\rho_{rta}(\lambda)} - 1 \right) \cdot \overline{L(T_{rta}(t), \lambda)} - \frac{\overline{L(T_{ham}(t), \lambda)}}{\rho_{rta}(\lambda)} \right] \right\} + \overline{\varepsilon_{obc}}(\lambda) \cdot \overline{L(T_{obc}(t), \lambda)} + \overline{L_{obc\_rfl}}(T_{sh}(t), T_{cav}(t), T_{tele}(t), \lambda)}{\sum_{j=0}^2 c_j \cdot \overline{dn_{obc}(t)}^j}$ | 112      |
| $\overline{L_{obc\_rfl}}(T_{sh}, T_{cav}, T_{tele}, \lambda) = \left[ \begin{aligned} &F_{cav} \cdot (1 - \varepsilon_{obc}(\lambda)) \cdot \overline{L(T_{cav}, \lambda)} + F_{sh} \cdot (1 - \varepsilon_{obc}(\lambda)) \cdot \overline{L(T_{sh}, \lambda)} \\ &+ F_{tele} \cdot (1 - \varepsilon_{obc}(\lambda)) \cdot \overline{L(T_{tele}, \lambda)} \end{aligned} \right]$  | 114      |

| Equations  | ATBD Eqn |
|--|----------|
| $\overline{dn_{obc}}(t) = \frac{1}{N_{cal}} \sum_{m=0}^{N_{cal}} dn_{obc}(t + m \cdot \Delta t_{frame})$ | 106      |
| Same $c_j$ values as in Table  |          |

### 2.4.2.5 Day Night Band Calibration Core Equations

**Table 39 Day Night Band Calibration Core Equations (Calibration)**

| Equations  | ATBD Eqn |
|--|----------|
| $\overline{L_{DNB}} = \frac{\sum_{i=0}^2 c_i [agg(N_F), N_P, N_G] \cdot dn_{DNB}^i}{RVS[N_F, N_P, N_H]}$ | 119      |
| $dn_{DNB} = DN_{DNB} - DN_{sv\_DNB}[N_F, N_P, N_G]$  | 120      |

### 2.4.2.6 Solar Diffuser View Data Processing Core Equations

**Table 40 Solar Diffuser View Data Processing Core Equations (Calibration)**

| Equations   | ATBD Eqn |
|---|----------|
| $F = \frac{RVS(\theta_{sd}, B)}{N_{acq}} \cdot \left(\frac{\overline{d_{se}}}{d_{se}}\right)^2 \cdot \sum_{n=0}^{N_{acq}-1} \left( \frac{\cos(\theta_{inc}(t_n)) \cdot \overline{L_{nsd}}(\phi_h(t_n), \phi_v(t_n), B)}{\sum_{j=0}^2 c_j \cdot \overline{dn_{sd}}(t_n)^j} \right)$  | 68       |
| $\begin{aligned} \overline{L_{nsd}}(\phi_h, \phi_v, B) &= (\tau_{sds}(\phi_h, \phi_v, \lambda) \cdot E_{sun}(\lambda, \overline{d_{se}}) \cdot BRDF(\phi_h, \phi_v, \lambda)) \\ &= \frac{1}{4\pi \cdot \overline{d_{se}}^2} \cdot (\tau_{sds}(\phi_h, \phi_v, \lambda) \cdot \Phi_{sun}(\lambda) \cdot BRDF(\phi_h, \phi_v, \lambda)) \end{aligned}$ | 67       |
| $\overline{dn_{sd}}(t_n) = \frac{1}{N_{SDfrm}} \sum_{m=0}^{N_{SDfrm}} dn_{sd}(t_n + m \cdot \Delta t_{frame})$  | 69       |
| $\phi_v = \arctan\left(\frac{\tan \theta_{inc}}{\sqrt{\tan^2 \phi_{inc} + 1}}\right)$   | 104      |
| $\phi_h = \arctan\left(\frac{\tan \theta_{inc} \tan \phi_{inc}}{\sqrt{\tan^2 \phi_{inc} + 1}}\right)$   | 105      |

### 2.4.2.7 Solar Diffuser SDSM

The Solar Diffuser Stability Monitor tracks the change in the reflectivity of the Solar Diffuser. Since the Solar Diffuser is used to calibrate the reflective bands of the VIIRS instrument, changes in its reflectivity directly affect the reflective calibration. The SD calibration is performed once per orbit when the orbit geometry allows it to be illuminated by the sun. At a longer interval, a command can be sent to the instrument to make the SDSM active during this period of illumination. Currently, the SDSM calibration is performed every orbit.

#### 2.4.2.7.1 SDSM Processing Logic

Figure 13 shows the SDSM Processing Block diagram.

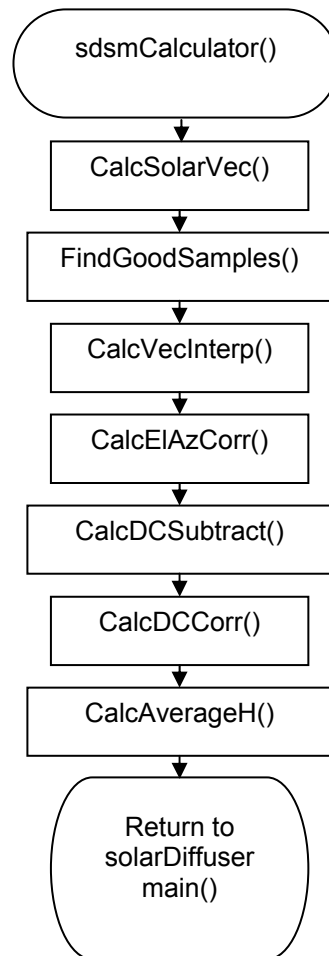


Figure 13 SDSM Processing Block Diagram

##### 2.4.2.7.1.1 SdsmCalculator

Main for the SDSM calibration class. Takes OBCIP data and LUT data to calculate the SDSM values. The following sub-sections cover the science logic that is now included in this new class.

##### 2.4.2.7.1.2 CalcSolarVec()

Compute sun direction in Lab, SD and SDSM coords and find which scans have good solar diffuser geometry (currently  $15.0^\circ < \text{dec} < 18.5^\circ$  and  $13.6^\circ < \text{azi} < 44.2^\circ$ , in lab coordinates) and good SDSM geometry (currently  $-0.7^\circ < \text{elev} < 0.7^\circ$  and  $-17.0^\circ < \text{azi} < 17.0^\circ$  in SDSM screen coordinates).

#### 2.4.2.7.1.3 FindGoodSamples()

Select sets of three scans (DC, SD, Sun views) from those selected by CalcSolarVec(). In other words, the first DC scan before the first scan with good geometry and the last SDSM scan before solar geometry goes bad, see Table .

**Table 41 Determining Good Data Set**

| Scan | View | Good solar angles | Good Data Set |
|------|------|-------------------|---------------|
| 1    | DC   | No                | No            |
| 2    | SD   | No                | No            |
| 3    | Sun  | No                | No            |
| 4    | DC   | No                | Yes           |
| 5    | SD   | Yes               | Yes           |
| 6    | Sun  | Yes               | Yes           |
| 7    | DC   | Yes               | Yes           |
| 8    | SD   | Yes               | Yes           |
| 9    | Sun  | Yes               | Yes           |
| 10   | DC   | Yes               | Yes           |
| 11   | SD   | Yes               | Yes           |
| 12   | Sun  | Yes               | Yes           |
| 13   | DC   | Yes               | No            |
| 14   | SD   | No                | No            |
| 15   | Sun  | No                | No            |
| 16   | DC   | No                | No            |

#### 2.4.2.7.1.4 CalcVecInterp()

Interpolate the solar position for each of the SDSM data sampling times. The scan fraction is referenced to the Solar Diffuser Sample time, see Figure 14.

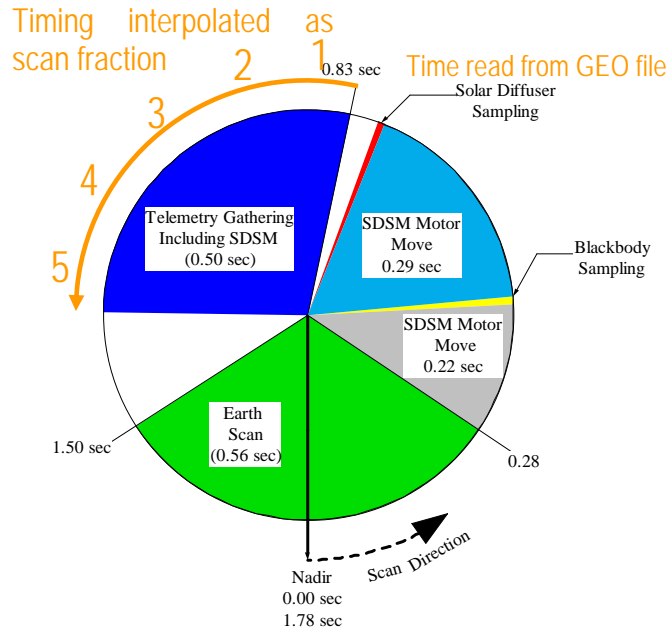


**Figure 14 Interpolation of Solar Position From Scan Fraction of Sample Times**

**2.4.2.7.1.5 CalcElAzCorr()**

Retrieve correction for the SDS, BRDF and SDSM given interpolated positions. First the solar position is converted to elevation and azimuth angles and these are used to fetch values from the correction arrays. The retrieval does a bilinear interpolation.

**2.4.2.7.1.6 CalcDCSubtract()**

Subtract the DC view from the SD view and Sun view. This expects sets of three (DC, SD, Sun) scans, but this was done in FindGoodSamples().

**2.4.2.7.1.7 CalcDCCorr()**

Apply the correction to the DC subtracted SD and Sun data.

**2.4.2.7.1.8 CalcAverageH()**

Calculate mean and standard deviation for h values for each detector/band for corrected data.

**2.4.3 Graceful Degradation**

The VIIRS SDR Solar Diffuser process contains no graceful degradation.

**2.4.3.1 Graceful Degradation Inputs**

None.

### **2.4.3.2 Graceful Degradation Processing**

None.

### **2.4.3.3 Graceful Degradation Outputs**

None.

### **2.4.4 Exception Handling**

No exception handling is performed in the VIIRS SDR Solar Diffuser process.

### **2.4.5 Data Quality Monitoring**

No data quality monitoring is performed.

### **2.4.6 Computational Precision Requirements**

The VIIRS SDR Solar Diffuser process uses double precision values in order to ensure the required accuracy.

### **2.4.7 Algorithm Support Considerations**

The DMS and INF must be running before the algorithm is executed.

### **2.4.8 Assumptions and Limitations**

The Solar Diffuser View Data Processing Unit needs the inputs identified in the two tables of Section 2.4.1.1 before the execution of the code.

## **2.5 Viirs SDR Bright Pixel Description**

Scattered light can contaminate pixels in the vicinity of bright objects in VIIRS scenes. Also, bright objects can lose light that is scattered to darker areas. Although the fraction of scattered light is low, for a sufficiently bright source near a dim nearby pixel, the scattered contribution can dominate the radiometric uncertainty. This condition is easily understood by considering the ocean's color and VIIRS ability to determine that color with a bright cloud in the nearby scene. Several EDRs (ocean color, land albedo, and sea-surface temperature) have exclusion conditions in the NPOESS System Spec around bright pixels, and call for a flag to indicate when scattering is above an acceptable level.

### **2.5.1 Interfaces**

#### **2.5.1.1 Inputs**

VIIRS Bright Pixel Inputs are listed in Table .

**Table 42 VIIRS Bright Pixel Algorithm Inputs**

| Input                            | Type   | Description   |
|----------------------------------|--------|---|
| VIIRS 750m (Moderate) SDR        | Binary | The VIIRS 750m SDR contains TOA radiances, reflectances (for reflective 'M' bands only) and brightness temperatures (emissive 'M' bands only) for each VIIRS pixel                      |
| Point Spread Functions (PSF) LUT | Binary | The VIIRS point spread functions (PSF) resolved to the resolution of the unaggregated samples for each bands.   |
| Band Replacement LUT             | Binary | This file contains proxy (substitution) bands to be used for saturated pixels, scale factor, and alternative maximum radiance. It also inputs the threshold limits for the 4-bit flags. |
| Bright Pixel Threshold LUT       | Binary | This file contains the threshold table by band for flag data to floating point translation.   |

**2.5.1.2 Outputs**

The output of this algorithm will be a 4-bit flag for each pixel in each band that characterizes the level of contamination of signal by scattered light.

The percentage of scattered light is defined to be:

$$\% \text{ scattered light} = \left| \frac{S_{scat}}{S_{meas}} \right| * 100$$

4-bit state flag:

- 0000 0.0 - 0.01% scattered light
- 0001 0.01 - 0.02% scattered light
- 0010 0.02 - 0.05% scattered light
- 0011 0.05 – 0.1% scattered light
- 0100 0.1 – 0.2% scattered light
- 0101 0.2 – 0.5% scattered light
- 0110 0.5 - 1.0% scattered light
- 0111 1.0 - 2.0% scattered light
- 1000 2.0 – 5.0% scattered light
- 1001 5 – 10% scattered light
- 1010 >10% scattered light
- 1111 calculation unreliable

VIIRS Bright Pixel Output is listed in Table .

**Table 43 VIIRS Bright Pixel Output Files**

| Output                                | Type   | Description  |
|---------------------------------------|--------|--|
| VIIRS 750m (Moderate) Bright Pixel ID | Binary | This data contains all Moderate band Flag data for Bright Pixel at pixel resolution. |

## 2.5.2 Algorithm Processing

### 2.5.2.1 Estimating % Scattered Light

Scattered light distribution is a property of the telescope & focal plane and is referred to as the near-field scattering. Bright Pixel Algorithm models the scattering with a point-spread function that is composed of a delta function with small epsilon tails. The measured scene is the true scene convolved with the PSF.

Definitions:

$$S_{true} = \text{true scene}$$

$$S_{meas} = \text{measured scene including scattered light}$$

$$P_{true} = \text{true PSF}$$

$$P_{meas} = \text{measured PSF}$$

$$\delta = \text{Dirac Delta Function}$$

$$\delta(i, j) = \begin{cases} 1 & \text{if } i = i_{center} \text{ \& } j = j_{center} \\ 0 & \text{otherwise} \end{cases}$$

$$i = \text{in-track sample index}$$

$$j = \text{in-scan sample index}$$

$$S_{meas} = P_{true} * S_{true}$$

The PSF here is a full optical PSF, including all the effects of Near-Field Scattering (NFS). This is sometimes also referred to as a Point Source Transmittance (PST), but it will be referred to as PSF here. The effect of NFS can be considered as a perturbation,  $\epsilon$ , with respect to the Dirac Delta function

$$P_{true} = \delta + \epsilon_{true}$$

$$P_{meas} = \delta + \epsilon_{meas}$$

The following normalization conditions apply to both the measured and the true PSF.

$$\sum_i \sum_j P(i, j) = 1$$

$$\sum_i \sum_j \epsilon(i, j) = 0$$

The true scattering in the scene is the difference between the measured scene and the true scene.

$$\begin{aligned} S_{scat} &= S_{meas} - S_{true} = P_{true} * S_{true} - \delta * S_{true} \\ &= (P_{true} - \delta) * S_{true} \\ &= \epsilon_{true} * S_{true} \end{aligned}$$

If the measured scene is convolved again with the PSF, it is found:

$$\begin{aligned}
S_{double\ conv} &= P_{meas} * S_{meas} \\
&= (\delta + \epsilon_{meas}) * (\delta + \epsilon_{true}) * S_{true} \\
&= (\delta * \delta + \epsilon_{meas} * \epsilon_{true} + \epsilon_{meas} + \epsilon_{true}) * S_{true}
\end{aligned}$$

Subtracting the measured scene from this gives what will be referred to as  $S'_{scat}$ .

$$\begin{aligned}
S'_{scat} &= S_{double\ conv} - S_{meas} = P_{meas} * S_{meas} - \delta * S_{meas} \\
&= (\delta + \epsilon_{meas} - \delta) * S_{meas} \\
&= \epsilon_{meas} * S_{meas} \\
&= \epsilon_{meas} * (\delta + \epsilon_{true}) * S_{true}
\end{aligned}$$

Then it can be written:

$$\begin{aligned}
S'_{scat} - S_{scat} &= (\epsilon_{meas} + \epsilon_{meas} * \epsilon_{true} - \epsilon_{true}) * S_{true} \\
\text{or} \\
S'_{scat} &= S_{scat} + (\epsilon_{meas} - \epsilon_{true} + \epsilon_{meas} * \epsilon_{true}) * S
\end{aligned}$$

which reduces to  $S'_{scat} = S_{scat}$  when  $\epsilon_{true} \cong \epsilon_{meas}$  and  $\epsilon_{true} * \epsilon_{meas} * S \cong 0$ .

As long as the measured NFS is a good estimate of the true NFS, and NSF is a small contribution to the whole PSF, then the difference between the doubly convolved scene and the measured scene is a good estimate of the scattering. Our estimate of scattered light then is:

$$\% \text{ scattered light} = \frac{S_{scat}}{S_{meas}} * 100 \cong \frac{S'_{scat}}{S_{meas}} * 100 \cong \frac{\epsilon_{meas} * S_{meas}}{S_{meas}} * 100$$

In addition to the above requirements that the measured scattering distribution be close to the real one and much smaller than one, there is another requirement here, that  $S_{meas} \gg S'_{scat}$ . Very close to a bright object, where the % scattered light is close to or greater than one, the exact value will become very uncertain. However, there is no uncertainty that the scattering is large, but the only thing that is uncertain is how large the scattering is going to be. Since it has been chosen that highest threshold of 10% for the flags, anything above this is flagged as >10% scattered light, so it will not matter whether it is, say, 20% or 40%. Either way, it is much too large an error to provide a meaningful EDR.

$\epsilon_{meas}$  as an estimate of  $\epsilon_{true}$

SBRS measures the LSF and Near-Field scattering. Until such measurements become available for the flight unit, the in-track and cross-track NFS contribution to the PSF will be based on a fit to a Harvey-Shack (H-S) BRDF model. H-S BRDF is translated into  $\epsilon_{meas}$ , using the angular separations in the BRDF to describe the scattering to adjacent samples in the in-track and in-scan direction.

$$\text{PSF} = \delta + \varepsilon_{meas}$$

The true scattering function,  $\varepsilon_{true}$ , is expected to differ from this, especially over the life of VIIRS as optical surfaces degrade with time, and SBRS has models to estimate this impact. So that our flags are conservatively pessimistic, end-of-life (EOL) estimates are to be used over the entire mission.

### 2.5.2.2 “Calculation Unreliable” Flag

The tails of the scattering distribution are notoriously difficult to measure since they are several orders of magnitude lower than the peak. The VIIRS near-field response (NFR) test FP-14 uses bright sources that saturate the central pixels to measure the tails and therefore it is expect to know  $\varepsilon_{meas}$  over several orders of magnitude. There will be some point, however, when the measured tails become unreliable. Computing the scattering fraction becomes problematic when both  $S_{meas}$  and  $S'_{scat}$  become very small, since the uncertainty of both is inversely related to the value.

A reasonable approach is to set minimum thresholds for each. The flag is then set if both  $S_{meas}$  and  $S'_{scat}$  are below their associated thresholds. For  $S_{meas}$ , a dim pixel threshold  $S_{lo\_thresh}$  is defined for each band. A reasonable choice for  $S_{lo\_thresh}$  is  $L_{min}$  or, for the emissive bands, is the black body radiance associated with  $T_{min}$ .

For  $S'_{scat}$  a threshold,  $S_{scat\_thresh}$ , will be based on test data. Determine the minimum  $\varepsilon_{meas}$  that is reliable and flag possible conditions where a reference bright target could scatter significant light beyond the measured tails. The bright target, as defined by the spec is at  $L_{max}$  and has an angular extent of 12 by 12 milliradians per the System Spec. If  $\theta$  is the angle which defines the limit of the measurement of the NFS, then  $S_{scat\_thresh} = S'_{scat}(\theta)$  where  $S'_{scat}(\theta)$  is computed for the bright target.

### 2.5.2.3 Creation of Non-Saturated Scene

Determining the % scattered light using the measured scene and a PSF has been considered; however, there is a difference between the scene needed to do this computation and a VIIRS SDR. The SDR is not a continuous field of radiance, which is what is necessary to do the convolution described above. Therefore, there are several features of the VIIRS SDR which need to be addressed to produce a continuous scene from the SDR.

- **Saturated radiance**

Values are assigned from a proxy band that has highly correlated radiances and substitute scaled radiances of the proxy band in place of the saturated data in cases where the pixel is saturated. Which proxy bands to use and the scale factors are controlled by a changeable LUT.

If no suitable proxy band is found, or if the radiance in the proxy band is saturated or missing, then default radiance based on maximum reflectance or brightness temperature are used

when available. This would be higher than Tmax or Lmax values and lead to a conservative upper estimate of the scattering.

- **In-scan angular resolution and Aggregation**

The PSF is a function of uniformly spaced pixels on the focal plane. Because of the size of the scattering PSF it is faster to convolve using an FFT. Computationally an FFT convolution requires a regular sample interval. Because the in-scan angular resolution changes across an aggregation zone boundary, each aggregation zone has a different angular resolution in-scan. To overcome this problem the aggregated pixels are “de-aggregated” by repeating them by the number of samples that were used in the original aggregation. A guard band would be added that would avoid aliasing of the FFT.

- **Bowtie and Edge of scan effects**

Re-pixelize is needed between the scans because of the “bowtie” overlap with adjacent scans. IDPS uses a common adjacency implementation to correct bowtie and edge of scan effects. This implement is not the same as is used in the science grade code which causes difference the outputs of the science algorithm to the science and operational implementation.

- **Missing radiance**

If the gap in radiance data is small, such as a single pixel, or a row of pixels, then the pixels are estimated by interpolating the nearest neighbors. If the gap is large, then it is filled in with proxy bands.

- **Scan & Granule limits**

The PSF is created to be as wide as or wider than a scan in the in-track direction. Reliable convolution depends on having guard regions around the scene that are about the size of the PSF. Granules are processed so that the granule before and the granule after is always available, so that scans adjacent to the first and last scan of the granule are available.

- **Scene edges**

In the usual processing mode, there is always a granule before and after the current granule. In the case where the process is just starting up, the IDPS algorithm should create a guard region by reflecting the first or last granule in the processing chain so that the flags can be calculated. The alternative is to set the “calculation unreliable” flag until the 2<sup>nd</sup> or 3<sup>rd</sup> scan. This is not part of the Science Grade Code. The IDPS Ops code uses the Common adjacency solution to pad the data with the previous and next scans providing all needed data for calculation.

#### 2.5.2.4 Common Adjacency Use In Bright Pixel

On Board Pixel trim in the SDR data must be replaced in order to provide for continuous data in on board pixel trim regions of each scan before convolution with the point spread function for calculation of the stray light percentages can be done. This replacement was described in the TM as being an area that must be modified by the IDPS operational baseline to use a modified version of the common IDPS operation method of on board bowtie deleted pixel replacement.

The provided implementation uses a spline average replacement as done with the bad data replacement. The TM NP-EMD-2007.510.0011.Rev.A describes this implementation as flawed and as an area the must be fixed in the IDPS operational solution. The method used was described in detail in the TM and has been the subject of a few meetings between IDPS and NGST. Because this has been a point of confusion in the past, a detailed explanation at this point of how this algorithm works has been included.

The first step in the replacement is to find the nearest neighbor for the bowtie deleted pixels in the previous or next scan as needed. The nearest neighbor once identified is then copied into the bowtie area, along with the in-track neighbors to the identified replacement pixel filling all missing bowtie pixels in the in-track direction in current scan being processed. This process is repeated for each cross-track (column) for all onboard bowtie deleted pixels. This is then continued for all scans of data being processed.

### **2.5.2.5 Data Convolution**

In the TM provided, along with explaining the needed changes for the on board pixel trim replacement, it also described a new approach for doing the point spread function convolution to replace the existing science implementation. The new approach is meant to remove discontinuities that can be produced during the convolution of the data. The science implementation takes the SDR data that has been updated to replace bad pixels, saturated pixels, and bowtie pixels and pads the data with the points spread function data and convolutes it with the PSF (point spread function) data. This is implemented in the science code as a by band calculation done once for each band.

IDPS operational implementation follows the method outlined in the TM by instead convoluting each scan separately in a 5-scan matrix. The 5-scan matrixes are made of the current scan as scan 3 of the 5-scan matrix. Scans 1 and 2 are made up of the previous two scans, and scans 4 and 5 are made using the next two scans. After the convolution is completed, only the current scan (scan 3 in the matrix) is maintained for use after the convolution.

Further differences were needed to implement this approach in the IDPS operational baseline for efficiency reasons. The code was modified to process the bowtie replacement on each matrix instead of the whole granule at once. The modification of the data from aggregated to unaggregated VIIRS space were also modified and moved to be done on the matrix of data to prevent duplication of work. Only the current scan is aggregated at the end to make the code more efficient.

### **2.5.3 Graceful Degradation**

The VIIRS Bright Pixel process contains no graceful degradation.

#### **2.5.3.1 Graceful Degradation Inputs**

None.

#### **2.5.3.2 Graceful Degradation Processing**

None.

#### **2.5.3.3 Graceful Degradation Outputs**

None.

#### **2.5.4 Exception Handling**

No exception handling is performed in the VIIRS Bright Pixel process.

#### **2.5.5 Data Quality Monitoring**

No data quality monitoring is performed.

#### **2.5.6 Computational Precision Requirements**

The VIIRS Bright Pixel process uses double precision values in order to ensure the required accuracy.

#### **2.5.7 Algorithm Support Considerations**

The DMS and INF must be running before the algorithm is executed.

#### **2.5.8 Assumptions and Limitations**

Bright Pixel implementation is currently limited to Moderate band data processing. Image band support is available with minor updates to the code.

### 3.0 GLOSSARY/ACRONYM LIST

#### 3.1 Glossary

Table 44 contains terms most applicable for this OAD.

**Table 44 Glossary**

| Term   | Description  |
|--|--|
| Algorithm                                    | A formula or set of steps for solving a particular problem. Algorithms can be expressed in any language, from natural languages like English to mathematical expressions to programming languages like FORTRAN. On NPOESS, an algorithm consists of: <ol style="list-style-type: none"> <li>1. A theoretical description (i.e., science/mathematical basis)</li> <li>2. A computer implementation description (i.e., method of solution)</li> <li>3. A computer implementation (i.e., code)</li> </ol>   |
| Algorithm Configuration Control Board (ACCB) | Interdisciplinary team of scientific and engineering personnel responsible for the approval and disposition of algorithm acceptance, verification, development and testing transitions. Chaired by the Algorithm Implementation Process Lead, members include representatives from IWPTB, Systems Engineering & Integration IPT, System Test IPT, and IDPS IPT.  |
| Algorithm Verification                       | Science-grade software delivered by an algorithm provider is verified for compliance with data quality and timeliness requirements by Algorithm Team science personnel. This activity is nominally performed at the IWPTB facility. Delivered code is executed on compatible IWPTB computing platforms. Minor hosting modifications may be made to allow code execution. Optionally, verification may be performed at the Algorithm Provider's facility if warranted due to technical, schedule or cost considerations.  |
| Ancillary Data                               | Any data which is not produced by the NPOESS System, but which is acquired from external providers and used by the NPOESS system in the production of NPOESS data products.  |
| Auxiliary Data                               | Auxiliary Data is defined as data, other than data included in the sensor application packets, which is produced internally by the NPOESS system, and used to produce the NPOESS deliverable data products.  |
| EDR Algorithm                                | Scientific description and corresponding software and test data necessary to produce one or more environmental data records. The scientific computational basis for the production of each data record is described in an ATBD. At a minimum, implemented software is science-grade and includes test data demonstrating data quality compliance.  |
| Environmental Data Record (EDR)              | <i>[IORD Definition]</i><br>Data record produced when an algorithm is used to convert Raw Data Records (RDRs) to geophysical parameters (including ancillary parameters, e.g., cloud clear radiation, etc.).<br><i>[Supplementary Definition]</i><br>An Environmental Data Record (EDR) represents the state of the environment, and the related information needed to access and understand the record. Specifically, it is a set of related data items that describe one or more related estimated environmental parameters over a limited time-space range. The parameters are located by time and Earth coordinates. EDRs may have been resampled if they are created from multiple data sources with different sampling patterns. An EDR is created from one or more NPOESS SDRs or EDRs, plus ancillary environmental data provided by others. EDR metadata contains references to its processing history, spatial and temporal coverage, and quality. |
| Model Validation                             | The process of determining the degree to which a model is an accurate representation of the real-world from the perspective of the intended uses of the model. [Ref.: DoDD 5000.59-DoD Modeling and Simulation Management]   |
| Model Verification                           | The process of determining that a model implementation accurately represents the developer's conceptual description and specifications. [Ref.: DoDD 5000.59-DoD Modeling and Simulation Management]  |
| Operational Code                             | Verified science-grade software, delivered by an algorithm provider and verified by IWPTB, is developed into operational-grade code by the IDPS IPT.   |
| Operational-Grade Software                   | Code that produces data records compliant with the System Specification requirements for data quality and IDPS timeliness and operational infrastructure. The software is modular relative to the IDPS infrastructure and compliant with IDPS application programming interfaces (APIs) as specified for TDR/SDR or EDR code.  |

| Term                       | Description  |
|----------------------------|--|
| Raw Data Record (RDR)      | <p><i>[IORD Definition]</i></p> <p>Full resolution digital sensor data, time referenced and earth located, with absolute radiometric and geometric calibration coefficients appended, but not applied, to the data. Aggregates (sums or weighted averages) of detector samples are considered to be full resolution data if the aggregation is normally performed to meet resolution and other requirements. Sensor data shall be unprocessed with the following exceptions: time delay and integration (TDI), detector array non-uniformity correction (i.e., offset and responsivity equalization), and data compression are allowed. Lossy data compression is allowed only if the total measurement error is dominated by error sources other than the data compression algorithm. All calibration data will be retained and communicated to the ground without lossy compression.</p> <p><i>[Supplementary Definition]</i></p> <p>A Raw Data Record (RDR) is a logical grouping of raw data output by a sensor, and related information needed to process the record into an SDR or TDR. Specifically, it is a set of unmodified raw data (mission and housekeeping) produced by a sensor suite, one sensor, or a reasonable subset of a sensor (e.g., channel or channel group), over a specified, limited time range. Along with the sensor data, the RDR includes auxiliary data from other portions of NPOESS (space or ground) needed to recreate the sensor measurement, to correct the measurement for known distortions, and to locate the measurement in time and space, through subsequent processing. Metadata is associated with the sensor and auxiliary data to permit its effective use.</p> |
| Retrieval Algorithm        | A science-based algorithm used to 'retrieve' a set of environmental/geophysical parameters (EDR) from calibrated and geolocated sensor data (SDR). Synonym for EDR processing.   |
| Science Algorithm          | The theoretical description and a corresponding software implementation needed to produce an NPP/NPOESS data product (TDR, SDR or EDR). The former is described in an ATBD. The latter is typically developed for a research setting and characterized as "science-grade".   |
| Science Algorithm Provider | Organization responsible for development and/or delivery of TDR/SDR or EDR algorithms associated with a given sensor.  |
| Science-Grade Software     | Code that produces data records in accordance with the science algorithm data quality requirements. This code, typically, has no software requirements for implementation language, targeted operating system, modularity, input and output data format or any other design discipline or assumed infrastructure.  |
| SDR/TDR Algorithm          | Scientific description and corresponding software and test data necessary to produce a Temperature Data Record and/or Sensor Data Record given a sensor's Raw Data Record. The scientific computational basis for the production of each data record is described in an Algorithm Theoretical Basis Document (ATBD). At a minimum, implemented software is science-grade and includes test data demonstrating data quality compliance.   |
| Sensor Data Record (SDR)   | <p><i>[IORD Definition]</i></p> <p>Data record produced when an algorithm is used to convert Raw Data Records (RDRs) to calibrated brightness temperatures with associated ephemeris data. The existence of the SDRs provides reversible data tracking back from the EDRs to the Raw data.</p> <p><i>[Supplementary Definition]</i></p> <p>A Sensor Data Record (SDR) is the recreated input to a sensor, and the related information needed to access and understand the record. Specifically, it is a set of incident flux estimates made by a sensor, over a limited time interval, with annotations that permit its effective use. The environmental flux estimates at the sensor aperture are corrected for sensor effects. The estimates are reported in physically meaningful units, usually in terms of an angular or spatial and temporal distribution at the sensor location, as a function of spectrum, polarization, or delay, and always at full resolution. When meaningful, the flux is also associated with the point on the Earth geoid from which it apparently originated. Also, when meaningful, the sensor flux is converted to an equivalent top-of-atmosphere (TOA) brightness. The associated metadata includes a record of the processing and sources from which the SDR was created, and other information needed to understand the data.</p>  |

| Term                          | Description  |
|-------------------------------|--|
| Temperature Data Record (TDR) | <p><i>[IORD Definition]</i><br/>                     Temperature Data Records (TDRs) are geolocated, antenna temperatures with all relevant calibration data counts and ephemeris data to revert from T-sub-a into counts.</p> <p><i>[Supplementary Definition]</i><br/>                     A Temperature Data Record (TDR) is the brightness temperature value measured by a microwave sensor, and the related information needed to access and understand the record. Specifically, it is a set of the corrected radiometric measurements made by an imaging microwave sensor, over a limited time range, with annotation that permits its effective use. A TDR is a partially-processed variant of an SDR. Instead of reporting the estimated microwave flux from a specified direction, it reports the observed antenna brightness temperature in that direction.</p> |

### 3.2 Acronyms

Table contains acronyms most applicable for this OAD.

**Table 45 Acronyms**

| Acronym  | Description   |
|----------|---|
| AM&S     | Algorithms, Models & Simulations                          |
| API      | Application Programming Interfaces                        |
| ARP      | Application Related Product                               |
| CDFCB-X  | Common Data Format Control Book - External                |
| DMS      | Data Management Subsystem                                 |
| DPIS ICD | Data Processor Inter-subsystem Interface Control Document |
| DQTT     | Data Quality Test Table                                   |
| E&A      | Ephemeris and Attitude                                    |
| EV       | Earth View  |
| FPA      | Focal Plane Array   |
| HAM      | Half Angle Mirror   |
| H-S      | Harvey-Shack  |
| IEO      | Instrument Engineering Order                              |
| IET      | IDPS Epoch Time   |
| IMG      | Imagery   |
| INF      | Infrastructure  |
| ING      | Ingest  |
| IP       | Intermediate Product                                      |
| IPO      | Input Processing Output                                   |
| LOS      | Loss of Signal  |
| LUT      | Look-Up Table   |
| MBN      | Max Band Number   |
| MDFCB    | Mission Data Format Control Book                          |
| MOD      | Moderate  |
| NCSA     | National Center for Supercomputing Applications           |
| NFR      | Near-Field Response                                       |
| NFS      | Near-Field Scattering                                     |
| OBC      | On-board Calibrator                                       |
| OBCBB    | On-board Calibrator BlackBody                             |
| PO       | Product Order   |
| PSF      | Point Spread Function                                     |
| PST      | Point Source Transmittance                                |
| QF       | Quality Flag  |
| RTA      | Rotating Telescope Assembly                               |
| SDR      | Sensor Data Record  |
| SDSM     | Solar Diffuser Stability Monitor                          |
| SI       | International System of Units                             |
| TBD      | To Be Determined  |
| TBR      | To Be Resolved  |
| TOA      | Top of the Atmosphere                                     |
| USES     | Universal Source Encoder for Space                        |

#### 4.0 OPEN ISSUES

Table 46 List of TBD/TBR

| TBX ID | Title/Description | Resolution Date |
|--------|-------------------|-----------------|
| None   |                   |                 |
|        |                   |                 |